UNIVERSITÁ DEGLI STUDI DI MILANO
DEPARTMENT OF AGRICULTURAL AND ENVIRONMENTAL SCIENCES – PRODUCTION, LANDSCAPE, AGROENERGY
DOCTORAL PROGRAMME IN AGRICULTURE, ENVIRONMENT AND BIOENERGY

CONTRIBUTIONS ON ADVANCED AUTOMATION FOR SELECTIVE PROTECTION TREATMENTS ON SPECIALTY CROPS

Doctoral Dissertation of:
Emanuele Tona

Supervisor:
Prof. Roberto Oberti

The Chair of the Doctoral Program:
Prof. Daniele Bassi

2017 – XXIX Cycle

Abstract

FOOD security and food safety are the main global objectives of today's agriculture. Within this framework, the recent growing sensibility of both policy makers and consumers for food safety themes appear to be a hopeful sign for the introduction of new strategies and technological systems in the next future's agriculture.

A particularly challenging issue for current crops management is the control of plant's diseases while avoiding environmental pollution. Precision pest management techniques (an emerging subset of precision agriculture suite) aim at facing this challenge by means of: i) sensing technologies for the early detection and localization of diseased areas in the canopy, and ii) variable rate technologies for the selective application of crop protection treatments on target areas.

In this dissertation, two innovative methodologies for hyperspectral crop's disease detection are presented. The measurements were acquired by means of a hyperspectral camera mounted onto a robotic manipulator which allowed to compose the subsequent hyperspectral scans (1 spatial dimension x 1 spectral dimension) into an hypercube (2D spatial x 1D spectral) of the imaged plant. The first disease detection method is based on the combinatorial selection of the most signifi-

cant wavelengths from the hypercube data by applying linear discriminant analysis, and the classification power of the optimal selected combination is then evaluated by applying a principal component analysis. The second method is based on a new spatial filter approach, acting along the different channels of the hypercube.

The two methods of detection are applied by discussing two case studies of diseases, both on cucumber plants. A first set of experiments was conducted on plants artificially inoculated with powdery mildew. A second and more extensive set of experiments was conducted on plants infected by the cucumber green mottle mosaic virus (CGMMV), which is nowadays considered one of the most dangerous diseases for the Cucurbitaceae family. The application of the two methodologies was successful in identifying the major symptoms of the diseases considered, and specifically the spatial filtering approach enable to detect the subtle morphological modifications in the plant tissue at rather early stage of CGMMV infection.

Due to the high cost and complexity of the technologies adopted in the disease detection and of precision spraying equipment, the second part of the thesis applies the classical methods of mechanization cost-analysis to investigate what are the economic thresholds, which may enable the introduction of new precision pest management technologies. To this aim, the analysis is focused on vineyard and apple orchard that represent a favourable case for introducing these kind of innovations, due to the high protection treatments costs typical for these specialty crops. Starting from the results obtained in research on precision spraying in speciality crops, the technical-economic analysis considers on three different technological levels of precision spraying equipment, associated with increasing levels of reduction of the distributed amount of pesticide. This reduction is assumed to be linked to the improved accuracy in targeting the application without affecting the biological efficiency of the treatment, and hence generating a net cost benefit for the farmer.

To gain insights into evaluating this benefit is of primary interest, since the profitability of precision spraying technologies will be a major driver for their adoption in speciality crops. Therefore, this study aims at: a) assessing the total costs associated to spraying equipment at the different technological levels considered; b) evaluating weather more advanced equipment can be profitable compared to current conventional sprayers.

Furthermore, this analysis was extended to a high-precision, robotic spraying platform, here considered as a perspective scenario for precision spraying technologies. For this specific case, the study aimed at assessing the maximum allowed cost for such a robotic platform, which could generate positive net benefits for the farmer thanks to the envisaged pesticide reduction.

Preface

DURING last few years the growing sensibility of both policy makers and consumers for food safety themes with the pressing of the technological advancement indeed are an hopeful sign for the introduction of the described strategies and technological systems in the modern agriculture.
In the introduction of the thesis a review of the motivation, history, regulations and the main techniques for precision pest management will be presented. The topics of interest are related to the use of agrochemicals with the environmental impact of their use on human health and environment with the main degradation routes of the most important pesticides. An extended presentation of the main strategies for precision pest management will be presented with a special focus on the disease recognition on leaves. At the end of the introduction chapter a literature review on economic analysis of precision spraying will be presented to introduce the economic sustainability of precision spraying system adoption.

Chapter 2 starts with a theoretical background of the main techniques and concepts applied during the experiments on cucumbers. A

special attention is given to the data processing techniques and imaging analysis. The description of the two methodologies developed will follow with the two experiments description. A new methodology for disease symptoms assessment is presented with the discussion of two case studies: the preliminary experiment was conducted on cucumber plants affected by powdery mildew aetiological agent. Thanks this case study the methodology was developed.

In chapter 3 the issue of adoption precision sprayer systems by the farmers will be investigated by applying the ASABE Standard methodology. At the beginning of the chapter there is a focus on the theoretical background on machine performance and machinery costs with a digression on the social impact of automation.

Contents

CHAPTER 1

Introduction

1.1 Purposes of the dissertation

The scientific work presented in this dissertation has two main objectives. The general framework in which it is inserted is the precision disease management agriculture and sensing strategies for disease recognition.
In the first part of the thesis a new methodology for disease symptoms assessment is presented with the discussion of two case studies: the first one on cucumber plants affected by powdery mildew. The methodology was developed using this case study. The second experiment is about cucumber green mottle mosaic virus (CGMMV) symptom detection on cucumber plants. CGMMV disease is one of the most dangerous in *Cucurbitaceae* family.

The measurements were performed using a hyperspectral camera

with high spectral and spatial resolution which during the second experiment was mounted into a robotic manipulator. In this studies various wavelengths combinations were selected for the disease detection coupled with a set of rules which permits the study of the reflected light which arrive from the canopy.

The second part of the dissertation deal with the technical-economic analysis on the possible adoption of high precision spraying equipment on the pest management in specialty crops coupled with advantage systems for disease detection. Starting from the results obtained in research on precision spraying in speciality crops, this study conducts a technical-economic analysis on three different technological levels of precision spraying equipment, associated with increasing levels of reduction of the distributed amount of pesticide. This reduction is assumed to be linked to the improved accuracy in targeting the application without affecting the biological efficiency of the treatment, and hence generating a net cost benefit for the farmer.
To gain insights into evaluating this benefit is of primary interest, since the profitability of precision spraying technologies will be a major driver for their adoption in speciality crops. Therefore, this study aims at: a) assessing the total costs associated to spraying equipment at the different technological levels considered; b) evaluating weather more advanced equipment can be profitable compared to current conventional sprayers.
Furthermore, this analysis was extended to a high-precision, robotic spraying platform, here considered as a perspective scenario for precision spraying technologies. For this specific case, the study aimed at assessing the maximum allowed cost for such a robotic platform, which could generate positive net benefits for the farmer thanks to the envisaged pesticide reduction.

The second analysis is strictly connected with the first part of the work due to it gives an idea of the economic limitations from the

farmers on adoption of sophisticated systems for disease detection and management. Furthermore, indirectly we have an idea of the time horizon of the introduction of new technologies.

1.2 Crop losses due to biotic stresses

Since the born of agriculture, humans had to protect their crops against yield loss from weeds, insect pests, and diseases. Harvest devastation by insects and fungal diseases is the main cause of the reduction of the crop yield causing problems in food and feed management and possible shortage.

The term *food security* describes the difference between the growing food demand of the world population and global agricultural output, further it describes the discrepancy between regional food demand and the presence of food. With food security it is included not only the food availability but also the physical and economic access to food.

Food imbalance has dramatically worsened during the recent decades, culminating recently in the 2008 food crisis Savary et al (2012). In accordance with FAO (2013) in the mid-2011, food prices were back to their heights of the middle of the 2008.

Most of the agricultural research conducted in the 20th century focused on increasing crop productivity as the world population and its food needs grew. To guarantee the progression a relevant role is given by the plant protection aspect. In fact, crop protection is able to avoid losses in the order of 20 % to 40 % of global agricultural productivity considering pathogens, animals, and weeds. Limit the focus on pathogens they represent roughly 20 % of direct yield losses (Oerke, 2006).

In general, the more intensive the system of cultivation, the larger are the potential losses due to harmful organism. This trend is given of one hand for the high intensity of the cultivation and in parallel for the increase in yield of modern cultivars. To overcome potential losses, crop protection has become more sophisticated and more effective, es-

pecially for developed countries (Oerke et al, 1994).
When we talk about crop losses we may refers to quantitative and/or qualitative issues. Quantitative losses result from reduced productivity, leading to a smaller yield per unit area. Qualitative losses from pests may result from the reduced content of valuable ingredients, reduced market quality, reduced storage characteristics, or due to the contamination of the harvested product with pests, parts of pest or toxic products of the pests.
Crop losses to weeds, animal pests, pathogens and viruses continue to reduce available production of food and cash crops worldwide, and some crop losses may not be avoidable for technological reasons.

1.2.1 Main strategies for ensuring food security

To ensure food security many techniques were introduced in modern agriculture. Part of these methods are intrinsic to the cultivation protocol, others include the use of external factors.
The first step to ensuring food production is the correct management of field: precision sowing techniques now enable the farmer to plan crop density and crop management on a selective basis in advance. In the last century there have been considerable changes and developments in techniques and crop rotations and soil fertility.
Plant breeding with the production of genotypes of useful plants, is another strategy to have suitable plants to grow under the conditions prevailing in the regions of cultivation and which give the highest possible yields of the best possible quality.
Considering now the methods which include external factors, the main inputs are pesticides. With this term we are considering a wide range of substances with ample fields of use. Pesticides are able to guarantee the increase of agricultural productivity. Pesticide includes insecticides, fungicides, herbicides, disinfectants and other substances or mixture of substances used to prevent or control any pest. Considering only the pre-harvest tasks, pests include vectors of human or animal diseases, unwanted species of plants or animal diseases; animals or or-

ganisms able to damage productive plants.
Focusing on chemical disease control, it represents an active strategy to protect plants from diseases, and started in the last century with the use of inorganic chemicals. The second generation of pesticides includes organic chemicals acting as surge protectans. Third generation fungicides are also organic but penetrate the plant tissue and control established infections. The fourth latest generation of compounds for disease control consists nonfungitoxic in vitrum that enhances resistance mechanism intrinsic to the plant and that interfere with the fungal infection process (Waard et al, 1993).
At the beginning of the use of chemical control one of the first compound was based on copper and sulphur to prevent the attach of powdery mildew and downy mildew diseases. To protect the canopy and save yields of the best techniques was the use of broad-spectrum fungicides like *dithiocarbamates* developed since the 1930s. These compounds have still a great importance in the protection of fruit and vegetables, cereals and speciality crops. Another group of broad-spectrum protective fungicides were the *phthalimides* but they were withdrawn completely due to the public health concerns. Referring in particular to vegetables and grapevine two groups very used are *chlorobenzenes* and *oxobenzenes*. The characteristic of all these fungicides is that they have a broad spectrum and block more than one stage of fungal metabolism. Due to the expiration of the patents broad-spectrum fungicides are cheap way to controlling fungal disease.
The introduction of systemic fungicides added a new dimension to the control of fungal diseases. These type of chemicals are able to penetrate into the tissue of the plant from the site of the application. This capability is extremely important because permits to cover also the already infected tissues. In this family we can find *guanidines*, *organophosphorus compounds*, etc. Among others *oxathline* fungicides have powerful systemic activity. The *pyrimidines* also include systemic fungicides suitable for dressing seed and for soil treatments and for controlling powdery mildew. The *imidazoles/triazoles* were an

important addition to the range of fungicides available. They are able to interfering with the membrane biosynthesis of fungi.
With the agents now available to control plant diseases, farmers are able to secure high yields from their crops. Systemic fungicides allow the control to start with the onset of the disease due to a curative and sometimes eradicative mode of action. The limit of chemicals and their diffusion is the onset of resistance phenomena.
In parallel with the diffusion of new chemical compounds also techniques of spreading are developing. The active control of crops and their genetics, of soil fertility via chemical fertilization and irrigation, and of pests via synthetic pesticides are hallmarks or the Green Revolution (Oerke, 2006).

1.3 Concerns regarding the use of plant protection products

In principle, pesticides are only registered for use if they are demonstrated not to persist in the environment considerably beyond their intended period of use. Nonetheless, residues of many pesticides are found ubiquitously in the natural environment Fenner et al (2013). Chemical degradation and metabolism are major mechanism of disappearance of pesticides after application to plants, animals or soil. The rates of degradation and metabolism are dependent on the chemistry of the compounds and factors such as temperature, humidity, light, surface of the crop (FAO, 2016b). A pesticide residue is the combination of the pesticide and its metabolites, degradates, and other transformation products.
The use of pesticides ensures less weed and pest damage to crops and a consistent yield. At the same time their use can have negative environmental impacts on water quality, terrestrial and aquatic biodiversity. Pesticide residues in food can also pose a risk for human health.
Hereafter are summarized the main environmental degradation routes and environmental occurrence in secondary compartments for top 10

pesticide classes are summarized (Fenner et al, 2013).

Dithiocarbamates (e.g. Mancozeb) are fungicides relatively used (7.1 % of global consumption). The main degradation route is acid-catalysed hydrolysis with the formation of potential NDMA precursors. In environment are rarely observed;

Organophosphates (e.g. Chlorpyrifos) are an insecticide relatively common (6.7 % of global pesticide use). The main degradation route is the microbial transformation (oxidation and hydrolysis) with the formation of glyphosate and AMPA frequently detected in groundwater; and clorpyrifos, diazinon, disulfuton detected in rainwater and remote lake waters;

Phenoxy alkanoic acids (e.g. 2,4-D) these compounds are herbicides relatively widespread (4.7 % of global pesticide use). The main degradation route is the microbial transformation (oxidative dealkylation and aromatic ring cleavage). Parent compounds are frequently detected in groundwater;

Amides (e.g. S-Metolachlor) are herbicides relatively widespread (4.2 % of global pesticide use). The main degradation route is the microbial transformation (hydrolysis and glutathione coupling. Secondary compounds are chloroacetanilides and their transformation products oxanilic (OXA) and ethanesulfonic acid (ESA). Secondary compounds are frequently detected in groundwater; metolachlor and alachlor detected in remote lake waters;

Bipyridyls (e.g. Diquat) which are common herbicides (3.2 % of global pesticide use). The formation of secondary compound is a very slowly biotransformation due to strong sorption to soil matrix. Secondary compounds are rarely observed due to they are mainly sorbed to sediments and soils;

Triazines (e.g. Terbuthylazine) belong to herbicides (2.3 % of global pesticide use). The microbial transformation (oxidative dealkylation and hydrolysis) lead to the formation of parent compounds

and hydroxyand dealkylated transormation products are frequently detected in groundwater (significantly beyond phase-out period). Furthermore, atrazine and DEA are detected in remote lake waters;

Triazoles and diazoles | (e.g. Propiconazole) belongs to fungicides (2 of global pesticide use). These substances are slowly transformation by microorganisms (oxidation) and by phototransformation of specific representatives. Among the parent compounds frutriafol is detected in remote lake waters;

Carbamates (e.g. pirimicarb) are insecticides/herbicides (2 % of global pesticide use). These components are transformed by microorganisms or base-catalyzed (hydrolysis of ester bond); some of them are phototransformed. Rarely are observed in environment;

Urea derivatives (isoproturon). These herbicides are transformed by microorganisms (oxidative dealkylation and hydrolysis). Parent compounds are frequently detected in groundwater;

Pyrethroids (e.g. cypermethrin) belong to insecticides (1.3 % of global consumption). The Microbial transformation (hydrolysis oxidation) and the phototransformation (direct and indirect) create parent compounds rarely observed due to mainly they are sorbed to sediments and soils.

Degradation of pesticides involves both biotic transformation processes mediated by microorganisms or plants, and abiotic processes such as chemical and photochemical reactions. When pesticides are handled improperly, they or their metabolites are toxic to humans and other species. Primary concern regarding the use of pesticides and in particular their residues is dietary. The intake of pesticide's residues can cause diseases and/or intoxications. Residues of the pesticides to which consumers are exposed often comprise not just the parent compound, but also metabolites produced in treated plants, environmental degradation products and possibly other pesticide-derived compounds.

Many studies showed health risk associated with the intensive use of pesticides connected especially with the farm workers. The effects in health are often chronic. Nevertheless, also the acute intoxications are common. It is also important to notice that often the absence of correlation in pesticide expenditure and yields seems to suggest that farmers are overusing pesticides in their farms (Rola, 1989).
The World Health Organization (WHO) and the United Nations Environmental Programme estimated that one to five million cases of pesticide poisoning occur among agricultural workers each year with about 20000 fatalities (Organization et al, 1990; Dennis, 2003). It was demonstrated that one of the main reason of poisoning is the lack of protective equipment and/or the use of defective equipment Andreatta (1998); Jeyaratnam (1990); Dennis (2003).

Direct and indirect negative effects of pesticide use on biodiversity have been shown by different studies (Young et al, 2001; Campbell and Cooke, 1997; Stoate et al, 2001; Marrs et al, 1991). Contamination of the environment from pesticides may result from spray drift, volatilisation, surface run-off, and subsurface loss via leaching/drainflow. Pesticides are second only to fertilizer (figure 1.2) in the amount applied and the extent of use (FAO, 2013). Referring to figure 1.1, which represents the global pesticide sales divided by region it is possible to note how in all the compartments present a growing trend in sales especially Asia, Latin America, and Eastern Europe. In addition, companies often charge lower prices for older products and in poorer markets, boosting sales. Africa uses far less pesticide than any other country. In figure 1.2 it is possible to see how the diffusion of pesticides is very spread in regions in which intensive farming is practiced. Where the land is limited like Bahamas or Mauritius the use is extremely high to maximize the production and contrast the spread of diseases. Japan, New Zealand, and Malaysia are in the same condition and the use is very intense. Different is the situation in China due to the status of developing country and its severe shortage of arable land compared with the high number of residents. Comparing with United

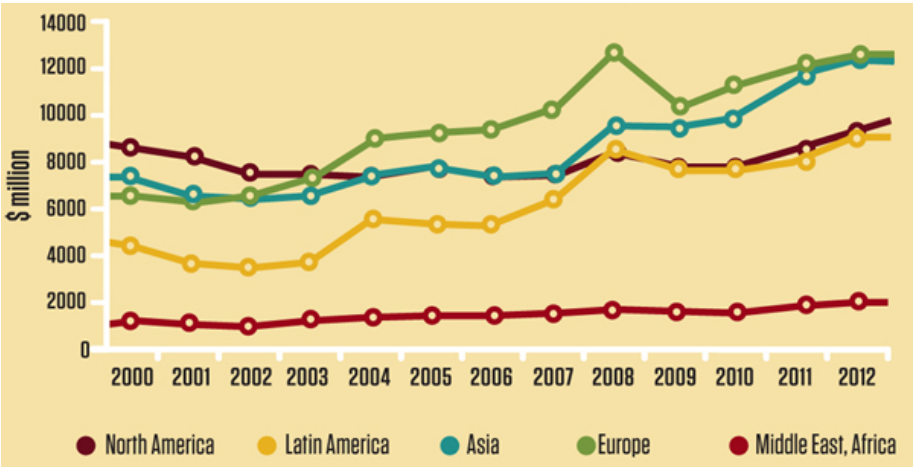

Figure 1.1: *Global pesticide sales by region (Anon., 2013).*

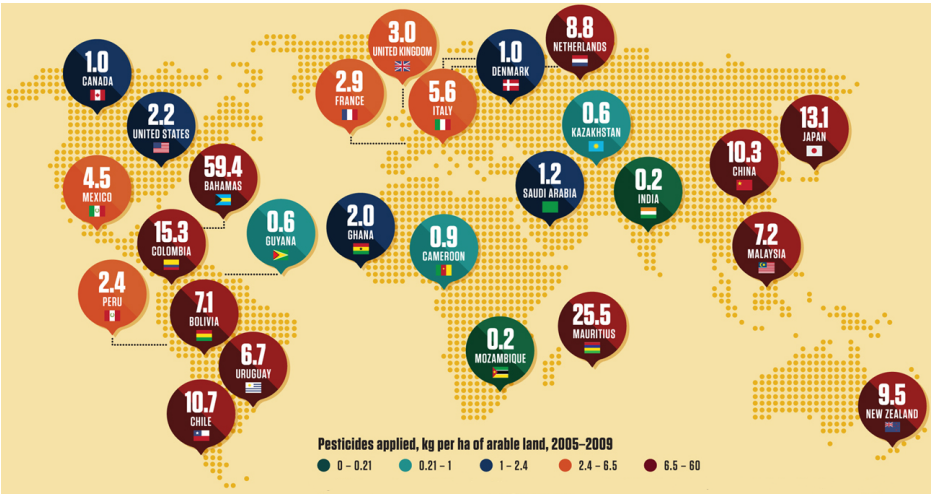

Figure 1.2: *Pesticide use around the world considering the arable lands FAO (2013).*

States we have here a lot of arable land with high extension, the farming is extensive, with a reduction of input used.
In rural Asia farmers used insecticides and herbicides liberally, giving them and their family members ready access to very toxic chemicals at moments of stress Hvistendahl (2013). The pesticide ingestion is the leading global means o suicide, and in Asia scientists said this is the one of the cause of the hight rates of suicide in Asia.

Long term studies of the effects of pesticides and other environmental chemicals were conducted by Mascarelli (2013), it was demonstrated throw research in lab animals and farm workers that chronic exposure to high doses of pesticides is associated with neuro-degenerative diseases such Parkinson's disease and cognitive deficits. In Europe where the demand of input is extremely high and the land available is relatively low or not equal-distributed we have a relative high use of pesticides especially in countries like Netherlands (greenhouse farming), Italy (intensive farming). The first large-scale risk assessment of organic chemicals in European rivers and lakes has revealed an extensive problem with pesticides. The problem is focused in greatest for insects and algae but concerns regard also the consumption of river water from humans without previous treatments (Malaj et al, 2014).
Malaj et al (2014) demonstrate that the levels of organic chemicals were high enough to likely cause chronic problems. These molecules contain carbon atoms, and they include pollutants such as pesticides, herbicides and other synthesized compounds. The team observed that pesticides were by far the most common guilty party. Another ubiquitous pollutant is polycyclic aromatic hydrocarbons which typically come from vehicle exhaust or petroleum spills from boats.

The global pesticide use can be anticipated to continue to increase, it means that the environmental impact of them and their residues is a present concern. Even if the new pesticide legislation in Europe puts more emphasis on hazard assessment, source control measures, and substitution blind spots in pesticides degradation are still present.

1.4 European legislation on pesticides and the impact on the machinery advancements

Pesticides usage can be reduced through integrated pest management (IPM), which uses information on pest populations to estimate losses and adjust pesticide doses accordingly (FAO, 2013).
In recent years one of the major interest of policy makers is the reduction of pesticide use in agriculture with the purpose of reducing negative impacts on environment and on food security. In Europe the main actions to protect human health and the environment regard to pesticides are:

Directive 128/2009 establishing a framework for Community action to achieve the sustainable use of pesticides;

Regulation 1107/2009 concerning the placing of plant protection products on the market;

Regulation 0083/1998 on the quality of water intended for human consumption which stipulates a maximum concentration of 0.1 μg l^{-1} for any single pesticide and its relevant metabolites in potable water;

Directive 60/2000 establishing a framework for Community action in the field of water policy which identifies a large number of particularly toxic, persistent or bioaccumulative polluting substances.

Directive 105/2008 on environmental quality standards in the field of water policy,

Directive 32/2002 on undesirable substances in animal feed;

Regulation 396/2005 on maximum residue levels of pesticides in or on food and feed of plant and animal origin.

Direct linked to the machine improvement is the pesticide distribution it is the Directive 2009/128/EC. Which is one of the strategic

themes of the 6^{th} *Environment Action Programme*. Many studies have been conducted about the precision spraying techniques because current farming practice provides the uniform application of pesticides into the field, even if several pests and diseases exhibit an uneven spatial distribution, with typical patch structures evolving around discrete foci, especially during the early stages of development (Everhart et al, 2013).

1.5 Main approaches for precision spraying in crop protection treatments

The mechanization and the intensification of agriculture in Europe, are important factor for the rationalization of the inputs (fertilizer, pesticides, fungicides) which are always applied uniformly without taking in account the variability of the environmental condition (soil type, crop density, or disease pressure) (West et al, 2003). Considering plant disease detection, recent development in agricultural technology have led to a demand for a new era of automated non-destructive management methods.

Pesticides are recognised to play a major role in environmental pressure and production costs of agricultural activity, as well as in public concerns about healthiness and wholesomeness products (Oberti et al, 2013). Then is present an increasing interest in developing suitable techniques and equipment able to selectively target the application of pesticides where and when needed by the crop.

Any system that aims to make a spatially targeted pesticide application needs a series of components, there is a detection part which permits to read the informations environmental conditions; a decision module and an application module. The advancement of the technology permits to improve the number of correct decisions of area unit in the field. The strong drive force in the advancement was thanks to the diffusion of sensors, especially global navigation satellite systems (GNSS), which permits the management of the target position in high

spatio-temporal variability (a peculiarity of agricultural fields). Satellite navigation systems such are now being widely developed for agricultural applications, reaching a very high accuracy.

Other important improvements deal with the decision module, which concerns the interpretation of the sensor's signals and the comparison with pre-setted rules. Calculation capacity today permits real-time applications disconnected from prescription maps. At the same time the use of treatment map means that an application system needs only to be loaded with those pesticide formulations that will be needed for treating a defined area (Miller, 2003). On the other hand, prescription maps are less flexible in managing unexpected conditions or changes.

Improvements in sensors and in decision systems are in parallel with the advancement of the delivery system. The main capability is to operate maintaining a good quality of spraying and uniformity over a wide range of dose rates.

Canopy characterization methods One of the techniques for disease treatment is the canopy volume detection due to the possibility of precise assessment of the target (Lee et al, 2010). For this case, the objective of saving pesticide is pursued by applying a variable spray rate adapted to the changing canopy volume or density, instead the uniform distribution rate adopted in conventional treatments. For the canopy volume assessment, there have been several attempts. The first method is the use of ultrasonic sensors, Turrell et al (1969) studied the changes in feature data of citrus tree over a period of time. From the work they observed that citrus trees and tree parts followed growth curves similar to non-woody plants. From 1980s laser technology was used for forest biomass and timber volume assessment through airborne laser profiling (Nelson et al, 1988). Other works were conducted through an helicopter-borne laser system by Nilsson (1996) using the combination of airborne LiDAR and satellite imagery.
The application of advanced technologies started later in 2004 by Wei and Salyani, they used a laser scanning system to measure citrus tree

height, width, and canopy volume reaching a good repeatability with a measurement error less than 5 %. More recently Ehlert et al (2008) estimate site-specific crop parameters such as plant height, coverage and biomass density which could be a major factor in optimizing crop harvesting methods.
Another step for the canopy density and volume assessment is represented by the use of ultrasonic sensing system. Giles et al (1988) and in 1989 investigate spray volume savings using an ultrasonic measurement which ranged an error rate less than 2 % on calibration targets and an average error of 10 % for apple and peach orchards applications. In the study of canopy volume assessment other groups of researchers made a comparison between a laser scanner and ultrasonic transducers in measuring canopy volume of citrus trees Tumbo et al (2002). Zaman and Salyani (2004) studied other technical aspects regarding the influence of travel speed on ultrasonic measurements. The third method used is based on light penetration of the canopy and are connected with leaf area index (LAI) determination (Jahn, 1979). On arable crops (Miller et al, 2000; Dammer and Ehlert, 2006; Van De Zande et al, 2009; Dammer and Adamek, 2012) by means of sensor-controlled spraying equipment, savings of pesticide reported to be in the range of 5 % to 30 %, while keeping an average biological efficacy similar to conventional uniform spraying. However, it is on speciality crops that this approach has the greater potential of savings. Specifically, onto bush and tree crops where the total amount of pesticides used (application rates and frequency of the treatments) is typically much higher than for arable crops. Furthermore, in these crops the volume and density of the canopy largely change during the growing season and, as well, gaps in the vegetation or variations in the canopy structure often occur among fields. To address this heterogeneity of spraying targets, the presence, size and density of canopy in bush and tree crops has been successfully sensed by multiple ultrasonic proximity sensors. The obtained site-specific information was then used to control the on/off switching of the nozzles in correspon-

dence of gaps in the canopy or when entering and exiting from tree crops rows. Examples of equipment adopting such approach in orchard and vineyard treatments were developed, among first, by Giles et al (1987); Balsari and Tamagnone (1998); Moltó et al (2001). More recently, Esau et al (2014) developed a similar system for blueberry crop, relying on a colour camera to detect the crop bush canopy to be sprayed selectively. These authors reported average savings from about 10 % to more than 35 %, compared to conventional sprayers without application control.

Further advances in implementing precision spraying on speciality crops were obtained by using the sensed canopy characteristics not just for the on/off switching of individual nozzles, but also to control the pattern of the spray proportionally to foliage density and according to the canopy geometry (i.e. to the plant's shape). Studies were conducted for and advanced sprayer control and an automatic tree inventory: Wellington et al (2012) had work in real time by adapting all parameters involved, it was used PWM control system with a duty cycle to control nozzles, but the main challenge was the utilization of a vehicle-mounted sensors to build a model of trees by accumulating LIDAR data in a 3D voxel density. LIDAR readings was processed by applying probabilistic models. To this aim, Solanelles et al (2006) developed an air-assisted sprayer for tree crops fitted with a LIDAR sensor for canopy characterization, and high-frequency PWM (pulse width modulation) solenoid operated nozzles, which enabled to continuously vary the delivered flowrate of each single nozzle in order to adapt it to the current spraying target. The obtained pesticide savings were estimated from 25 % to 45 % compared to conventional treatments. Gil et al (2007) developed for vineyard applications a similar system equipped with six electro valves, obtaining continuously variable flow rate at three different height portions of the canopy.

In addition to the delivery rate of liquid spray, Balsari et al (2008) addressed also the problem of controlling the air-assist flow rate, with the aim of improving the targeting and deposition of pesticide; i.e.

reducing off-target spray losses. Their prototype included adjustable air ports allowing to obtain a vertical spray profile with three separate bands on each side, individually controlled according to the characteristics of the canopy volume sensed in real-time by ultrasound transducers. A similar solution, based on PWM controlled nozzles and a mechanically adjustable air-assist flow, especially designed for the precision spraying of young (i.e. small canopies) citrus tree, has been proposed by Khot et al (2012) who estimated a possible reduction of almost 50 % of pesticide.
Vieri et al (2013) went further in this approach by developing an orchard-vineyard sprayer able to automatically vary the distribution pattern of the air-assist flow, to adapt it to the canopy volume and shape. This was obtained by means of electric actuators able to control in real time the inlet air flow rate and the delivering angle of four independent air ports. From the results of preliminary tests, the authors envisaged a possible reduction of about 50 % in pesticide while maintaining an acceptable spray deposition. Osterman et al (2013) addressed the same objective by developing a three, hydraulically-driven, spraying arms prototype with height degrees of freedom when configuring the spraying and air-assist pattern on a side of the trees row. Also in this case the sensed canopy's shape was real-time processed to vary the pose of the air-assist and spray delivery devices.

Reasoning on the importance of Precision Pest Management (PPM), which aim to target chemicals where and when needed at an appropriate dose, many pathogens cause discrete foci of disease within crops due to uneven arriving of the pathogens in the field. In many polycyclic diseases, the dispersal of new propagules, predominantly around the original foci, intensifies the development of patches of disease (McCartney and Fitt, 1998). The fundamental rationale of this selective approach relies on the uneven spatial distribution exhibited by the symptoms of several diseases, with typical patch structures evolving around discrete foci, especially during the early stages of infection development (Everhart et al, 2013; Spósito et al, 2008; Waggoner et al, 2000).

The targeted spraying of disease foci (and of surrounding buffer areas) can control the infection establishment and prevent its epidemic spread to the whole field (West et al, 2003), while significantly reducing the total amount of pesticide applied.

The fungal action in plants Fungi which infect plants are organism unable to photo-assimilate, they derive their nutrition from the plant's internal flow. At the end of the cycle fungi produce spores which are able to survive in extreme circumstances until they infect other plants (Bravo, 2006). Usually fungi are host specific, it means that the spores are able to germinate only in the specific host. When it happens usually the reaction of the host is extremely circumscribed and difficult to see with naked eye.

Due to the parasitism in which the fungus live, it is interested in maintaining the plant tissue alive, but at the same time it is settled into the plant intercellular and intracellular structures. This presence interferes with the plant's immunity system; the fungus takes control of the metabolism of the infected cells. This condition forces the host to change its photosynthetic metabolism into a respiratory environment. The chlorophyll content does not change until a later stage of the infection, where infected cells start to die of. Even if the chlorophyll content derived from fluorescence is almost the same, the efficiency for assimilating the harvested light clearly chanced accordingly to the fluorescence intensity (Peterson and Aylor, 1995).

The phenomena is caused by the protection of the chlorophyll complex against photo-oxidation. When the chlorophyll is too much illuminated, photo-oxidation damage can occur under the form of triplet excited chlorophyll. The chlorophyll photo-protection can be realized in two different ways. One is called Non-Photochemical Quenching (NPQ), which is activated by carotenes and pool of β-carotene derived xanthophylls: violaxantin and zeaxantin. De-epoxidation of violazantin by excess energy of chlorophyll into zeaxantin helps the discharging of the chlorophyll complex during the saturation event of the

chloroplast. Further on zeaxantin changes into violaxantin by epoxidation and thereby releases heat. This last part of the xanthophyll cycle is called thermal relaxation. The excessive light energy, which could not be assimilated through neither photosynthesis nor NPQ is fluoresced. The initial peak fluorescence is a measure for the plant's chlorophyll content (Bravo, 2006).
The presence of the fungus inside the plant influence the composition of the leaf and the biochemistry of the leaf itself. Healthy plants appear green since the green light band is reflected relatively efficiently compared to blue, yellow and red bands which are absorbed by photoactive pigments. Furthermore, with the advancing of the symptoms also the structure of the leaf results influenced and conditioned by the pathogen activity. The interpretation and the reading of the interaction of light with plant is able to give important informations about the disease recognition.

Disease symptoms recognition techniques The laboratory analysis for the disease characterization are represented by molecular methods. This type of techniques are the reference for the comparison with the indirect methods for disease characterization. Molecular methodology is very sensitive (ranged between 10 and 10^6 cfu ml^{-1}) but difficult to use in real time applications. One of the commonly used diseased molecular detection method is ELISA (enzyme-linked immunosorbent assay) and PCR (polymerase chain reaction). The former method consists in the injection into an animal of a microbial protein called antigen. In presence of the disease causing microorganism (antigen), the sample would fluoresce confirming the presence of a particular plant disease. In PCR-based disease detection, the genetic material (DNA) of the disease-causing microorganism is extracted, purified and amplified Sankaran et al (2010).
The methods just described present limitations because they are time-consuming and labour-intensive. The main steps are the sample prepa-

ration and the analysis itself which include the use of costly reagents. Different is the situation for indirect methods for disease detection which, for example, use the interaction of plant with light to recognize the disease. These techniques in fact have the potential to be applied in real time applications and are relatively guaranteeing a certain repeatability.

The properties of light are medium to understand the read the surrounding environment, for this purpose optical-based sensors for disease detection have been developed. They offer non-destructive and fast detection capabilities along with low weight and dimensions and thus simple system integration (Sankaran et al, 2010). The differences in energy per photon also have implications for sensing. For photons from longer wavelengths, either very sensitive sensing devices are needed or a larger area is required in order to get a sufficient amount of energy Heege (2015). Thus a balance between wavelengths and spacial resolution might be necessary.
Another important factor for the detection besides the spacial resolution is the source of the light which can be natural (the sun is the most important) or artificial. The radiation of a body depends mainly in its temperature, for example the sun has a very high temperature in fact the radiation which arrive on heart is of ultraviolet, visible and some infrared radiation. On the other hand, the energy emitted from the surface of the earth is mainly in thermal infrared range.

Regarding the interaction between a body and the light we can say that a body can emit, reflect, absorb and transmit radiation. Every body with a temperature above 0°K discharges photons. When a photon hits a particle in its rote and change the direction this is a *reflected radiation*. When the energy of the photons is used by the matter with which they come in contact heating the body or for photosynthesis we talk about *absorbed radiation*. Finally, *transmitted radiation* is the remain radiation which pass through the body.
When we measure the light reflected by leaves we are looking to its *reflectance*. The reflectance in plants is almost constant for healthy

ones; alterations of the reflectance can be considered as an inference of a leaf compositional change. Diseases can affect the optical properties of leaves at many wavelengths, thus disease detection systems may be based on spectral measurements in different wavebands or a combination of them.

Spectroscopy and imaging techniques are unique disease monitoring methods which can be useful for PPM, the spectroscopic and imaging techniques could be integrated with an autonomous agricultural vehicle that can provide information on disease detection at early stages to control the spread of plant diseases Sankaran et al (2010).
When we measure the light coming from the plant, considering an healthy one, we are reading the *spectral signature* of the plant itself (Lee et al, 2010). Leaf reflectance is defined as the proportion of the irradiated light reflected by the leaf. Usually the reflected spectrum in healthy plants present common features:

- Low reflectance at visible wavelengths (VIS = 400 - 700 nm) due to the strong absorption of the photo-active pigments;
- high reflectance in the near infrared (NIR = 700 - 1200 nm) in which there is the strongest interaction with the tissue of the leaf;
- low reflectance in wide wavebands of the long-wave infrared part of the spectrum (SWIR = 1200 - 2400 nm)

In figure 1.3 is showed the typical reflectance vegetation spectrum, with some of the most significant wavelengths associated with main components of the leaf tissue. Disease can affect the optical properties of leaves at many wavelengths, depending on which tissue of the leaf is damaged, thus disease detection systems may be based on spectral measurements i different wavebands. One of the most significant channel is around 670 nm, usually defined as *red edge*. In this point there is a sharp transition in the reflectance spectrum from low VIS reflectance to high NIR reflectance. In this point usually there is the maximum

chlorophyll's absorbance value; which result often corrupted in diseased plants.

The identification is a matter of careful analysis of the spectrum which

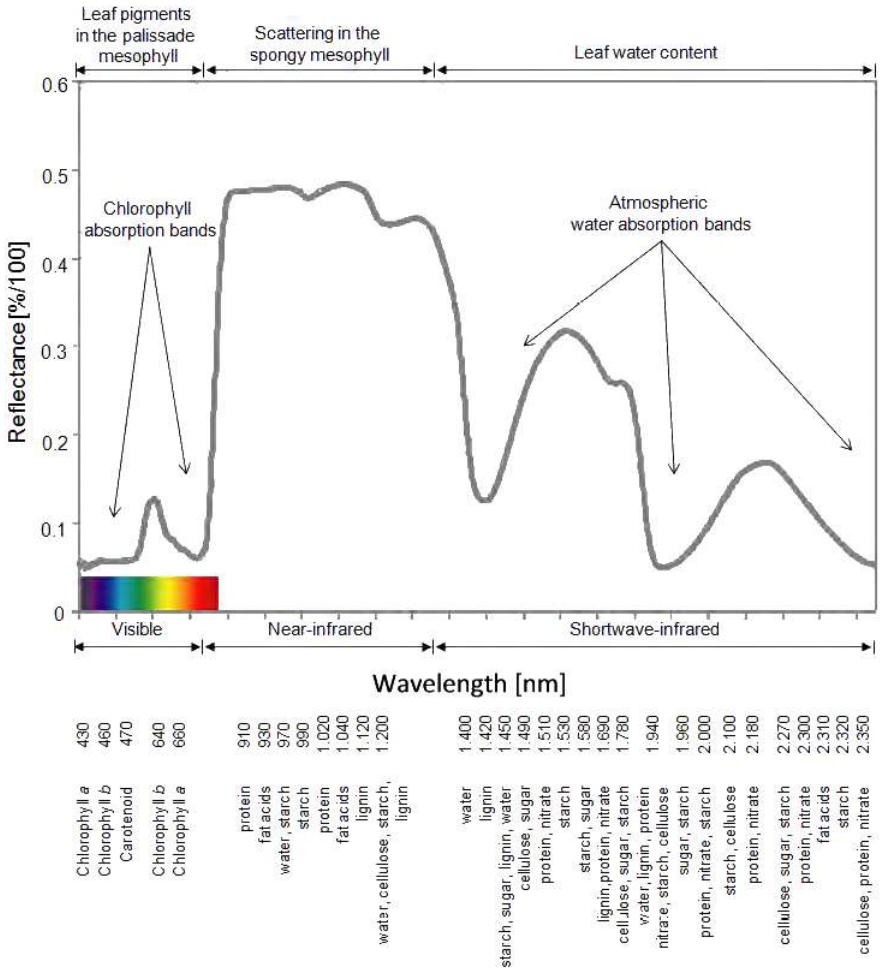

Figure 1.3: *Vegetation reflectance spectrum from visible to shortwave-infrared spectrum.*

can include mathematical processing of spectral data. The analysis can be done with a full spectrum approach or a discrete waveband one. For our analysis we develop a discrete waveband algorithm.

The real issue and interesting challenge in precision pest management remain the recognition of the disease symptoms and the early

identification of disease foci in field. Different methods are available for this purpose. We pass from machine olfaction systems such as electronic nose to foliar optical methodologies (fluorescence, thermography, hyperspectral imaging).

Thermography Images obtained with regular cameras, are two-dimensional slices representing scenery in one or more spectral regions. Images in other wavebands such as near-infrared part of the spectrum are obtainable with special sensors and cameras. Thermography for example is a technique that acquires images of thermal radiation between 8 and 15 μm. The object under investigation emits a certain thermal radiation depending on the temperature of this object and its emissivity. Plant radiation can be estimated through the thermal radiation captured by a thermal camera and the emissivity of the plants. The response of the plant in thermal radiation responds to a physiological status: when the plant is in a stress condition tends to close the stomata causing that CO_2 and H_2O are not exchanged which causes a greenhouse effect in the leaf (Lee et al, 2010).

Fluorescence Fluorescent radiation can be traced back to photons that did enter an absorption process in plants. Fluorescence happen after artificial excitation of the photosystems of a plant and the observation of the relevant responses in from of fluorescent light. In particular fluorescence is light emitted during absorption of radiation of some shorter wavelength.
Irradiating the chloroplasts with blue or actinic light will result in some re-emission of the absorbed light by the chlorophyll. The proportion of this light compared to the irradiation is variable and depends on the plant's ability to metabolize the harvested light. The plant gain energy in form of ATP (Adenosine triphosphate) throw the mitochondrial activity. Whether the photosynthetic receptors are exited with a very strong blue light beam, the chloroplast Light-Harvesting Complexes

(HCL) become completely saturated. The excitation is not associated with the complementary activation of the photosynthetic metabolic pathway; this misalignment causes the need of the HCL to discharge its excess excitation energy into lower energy photons in form of red emission. Common ranges for plant fluorescence are either the blue to green region extending from about 400 to 600 nm or the red to far-red region from approximately 650 to 770 nm wavelength. This fluorescence is strictly correlated with the chlorophyll concentration, and can be utilized to monitor nutrient deficiencies, environmental conditions based stress levels, and diseases in plants (Cerović et al, 1999; Belasque Jr et al, 2008). Daley (1995) found sub-millimiter sized high fluorescence emission spots that corresponded with TMV infection points on tobacco leaves. Bodria et al (2002) observed fluorescence spots,on wheat laves 2-3 days after inoculation with *Puccinia recondida* spores.
The fact that the fluorescence always has high wavelengths than the respective exciting light means that the fluorescence light has lower intensity.

Hyperspectral imaging Recently hyperspectal imaging is gaining a considerable interest for its application in precision agriculture. In the hyperspectral imaging, the spectral reflectance of each pixel is acquired for a range of wavelengths in the electromagnetic spectra (see section 2.3.1 for technical details). The hyperspectral technique is used in various applications such as monitoring of the food quality: Aleixos et al (2002) used multispectral imaging of citrus fruits to assess the quality of the fruits for developing a machine vision system. Gowen et al (2007) explored the food quality and food security applications. Huang and Apan (2006) provides the physiological condition of the plants.

Considering the fungal infections, the reflectance variations can be various (Mahlein et al, 2010). For the study of many crop proper-

ties one successful approach is the use of reflectance indices. Spectral indices are able to condensate the informations of the reflectance electromagnetic spectrum to obtain useful the discrimination between healthy and diseased plants. For example, Huang et al (2007) to study *Puccinia striiformis* symptoms used the photochemical reflectance index (PRI):

$$PRI = \frac{R_{531} - R_{570}}{R_{531} + R_{570}}$$

where the form R_{xxx} represents the reflectance at a specific wavelength.
Oberti et al (2012) to analyse symptoms of powdery mildew in grapevine used the following spectral indices:

$$I_1 = \frac{R_{660}G_{580}}{NIR_{800}^2} \quad \text{and} \quad I_2 = \frac{R_{660}}{R_{660} + G_{580} + NIR_{800}}$$

For the studying of fungi is reasonable to analyse systematically mathematical combinations of discrete narrow wavelengths along a sensible full spectrum. Nevertheless, this systematic searching will be immense due to many different fungi and various crops should be considered (Heege, 2015).

In figure 1.4 are summarized the various phases of infection of a foliar disease from the first metabolic changes to the advanced symptoms, associated to the main detection techniques. Three phases are defined: infection, early senescence and advanced stressed plant.

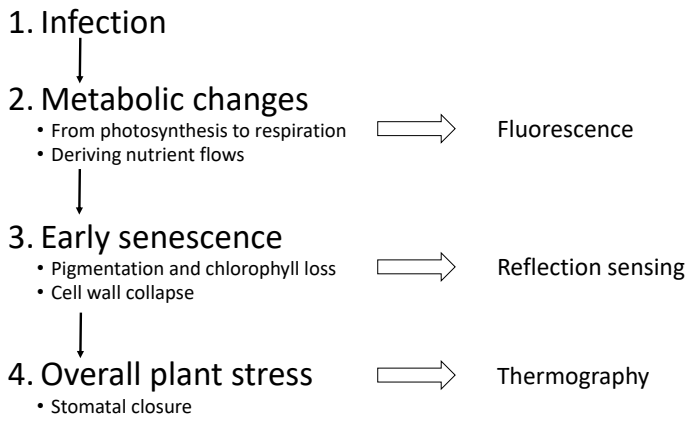

Figure 1.4: *Most relevant indirect measurement techniques associated to the stage of infection of a foliar disease (Bravo, 2006).*

1.6 Perspective of disease detection

The objective of selectively targeting pesticide on disease areas in speciality crops has recently gained some interest among researchers. Li et al (2009) considered this concept in a lab setup by using artificial labels to simulate spraying targets to be detected by a stereoscopic colour camera. Larbi et al (2013) while focussing on the problem of multispectral sensing of the young foliage in citrus canopy, they also envisaged for further research the possible selective spraying of immature leaves, being the channel trough which Huanglongbing disease infects citrus trees.

Regarding the robotic selective spraying in recent years Oberti et al (2016) reported the first fully automatic tests of selective spraying of disease areas In speciality crops, by using a reconfigurable, multifunction agricultural robot developed in the EU-project CROPS (www.crops-robot.eu). One of the main purpose of the project was the development of an automated platform for disease management provided with sensors to detect and manage symptomatology on plants and this was the first experiment conducted on totally automatic, selective spraying of diseases in speciality crops Oberti et al (2016). To identify disease

symptoms a R-G-NIR multispectral camera was used. Data were processed with dedicated algorithms, instead the treatment was guaranteed by a ROS[1] based communication framework.
In a series of greenhouse experiments conducted on grapevine plots exhibiting different levels of powdery mildew disease symptoms, the CROPS robotic system was demonstrated to autonomously detect the disease foci within healthy canopy, and to selectively spray them by means of a sprayer end-effector. The results of these experiments were evaluated basing on deposition of spray on targets, with the implicit assumption of a contact action treatment on the disease, obtaining a reduction of applied pesticide from 65 % to 85 % (depending on disease levels and spatial distribution of foci) when compared to a conventional homogeneous spraying of the canopy. Spite their preliminary nature, these experiments represent a first demonstration of the possibility to develop such an advanced stage of precision spraying in speciality crops. The robotic manipulator used during the experiment was equipped with a precision-spraying end-effector (Malneršič et al, 2012) and configured for this application. The robotic system was tested on powdery mildew disease symptoms and was able to cover at least 85 % of the disease area, reducing the healthy area covered from 5 % to 20 % of the total canopy are. The total pesticide amount reduction was between 65 % and 85 % comparing to a conventional homogeneous spraying of the canopy.
The idea behind the described system is the possibility to perform non-destructive measurements without a direct contact with the sample and can be operated from almost any desired distance. The measurement regards the sensing of instantaneous phenomena, suitable for on-the-go measurements from a vehicle during normal field operation inspecting the vertical stucture of the canopy. The detection it was at a sub-centimetre scale. PPM can be an occasion for reducing the environmental impact, and health issues (section 1.3) and to have a reduction in economic pressure on the agricultural farm. The selective targeting

[1] Robot Operating System (Quigley et al, 2009).

of pesticide application only where and when it is needed by the crop.

1.7 Literature review on economic analysis of precision spraying

Beside the technical issues, the economic farm management is main limit for adopting precision technologies for disease management by farmers. Economic analysis on adoption of precision technologies in sprayers has so far been limited to boom-equipment for arable crops protection, mostly by studying the savings obtained with spot application of herbicide on weed patches, or by avoiding spraying overlaps due to swath errors and to irregular shaped or edged field.
Among the first, Bennett and Pannell (1998) analysed the potential profitability of a weed-activated, on-off sprayer to be used for pre-emergence application of glyphosate in a 1000 ha, Western Australia's hypothetical wheat farm. The authors estimated the investments and operative costs of the precision spraying equipment and the associated savings of herbicide, by assuming different patchy weed populations to be sprayed only above predefined threshold of weed density. They concluded that, for the considered scenarios, the costs of the technology were still too high for the net benefits to be positive. Timmermann et al (2003), in a four years experiment on herbicide site-specific spraying of arable crops based on manual weed mapping, computed that the obtained herbicide savings were on average 33 € ha^{-1} per year, but they did not quantified the associated costs of automatic sensing and patch spraying technologies.
Batte and Ehsani (2006) evaluated the potential benefits for a high-accuracy RTK-GPS guidance system combined with control of individual sprayer nozzles, in comparison to investment and operative costs of conventional boom-sprayers with foam marker guidance used in arable crops. In their analysis, they assumed a cost of sprayed material of 27 USD ha^{-1} per application, two chemical applications per year, and 10 years of service life for the sprayers. The authors, by con-

sidering simulated farm fields with different shapes and with or without presence of waterways, quantified the savings due to difference of swathing accuracy (overlapped spray area) in term of additional passes and over-sprayed material, finding that a farm size between 486 ha and 729 ha was needed to justify the investment in precision spraying technology. With a similar approach, Larson et al (2016) analysed the profitability of automatic nozzles control for a 27.4 m boom, specifically considering field geometry (i.e. size and shape) obtained for 44 cotton and corn real farm fields in Tennessee, USA. The authors suggested that the Perimeter-to-area ratio (P/A) of field geometry may be a useful index to consider when evaluating investments in boom-sprayers precision technologies. They estimated that, for a typical size of cotton farm among those considered, investing in automated boom-control was not profitable for fields with P/A = 0.01, but was generally profitable for fields with P/A $\geq$ 0.02.

Esau et al (2016) analysed the economics of precision spraying technologies on boom-sprayers used for wild blueberries farming. The authors compared the cases of a 13.7 m tractor-mounted boom sprayer equipped with conventional manual control and foam marker guidance assistance, with one equipped with high-accuracy guidance system and individual nozzles control actuated by vegetation sensing. By considering two simulated fields with 30% weed coverage during pre-emergence herbicide applications, and with 80% crops coverage during fungicide applications, basing on 9 spray passes over 2-year production cycle, the authors computed an average reduction of 44% on operative costs (from 2110 CAD ha^{-1} to 1137 CAD ha^{-1}) thanks to avoiding over-spraying due to swath errors (assumed to be on average 9%), and to the savings obtained by spot application.

Prior technical-economic analyses have not addressed precision technologies for spraying equipment used on speciality crops, i.e. air-assisted sprayers travelling along crop's rows (trees, vines, bushes) and applying pesticide onto a vertical canopy wall.

However, from the above mentioned research works it can be drawn

that the major factors influencing the profitability of introducing precision technologies on sprayer equipment are in general: the investment costs of the technology; the amount and value of the inputs saved per unit of area; the spatial variability of the inputs needed by the crop; the size of the farm area operated by the equipment.

CHAPTER 2

Methodology development for hyperspectral disease detection

2.1 Theoretical background

2.1.1 Hyperspectral disease detection

Disease detection and monitoring in greenhouses are conducted manually by experts and for this reason are limited to human boundaries: resource availability, low sampling rate, non-uniformity in performance and high monitoring costs (Schor et al, 2016). How it was explained in the previous chapter automation can have a positive impact also in disease detection and monitoring facilitating targeted and timely disease control which can lead to increased yield, improved crop quality and massive reduction in applied pesticides (see chapter 3). In perspective the less use of pesticide is correlated with a decreased risk for

environment and for human health (section 1.3).

In the study of disease and in general health status in plants, hyperspectral imaging is gaining considerable interests (see section 2.3.1 for technical details). These techniques are used in remote and proximal sensing experiments in field agriculture, but also in monitoring the quality of food. The implementation of such system in robotic application remains not available in the market due to are technologies still expensive and immature for the real field application. It is important to underline that both legislation and technical advancement are pushing to the development and the application of techniques for reducing the impact of pesticides for the farm management.
In the hyperspectral imaging, the spectral reflectance of each pixel is acquired for a range of wavelengths in the electromagnetic spectra. The resulting information is a set of pixel values at each wavelength of the spectra in the form of an image. Spectroscopy and imaging techniques are unique disease monitoring methods which can be useful for PPM, the spectroscopic and imaging techniques could be integrated with an autonomous agricultural vehicle that can provide information on disease detection at early stages to control the spread of plant diseases Sankaran et al (2010).
Plants interact with electromagnetic radiation in different ways: absorption, reflection, emission, transmission and fluorescence. Light measurement techniques are very helpful for detecting these properties. The assumption of the foliar disease detection with light measurement starts from the hypothesis that diseased plants interact with lights differently than healthy ones.
When we measure the light coming from the plant, considering a healthy one, we are reading the *spectral signature* of the plant itself (Lee et al, 2010). Leaf reflectance is the proportion of the irradiated light reflected by the leaf.
In the study of disease hyperspectral imaging is used in remote and proximal sensing experiments in field agriculture, but also in monitoring the quality of food. The spectral reflectance of each pixel is ac-

quired for a range of wavelengths in the electromagnetic spectra with the resulting information of a set of pixel values at each wavelength of the spectra in the form of an image.

2.1.2 Wavelengths selection

One of the main issues in hyperspectral imaging for plant disease detection are the selection of specific bands which have the information about the symptoms of the disease on the leaf. The main approach to study the electromagnetic spectra of different symptoms are statistical classification algorithms. For example Bravo et al (2003) develop a discrimination model using quadratic discriminant analysis (QDA) investigating hyperspectral imaging for the early detection of rust disease in winter wheat. Moshou et al (2004) for the same crop but studying yellow rust implemented a method based on QDA, self-organizing map (SOM), and multilayer perceptrons based artificial neural network. Zhang et al (2006) collect hyperspectral data from *Phytophthora infestans* in tomato field, they used principal component analysis and cluster analysis for the elaboration obtaining remarkable results in detection middle to late stage symptoms. Zhang et al (2006) stated that understanding the light responses of unique biological features might increase discrimination accuracy since one should then be able to reduce the impact of soil background on spectral measurements, utilizing the most sensitive wavelengths to discriminate healthy and diseased tomatoes.
Malthus and Madeira (1993) studied the effect of *Vicia faba* leaves infected by *Botritis fabae*. They found a significant influence of the response to light in the visible part of the spectrum and a decrease of the response in near infrared for diseased plants. Both responses are attributable to the collapse of leaf cell structure as the fungus spread. Recently Lee et al (2016) applied hyperspectral imaging to detect cucumber green mottle mosaic virus on seeds of the "Sambok Honey" cultivar. To analyse the data chemometric models were used in particular partial least-squares discriminant analysis (PLS-DA) and Least-

squares support vector machines (LS-SVM) method. Authors propose that phenolic components are the key factor for discriminating between virus infected and healthy seeds because major peaks of beta coefficients were consistent with the absorption peaks of the phenolic components. During the experiment it was possible to localize the symptoms in the seeds: physiochemical changes in seeds were generally located in the centre.
Zhang et al (2003) conduct an experiment in remote sensing on tomatoes. The experiment was conducted to collect the canopy spectral reflectance of tomato plants in a diseased field. The spectral reflectance of the field samples indicated that the near infrared region was much more valuable than the visible range comparing healthy and diseased plants. The developed methods were based on minimum noise fraction transformation (MNF), multi-dimensional visualization, pure pixels endmember selection and spectral angle mapping (SAM).

Relatively few studies have been conducted on the spatial informations obtainable with hyperspectral images. The combination of spacial and spectral informations can give important improvement in the symptoms recognition.
Recent advances in hyperspectral remote sensor technology allow the simultaneous acquisition of hundred of spectral wavelengths for each image. The high spectral resolution is coupled with an high spatial resolution of the sensor which enable also the analysis of small spatial structures in the image. During the last decade a lot of scientists have been build accurate hyperspectral classifiers, most of them are based on remote sensing for the classification of structures in the view. Among others signal processing methods the feature reduction and Bayesian models have been reported (Landgrebe, 2005). Ham et al (2005) investigate two approaches based on the concept of random forests classifiers. The classifier proposed incorporates bagging of training samples and adaptive random subspace feature selection within a binary hierarchical classifier. Ratle et al (2010) used a semi-

supervised neural networks for efficient hyperspectral image classification. Also kernel methods have been investigated (Camps-Valls et al, 2009).

2.1.3 Principles of the line imaging spectrography

Line Imaging Spectrography (LIS) is the simultaneous acquisition of different spectra from reflective points in the sensor's field of view placed along the line. It gives us an high spatial resolution enabling the detection of symptomatic areas along a spatial range and not like a spectrophotometer which has only one sensible point for the acquisition (Bravo, 2006).
In LIS the light is gathered by an objective and brought to a very narrow slit. After collimating the light in a parallel beam, a first prism diffracts incoming radiation and projects this light a grating device. Owing to the specific inclination of the diffracted light compared to position of the grating device, light is being decomposed into its spectrum. The decomposed light is oriented along the optical axis of the spectrograph where a CCD or CMOS sensor is used to collect the incoming light and estimate its intensity at every waveband in the sensitive range of the instrument.
To record the data the condition is that the incoming light have to cover the sensitive range of the camera (in our case 400 - 1000 nm); the camera itself should be large enough to collect all spectral radiation of interest maintaining a high signal to noise ratio. If the f-stop number[1] is too small the spectrograph will be filled by light, causing unwanted reflections inside the optical instrument.

The hypercube

The movement of the hyperspectral camera along the x axis of the acquisition permit to generate an image with three dimensions called

[1]The f-stop number (focal ratio) expresses the diameter of the spectrograph aperture in terms of the effective focal length of the lens. For example f/8 represents an aperture diameter that is one-eight of the focal length.

hypercube. The output of the camera is an image with composed of an x, y, and z axis. In x and y axis is stored the spatial information of the acquisition and in particular y is fixed and depends on the sCMOS sensor size, x varies with the angle covered during the acquisition. In z are stored the informations relative to the electromagnetic spectrum intensity. In figure 2.1 there is a representation of the hypercube in which are stored the spatial and spectral informations.
As example the file generated by the camera is encoded in Band Interleaved by Line typology. To read this type of file additional information is needed, such as the numbers of rows, columns, and bands. This information are supplied in a header file, when the file is loaded is a multidimensional array. In the spectral domain pixels are represented by vectors for which each component is a measurement corresponding to specific wavelengths. The size of the vector is equal to the number of spectral bands that the sensor collects. With increasing dimensionality of the images in the spectral domain, theoretical and practical problems arise (Fauvel et al, 2013). In high-dimensional spaces normally distributed data have a tendency to concentrate in the tails which is in contradiction with its bell-shaped density function (Jimenez and Landgrebe, 1998).

Optical principle of the hypercube building

The camera output is one line of image at a time, the x dimension is recorded for every frame, and the y dimension is created by moving the target or the sensor depending on the system type. It is easy to understand that the formation of the hypercube, how is conceived, can be affected of distortions of the spatial axes in comparison with the reality.
To maintain the proportion of the image it is possible to define the speed of the target or the frame rate. Usually to perform the aspect ratio adjustment it possible to follow the following steps:

- image an object of a known size, with a simple geometry, such

as a circle or a square

the larger the object the better as long as the object is within the field of view of the sensor

the object should e something that can be easily seen by the sensor in use

- open the recorded image in a viewer
- measure the width (x) and the height (y) of the object in pixels in the image;
- calculate the ratio x/y

  if the ration is smaller than 1 either the scanning speed is too fast or the frame rate is too slow

  if the ratio is greater than 1, the scanning speed is too slow or the frame rate is too fast

To change the frame rate of the sensor it is necessary to multiply the current frame rate with the calculated multiplier, and set the result as the new frame rate; conversely if we want change the scanning speed it is necessary to divide the current scanning speed with the calculated multiplier and set the result as the new scanning speed.

2.1.4 Image processing

The hypercube in its spacial dimension can be treated with digital image processing techniques. These digital methods are characterized by the need for extensive experimental work to establish the viability of proposed solution to a given problem Gonzalez et al (2003). An important characteristic underlying the design of image processing systems is the significant level of testing and experimentation that normally is required before arriving at an acceptable solution.

Digital image representation A single layer of the hypercube is a two-dimensional function, $f(x, y)$, where x and y are spatial coordinates,

and the amplitude of f at any pair of coordinates (x, y) is called intensity. The term gray level is used often to refer to the intensity of monochrome images. In a RGB color system a color image consists of three individual monochrome images, referred to as the red (R), green (G) and blue (B) primary images. When x, y, and f are all finite, discrete quantities, we call the image a digital image. Each point defined from the coordinate x and y is commonly denoted as pixel.
Assuming that an image $f(x, y)$ is sampled so that the resulting image has M rows and N columns, we say that the image is of size $M \times N$.

$$f(x,y) = \begin{bmatrix} f(0,0) & f(0,1) & \dots & f(0,N-1) \\ f(1,0) & f(1,1) & \dots & f(0,N-1) \\ \vdots & \vdots & & \vdots \\ f(M-1,0) & f(M-1,1) & \dots & f(M-1,N-1) \end{bmatrix}$$

Expressing the sampling and quantization in formal mathematical terms let Z and R denote the set of real integers and the set of real numbers, respectively. The sampling process may be viewed as partitioning xy plane into a grid, with the coordinates of the center of each grid being a pair of elements from Cartesian product. Z^2, which is the set of all ordered pairs of elements (z_i, z_j), with z_i and z_j being integers from Z. Hence, $f(x, y)$ is a digital image if (x, y) are integers from Z^2 and if f is a function that assigns a grey-level value (real numbers from R) to each pair of coordinates (x, y).

Spatial filtering concepts In image analysis the monochromatic image represents the input of signal processing algorithms from which it possible to obtain an image or a set of characteristics or parameters related to the image. If from an image we decide to analyse sub-images we talk of *regions of interest* (ROIs). Different operations can be performed on an image following the ROI criteria and applying different methodologies.
The digital filter concept was used to study our collection of images.

The concept of linear filtering has its roots in the use of the Fourier transform for signal processing in the frequency domain. Digital linear filtering is the operation of multiplying each pixel in the neighbourhood by a corresponding coefficient and summing the results to obtain the response at each point. The application of the filter is based on a mask or window of significant amplitude which perform the operation along the image of interest. There are two closely related concepts very important to perform the linear spatial filtering: the first one is the *correlation*; other is *convolution*. Correlation is the process of passing the mask w by the image array f; convolution is the same process, except that w is rotated by 180°prior to passing it by f. The correlation of a filter mask $w(x, y) \star f(x, y)$, is given by the expression

$$w(x,y) \star f(x,y) = \sum_{s=-a}^{a} \sum_{-b}^{b} w(s,t) f(x+s, y+t)$$

This equation is evaluated for all values of the displacement variables x and y so that elements of w visit every pixel in f, which we assume has been padded appropriately. Constant a and b are given by $a = (m-1)/2$ and $b = (n-1)/2$. For notational convenience, we assume that m and n are odd integers.
In a similar manner, the convolution of $w(x, y)$ and $f(x, y)$, denoted by $w(x, y) \star f(x, y)$, is given by the expression

$$w(x,y) \star f(x,y) = \sum_{s=-a}^{a} \sum_{-b}^{b} w(s,t) f(x-s, y-t)$$

where the minus signs on the right of the equation rotate the f of 180°. The nonlinear spatial filtering is based on neighbourhood operations also, and the mechanics of sliding the center point of an $m \times n$ filter through an image are the same previous discussed but, nonlinear spatial filtering is based on nonlinear operations. It means that whereas linear spatial filtering is based on computing the sum of products (linear operation), nonlinear filtering operations involving the pixels in the

neighbourhood encompassed by the filter. For example, letting the response at each center point be equal to the maximum pixel value in its neighbourhood is a nonlinear filtering operation.
An important consideration implementing neighbourhood operations for spatial filetering is the issue of what happens when the center of the filter approaches the border of the image. Considering simple square mask of size $n \times n$ at list one edge of such mask will coincide with the border image when the center of th mask is a a distance of $(n - 1)/2$ pixels away from the border of the image. The simple and most effective way to obtain a perfectly filtered result is to accept a somewhat smaller filtered image by limiting the excursions of the center of the filter mask to a distance no less than $(n - 1)/2$ pixels from the border of the original image (Gonzalez and Woods (2008)). In such way the resulting filtered image will be smaller than the original, but all the pixels in the filtered image will have been processed by the entire mask. This was the approach developed during the experiment.

2.1.5 Spectral image processing

Studying the hypercube from the z axis it is possible to read the intensity of the spectrum along the sensibility of the sensor. It's very important to note that the different parts of the camera system can fade in their performance over time, temperature or environment in general. This is a crucial point in the spectra acquisition, one of the most important factor is the stability of the light source during image acquisition. If the light source should render unstable due to the bulb itself or the associated power supply, than any image acquired will suffer from undesidered artefacts.
It is therefore important to conduct a acquisition procedure where the sensitivity towards these external factors are minimized. The best approach is to acquire white reference and dark current as often as possible to capture any drift (Arngren, 2011).

Dark signal subtraction Every sensor when is not illuminated shows a dark current, which is mostly due to temperature dependant excitation. The noise created by the current can cause a bias in the calculation, it is important to subtract this signal from raw data before the processing.
To estimate this signal is possible to cover the objective or close the shutter and acquire a set of a completely dark images at the same exposure time and gain as the measurements. At the same time is also possible to acquire one dark image for each measurement.
The dark signal correction can be expressed as in the following equation:

$$A(s,\lambda) = R(s,\lambda) - dc \tag{2.1}$$

where A is the dark current corrected image, R is the raw image, dc represents the dark current, s is the observation number (camera pixel coordinate) along spacial dimension, λ represents the camera channel dedicated to the spectral information.
In our case the output of the camera is an hyperspectral data cube or hypercube with i, j, k coordinates. If we have a reference cube X_{ref} and a dark current cube X_{dark}. Using these two hyperspectral images a single compensated line scan image can be calculated from the measured image X_{means} by

$$X_{ijk}^{comp} = \frac{X_{ijk}^{means} - X_{jk}^{dark}}{X_{jk}^{ref} - X_{jk}^{dark}} \forall i \tag{2.2}$$

Data normalization Reflection variability between images and irradiance differences for all measured spectra in the same acquisition give the need to normalize the data acquired. It means that the different illumination due to scene variation may cause the variation of a camera pixel at a certain wavelength.
Leaf reflectance can be calculated using the proportion of reflected light, at a certain waveband, to the total incoming light of the leaf. It should be noted that it is not feasible to measure this incoming light

on each leaf. By employing the gray 50% reflectance standard and assuming that illumination conditions are equal in the same image self-reflectance can be estimated. Using the dark corrected image (A) calculated by the equation 2.1, the reflectance-normalized matrix B can be defined in percent through the following:

$$B(s, \lambda) = \frac{A(s, \lambda)}{A(P_{ref}, \lambda)} \tag{2.3}$$

where s is the observation number along the spatial axis, λ is the wavelength, and P_{ref} is the position of the reflectance standard along the spatial axis.

2.1.6 Exploratory data analysis

After the data normalization all the wavelengths intensity are in the same range. This condition permits to compare the different groups of spectra trying to understand patterns eventually present in the data. This process can be defined as *exploratory data analysis*. Tukey (1977) provided a detailed description for exploratory data analysis (EDA) as a numerical detecting work. This type of analysis permits to examine the data without any preconceived ideas about the phenomena being studied. The EDA preliminary involve visualizing the relationship between samples and between variables without assign them to groups.
Among the EDA techniques an important one is the principal component analysis (PCA). PCA is the most flexible general purpose approach, but suffers when there are many different groups Brereton (2009). Nevertheless, PCA is still an excellent method for preliminary visualization, natural scientists of all disciplines, from biologists, geologists, and chemists have caught on to these approaches over the past few decades.
The main purpose of the PCA is to reduce the dimensionality from p to d, where $p < d$, at the same time accounting for as much of the variation in the original data set as possible. PCA involves an abstract mathematical transformation of the original data matrix. In addition,

the observations in the new principal component space are uncorrelated. The hope is that we can gain information and understanding of the data by looking at the observations in the new space. In order to explain the statistical method, the sample covariance matrix algorithm will be presented.

PCA using the sample covariance matrix We start with the centered data matrix X_c that has dimension $n \times p$. The defined matrix is centered about the mean of the observation for the determined variable. Then we form the sample covariance matrix S as

$$S = \frac{1}{n-1} X_c^T X_c$$

where T denotes the matrix transpose. The jk-th element of S is given by

$$s_{jk} = \frac{1}{n-1} \sum_{i=1}^{n} (x_{ij} - \bar{x_k}); \; j,k = 1,\ldots,p$$

with

$$\bar{x}_j = \frac{1}{n} \sum_{i=1}^{n} x_{ij}$$

The next step is to calculate the eigenvectors and the eigenvalues of the matrix S. The eigenvalues are found by solving the following equation for each l_j, $j = 1,\ldots,p$

$$|S - lI| = 0 \tag{2.4}$$

where I is a $p \times p$ identity matrix and $|\bullet|$ denotes the determinant. The equation 2.4 produces a polynomial equation of degree p.
The eigenvectors are obtained by solving the following set of equation for a_j

$$a_i a_i^T = 1$$

$$a_j a_i^T = 0$$

for $i,j = 1,\ldots,p$ and $i \neq j$
A major result in matrix algebra shows that any square, symmetric,

non-singular matrix can be transformed to a diagonal matrix using

$$L = A^T S A$$

where the columns of A contain the eigenvectors of S, and L is a diagonal matrix with the eigenvalues along the diagonal. By convention, the eigenvalues are ordered in descending order $l_1 \geq l_2 \geq \cdots \geq l_p$, with the same order imposed on the corresponding eigenvectors.
We use the eigenvectors of S to obtain new variables called *principal components* (PCs). The j-th PC is given by

$$z_j = a_j^T (x - \bar{x});\ j = 1, \ldots, p \tag{2.5}$$

and the elements of a provide the weights or coefficients of the old variables in the new PC coordinate space. It can be shown that the PCA procedure defines a principal axis rotation of the original variables about their means, and the elements of the eigenvector a are the direction cosined that relate the two coordinate systems. Equation 2.5 shows that the PCs are linear combinations of the original variables.
We transform the observations to the PC coordinate system via the following equation

$$Z = X_C A \tag{2.6}$$

The Z matrix contains the *principal component scores*. Note that these PC scores have zero mean and are uncorrelated. We could also transform the original observations in X by similar transformation, but the PC scores in this case will have mean $\bar{z}$. We can invert this transformation to get an expression relating the original variables as a function of the PCs, which is given by

$$x = \bar{x} + Az$$

To summarize: the *transformed variables* are the PCs and the individual *transformed data values* are the PC scores.

2.1.7 Two class classifier

The purpose of two class classifier is reformulate the problem as a classification problem, which involve the use of the samples to determine whether there is a relationship between interesting properties of the samples and the analytical data, and if there is so, to determine what this relationship is, in the form of a mathematical model. Once the model is set up, the objective is to determine is a new sample belongs to a determined group.
There are numerous approaches in the literature to classify between two or more groups. During the work it was used a two class classifier, linear discriminant analysis.

Linear discriminand analysis (LDA) Linear discriminant analysis is a method used in statistics, pattern recognition and machine learning to find a linear combination of features which characterized or separates two or more classes of objects or events. The LDA takes the different variance of each variable into account, but has an additional property that it also takes into account the correlation between the variables: if there are 20 variables, for example, and 19 convey similar information will be correlated and as such should not be weighted too much.
The characteristic of the LDA is to produce a linear boundary between two classes. The algorithm used during our work is the Fisher one (Fisher, 1936), to evaluate the distance to each class centroid a measured distance called Mahalanobis was used:

$$d_{ig}^2 = (x_i - \bar{x}_g) S_p^{-1} (x_i - \bar{x}_g)'$$

where S_p is the pooled variance-covariance matrix, calculated for two classes as follows:

$$S_p = \frac{(I_A - 1)S_A + (I_B - 1)S_B}{I_A + I_B - 1}$$

and where S_g is the symmetric variance-covariance matrix for class g of dimension $J \times J$ whose diagonal elements correspond to the variance of each variable and whose off-diagonal elements are the corresponding covariance between each variable. The Mahalanobis distance based on variance-covariance matrix is based on the entire dataset, rather than for each class independently.
The classifier was created assuming that the model has the same covariance matrix of each class; only the means vary. It was computed the sample mean of each class. Then the sample covariance by first subtracting the sample mean of each class from the observations of that class, and taking the empirical covariance matrix of the result.
The weighted classifier was built supposing M is a N-by-K class membership matrix: M_{nk} = 1 if the observation n from class k; M_{nk} = 0 otherwise.
The estimate of the class mean for unweighed data is

$$\hat{\mu}_k = \frac{\sum_{n=1}^{N} M_{nk} x_n}{\sum_{n=1}^{N} M_{nk}}$$

The unbiased estimate of the pooled-in covariance matrix for unweighed data is

$$\hat{\Sigma} = \frac{\sum_{n=1}^{N} \sum_{k=1}^{K} M_{nk} (x_n - \hat{\mu}_k)(x_n - \hat{\mu}_k)^T}{N - K}$$

After the determination of the model it was examined the resubstitution error how difference between the response training data and the predictions the classifier makes of the response based on the input training data. If the resubstitution error is high, you cannot expect the predictions of the classifier to be good. The confusion matrix shows how many errors, and which types, arise in resubstitution. When there are K classes, the confusion matrix R is a K-by-K matrix with $R(i, j)$ equal to the number of observations of class i that the classifier predicts to be of class j.
In detail for the LDA we consider a set of n p-dimensional observations $x_1, \ldots, x_n$, with n_1 samples labeled as belonging to class 1 (λ_1)

and n_2 samples as belonging to class 1 (λ_2).
We will denote the set of observation in the i-th class as Λ_i. Given a vector w with unit norm, we may form a projection of the x_i onto a line in the direction of w using:

$$y = w^T x$$

where T denotes the matrix transpose. We want to choose w in order to provide a linear mapping that provides maximal separation of the two classes. One natural measure of separation between the projected points y_i is the difference between their means. We may calculate the p-dimensional sample mean for each class using the following equation

$$m_i = \frac{1}{n_i} \sum_{x \in \Lambda_i} x$$

the sample mean for the projected points is given by

$$\tilde{m}_i = \frac{1}{n_i} \sum_{y \in \Lambda_i} y = \frac{1}{n_i} \sum_{x \in \Lambda_i} w^T x = w^T m_i$$

we can use the last equation to measure the separation of the means for the two classes

$$|\tilde{m}_1 - \tilde{m}_2| = |w^T (m_1 - m_2)|$$

where $|\bullet|$ denotes the determinant. To obtain good class separation, and hence a good classification performance, we want the separation of the means to be as large as possible standard deviation for the observation in each class. We will use the scatter as our measure of the standard deviations. The scatter for the i-th class of projected data points is given by:

$$\tilde{s}_i^2 = \sum_{y \in \Lambda_i} (y - \tilde{m}_i)^2$$

We define the total within-class scatter to $\tilde{s}_1^2 + \tilde{s}_2^2$. The LDA is defined as the vector w that maximizes the function:

$$J(w) = \frac{|\tilde{m}_1 - \tilde{m}_2|^2}{\tilde{s}_1^2 + \tilde{s}_2^2}$$

A little bit of linear algebra manipulation (Duda et al, 1973) allow us to white the solution of the maximization as:

$$w = S_w^{-1}(m_1 - m_2)$$

where S_w is the within-class scatter matrix defined by:

$$S_w = S_1 + S_2$$

and

$$S_i = \sum_{x \epsilon \Lambda_i} (x - m_i)(x - m_i)^T$$

Note that the matrix S_w is proportional to the sample covariance matrix for the pooled p-dimensional data. Interestingly, it turns out that the LDA is the linear mapping with the maximum ratio of between-class scatter S_B to within-class scatter, where

$$S_B = (m_1 - m_2)(m_1 - m_2)^T$$

The input vectors data now reside in one dimension.

2.1.8 Applied technique for data reduction

The purpose of the experiment is the definition of a certain number of wavelengths, to selectively choose the channels of interest data processing exploited the binomial coefficient technique. The number of ways of picking k unordered outcomes from n possibilities, known as binomial coefficient (Brualdi, 1977) or choice number and read "n

choose k", is described by this equation:

$$ {}_nC_k \equiv \binom{n}{k} \equiv \frac{n!}{k!(n-k)!} $$

where $n!$ denotes a factorial. For example, considering $\binom{4}{2}$ combinations of two elements out of the set $\{1,2,3,4\}$, namely $\{1,2\}$, $\{1,3\}$, $\{1,4\}$, $\{2,3\}$, $\{2,4\}$, and $\{3,4\}$. These combinations are known as *k-subsets*.
In detail the binomial coefficients $\binom{n}{k}$ for all nonnegative integers k and n, is equal to zero if $k > n$ and that $\binom{n}{0} = 1$ for all n. If n is positive and $1 \leq k \leq n$, then

$$ \binom{n}{k} = \frac{n!}{k!(n-k)!} = \frac{n(n-1)\dots(n-k+1)}{k(k-1)\dots 1} \tag{2.7} $$

but we have that

$$ \binom{n}{k} = \binom{n}{n-k} $$

This relation is valid for all integers k and n with $0 \leq k \leq n$. We also derived Pascal's formula, which asserts that

$$ \binom{n}{k} = \binom{n-1}{k} + \binom{n-1}{k-1} $$

By using Pascal's formula and the initial information

$$ \binom{n}{0} = 1 \text{ and } \binom{n}{n} = 1, \ (n \geq 0) $$

the binomial coefficients can be calculated without recourse to the formula 2.7. When the binomial coefficients are calculated in this way, the results are often displayed in an infinite array known as *Pascal's triangle* (Pascal, 2011):

n \ k	0	1	2	3	4	5	6
0	1						
1	1	1					
2	1	2	1				
3	1	3	3	1			
4	1	4	6	4	1		
5	1	5	10	10	5	1	
6	1	6	15	20	15	6	1

Each entry in the triangle, other than those equal to 1 occurring on the boundary of the triangle, is obtained by adding together two entries in the row above: the one directly above and the one immediately to left. This is in accordance with Pascal's formula. For instance, in row $n = 6$, we have

$$\binom{6}{3} = 20 = 10 + 10 = \binom{5}{2} + \binom{5}{3}$$

Many of the relations involving in binomial coefficients can be discovered by the examination of Pascal's triangle.

2.1.9 Robot position and rotation

During the experimentation a robotic manipulator was used. To perform the camera acquisitions it was necessary the study of robot kinematic. The position and orientation of a rigid body in space are collectively termed the *pose*. In these terms the robot kinematics describes the pose, velocity, acceleration, and all higher-order derivatives of the pose of the bodies that comprise mechanism.

A coordinate reference frame i consists of an origin, denoted O_i, and a triad of mutually orthogonal basis vectors, denoted ($\hat{x}_i$, $\hat{y}_i$, $\hat{z}_i$), that are all fixed within a particular body. The pose of a body will always be expressed relative to some other body, so it can be expressed as the pose of one coordinate frame relative to another.

The position of the origin of coordinate frame i relative to coordinate frame j can be denoted by 3×1 vector

$$ {}^{j}p_i = \begin{pmatrix} {}^{j}p_i^x \\ {}^{j}p_i^x \\ {}^{j}p_i^x \end{pmatrix} $$

The components of this vector are the Cartesian coordinates of O_i in the j frame, which are the projections of the vector ${}^{j}p_i$ onto the corresponding axes.
To define the rotation matrices we have the coordinate frame i relative to coordinates frame j can be denoted with $({}^{j}\hat{x}_i\ {}^{j}\hat{y}_i\ {}^{j}\hat{z}_i)$, which when written together as a 3×3 matrix known as the rotation matrix. The components of ${}^{j}R_i$ are the dot products of basis vectors of the two coordinate frames.

$$ {}^{j}R_i = \begin{pmatrix} \hat{x}_i \cdot \hat{x}_j & \hat{y}_i \cdot \hat{x}_j & \hat{z}_i \cdot \hat{x}_j \\ \hat{x}_i \cdot \hat{y}_j & \hat{y}_i \cdot \hat{y}_j & \hat{z}_i \cdot \hat{y}_j \\ \hat{x}_i \cdot \hat{z}_j & \hat{y}_i \cdot \hat{z}_j & \hat{z}_i \cdot \hat{z}_j \end{pmatrix} $$

Because the basis vectors are unit vectors and the dot product on any two unit vectors is the cosine of the angle between them, the components are commonly referred to as direction cosines.
An elementary rotation of frame i about the ${}^{j}z_i$ axis through and angle θ is

$$ R_Z(\theta) = \begin{pmatrix} \cos\theta & -\sin\theta & 0 \\ -\sin\theta & \cos\theta & 0 \\ 0 & 0 & 1 \end{pmatrix} $$

while the same rotation about the $\hat{y}_j$ axis is

$$ R_Y(\theta) = \begin{pmatrix} \cos\theta & 0 & \sin\theta \\ 0 & 1 & 0 \\ -\sin\theta & 0 & \cos\theta \end{pmatrix} $$

and about $\hat{x}_j$ axis is

$$R_X(\theta) = \begin{pmatrix} 1 & 0 & 0 \\ 0 & \cos\theta & -\sin\theta \\ 0 & \sin\theta & \cos\theta \end{pmatrix}$$

Rotation matrices are combined through simple matrix multiplication such that the orientation of frames i relative to frame k can be expressed as

$$^{k}R_i = {}^{k}R_j^{j}R_i \tag{2.8}$$

In summary, ${}^{j}R_i$ is the rotation matrix that transforms a vector expressed in coordinate frame i to a vector expressed in coordinate frame j.

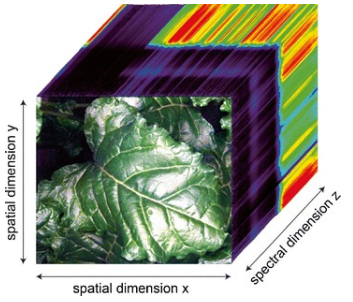

(a) *Hypercube scheme*

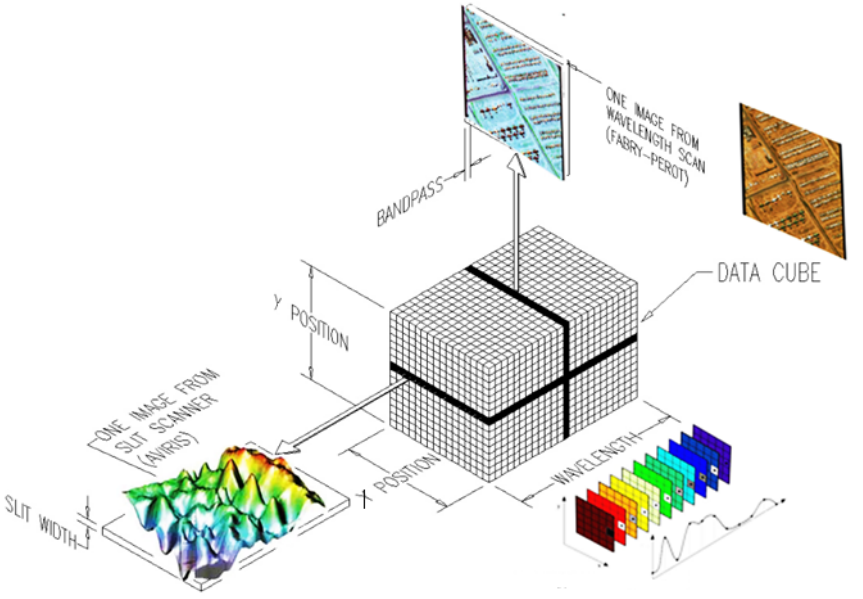

(b) *Hypercube data storage representation*

Figure 2.1: *Hypercube representation with the scheme of the data storage system.*

2.2 Plants and diseases studied

During the experimentation cucumber plants (*Cucumis sativus* L.) were studied, the disease symptomatology analysed is caused by powdery mildew during the preliminary experiment and cucumber green mottle mosaic virus (CGMMV) in the main investigation.
Cucumbers are from the family of *Cucurbitacea* taxonomy isolated from other families. The family *Cucurbitaceae*, consists of about 120 genera and more than 800 species (Welbaum, 2015).
Commercial cucumber cultivars are warm-season, frost-sensitive annuals. Usually cucumbers grow up to 2 m tall and 5 m long with a climbing habit. *C. sativus* is a morphologically variable annual herbaceous climber. The stems are prostate, angular, and covered in white pubescence. Stipulas are absent, and the plant bears unbranched axillary tendrils up to 30 cm long 10 to 16 cm long petioles. The pubescent leaves are alternatively arranged on 10-16 cm long petioles, simple, basally cordate, and apically acute whit 3-7 palmate lobes (Mnzava and Ngwerume, 2004; Zomlefer, 1994).
Cucumber plants exhibit monoecious (separate male and famale flowers on a plant), andromonoecius (separate perfect and male flowers on the same plant), or gynoecius (all female) sex expression. The expression can be controlled by genetics or chemicals.

Flowers occur at the nodes, staminate in clusters or singly with only one flower in a cluster opening at a time. Flowers are open for a single day and if not adequately pollinated rapidly abort. The fruit is an indehiscent cylindrical berry with many seeds. They can be spherical, blocky, oblong or elongated in shape and variable size. Cucumber are glabrous, and can be smooth or warty, yellow or green, ranging from 5-100 cm long and weight 50 g to 4 kg. Each plant produces up to 25 fruits. Cucumber fruits are consumed immature when their flavour is mild and seeds are small and underdeveloped.

Cucumbers have an important role in agricultural economy, they

are consumed raw or pickled. Mature uncooked cucumbers bring relief for individuals suffering from celiac disease and promote skin health. The fruit is also valuted in the cosmetic industry, used to soften the skin.
The seed can be used to expel parasitic worms. The seedlings are toxic and should not be consumed.
Cucumber growing is very important because it has a high rate of consumption; with reference to the World market consumer from 1970's preference and per-capita use of pickling cucumbers began to increase. Analysing FAO (2016a) statistics the world production of cucumber increased in the last 30 years of 6 times (figure 2.2).

Total world production of cucumbers and gherkins in 2011 was estimated to be approx 2 million hectares. Compared with other vegetables, cucumber occupies fourth place in importance in the world, following tomato, cole crops, and onion. The best world producer is China with the 34% of total production.

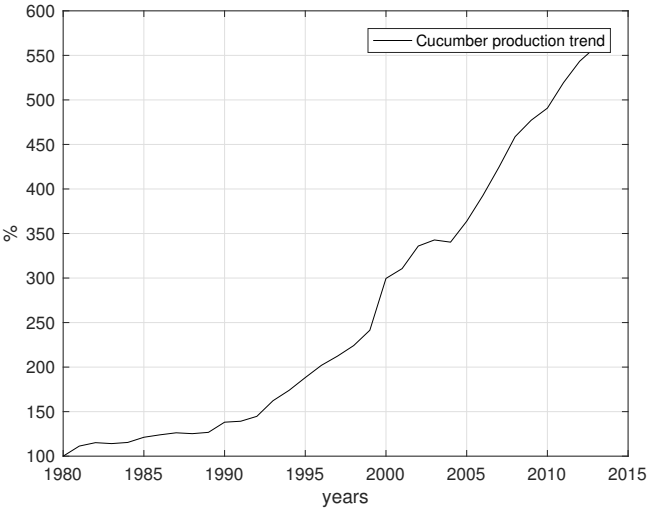

Figure 2.2: *Cucumber production trend indexed in 1980. Elaboration of FAO (2016a) statistics.*

2.2.1 Powdery mildew on cucumbers

Powdery mildew fungi are obligate plant pathogens that attack approximately 10000 species of plans belonging to more than 1600 genera (Agrios, 2005). P. mildew fungi obtain their nutrients from living cells of their host plants through feeding organs called haustoria.
Powdery mildew appears as spot patches of a white to greyish, powdery, mildewy growth on young plant tissues or as entire leaves and other organs being completely covered by the white powdery mildew.

Powdery mildew fungi are very common and severe in warm, dry

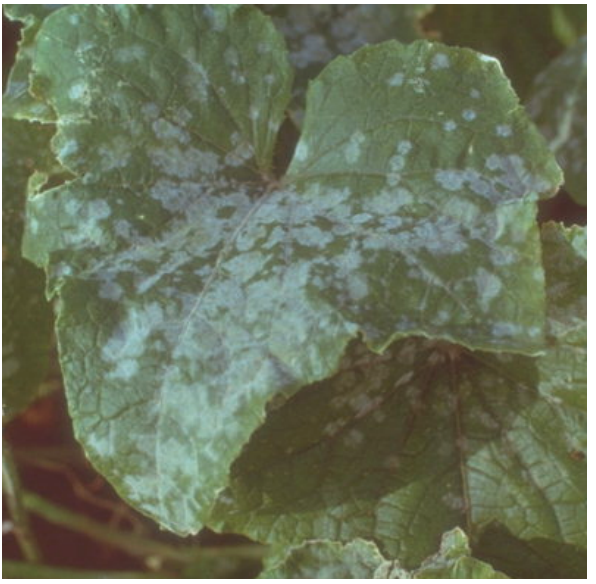

Figure 2.3: *Powdery mildew symptoms on Cucumber plants (INRA, 2016).*

climates, because their spores can be released , germinate, and cause infection even when there is no film of water on the plant surface as log as the relative humidity in the air is fair high. growth on young plant tissues or as entire leaves and other organs being completely covered by the white powdery mildew. The control of this pathogen is difficult some of them have develop resistance and are no longer controlled by some systemic fungicides.
Powdery mildew is one of the most important disease in cucumber (fig-

ure 2.3) with downy mildew and damping-off, under field and greenhouse conditions in most areas of the world. This disease is a major production problem due to reduction of yield, decrease in the size or number of fruit or decrease in the length of the harvest period. Premature senescence of infected leaves can result in reduced market quality because fruit become sunburnt or ripen prematurely or incompletely.
Among others the pathogen in cucumber is *Erysiphe cichoracearum* and *E. polygoni*, other are *Podosphaera fuliginea* also known as *P. xanthii*.
Powdery mildew develops on both leaf surfaces, petioles, and stems. The growth is primarily asexual through spores called conidia. It usually develops first on crown leaves, on shaded lower leaves and on leaf undersurfaces. Usually older plants are affected first, whit the infection leaves wither and die.

2.2.2 Cucumber green mottle mosaic virus (CGMMV)

Cucumber green mottle mosaic virus (CGMMV) is one of the most important viruses that exert influence, such as serious distortion and decomposition on the plant family Cucurbitaceae. According with Agrios (2005), cucumber mosaic virus occur worldwide, infects more different kinds of plants than any other virus, and causes mosaics, stunting of plants, and leaf and fruit malformations. Cucumoviruses are very infective and can be transmitted by insects like aphids, from infected seeds or mechanically handling the plants.
The virus infects and multiplies in phloem and parenchyma cells. Virus particles may appear scattered in the cytoplasm, the vacuoles, and, possibly the nucleus, and they may be aligned in multiple files in the cytoplasm or in single file passing through plasmodesmata. The control of the virus is very difficult, it depends primarily on breeding and use of resistant varieties. Moreover continuous increase of the consumption and trade of seeds among nations have led to hight risk of spreading the disease (Lee et al, 2016).

(a) *Old leaf yellowing (PCA, 2016)*

(b) *Young leaf mottling and shape deformation (USDA, 2016)*

Figure 2.4: *CGMMV symptoms characteristics in cucumber leaves.*

Regarding the symptoms, cucumber mosaic affects plants by causing mottling or discolouration and distortion of leaves, flowers, and fruits (figure 2.4). Symptoms on young leaves are vein clearing and crumpling may be visible (figure 2.4b), while mature leaves may show mottling or mosaic patterns, or look pale, yellow, or bleached (figure 2.4a). Young seedling symptoms may be indistinct or difficult to recognise as being caused by a virus. In severe infections, embryonic leaves may become yellow, but symptoms may not be apparent until more mature leaves emerge The quantity and the quality of the yield is reduced. Already four or five days after inoculation the young developing leaves become mottled, distorted and wrinkled and their edges begin to curldownward. The dangerousness and the variability of the symptoms were the reason why we decided to study this disease.
Once a few plants have become infected with CGMMV, insect vectors and humans during their cultivating and handling of the plants spread the virus to many healthier plants. A study in India (Vani et al, 1993) has isolated CGMMV from river and irrigation water, indicating the virus can spread under natural conditions once plants in the field or greenhouse become infected.

The great symptoms variability - from colour variation to leaf shape

distortion - with the extreme pathogenicity and danger of the virus are the main reasons for the choice of this pathogen for the experimentation. Contextually the economic losses deriving from the disease are substantial and involve the whole Cucurbitaceae family.

2.3 Measurements setup

2.3.1 Image acquisition system

To conduct the experiment, it was used a hyperspectral camera manufactured by the SPECIM® company (figure 2.5). It is a line-scan camera sensitive from in the Vis-NIR range approx. 400 - 1000 nm. Compared to a multispectral camera in which we are able to acquire images in few discrete wavebands in hyperspectral cameras we cannot acquire an entire image at once. In fact, the camera is equipped of a high speed sCMOS sensor which permits an image frame-rate in the range of 1 to 100 Hz, this sensor has 1600 spatial pixels and 840 spectral channels. The spectrograph present inside the camera has a spectral resolution (FWHM) of 2.9 nm.
One important characteristic of the camera is the possibility to sample the light spectrum at steps of 0.63 to 5.07 nm. This peculiarity is given by the adjustable spectral binning. It means that we are able to bin the channels along the spectrum with two advantages, the former is adapt the sensibility of the sensor to our needs, the latter is the reduction of the quantity of data recorded with a resilience in the experiment setup. Another peculiarity of this system is the spacial binning properties, thanks to which it is possible to impose the resolution of the acquisition and the quantity of data recorded.
Exposure time range goes from 8.1 to 100 ms. An advanced optic system developed by Schneider® (Xenoplan™ 1.9/35 C-mount) is used to direct the light to the objective into the spectrograph.
The hyperspectral camera during the experiment was coupled with a scanner system controlled by the Lumo software. The servo motor permits to cover an arc with defining the starting and the ending position,

(a) *VIS-NIR Camera* **(b)** *Xenoplan™ 1.9/35*

Figure 2.5: *Camera equipment used during the experimentation*

contemporary it is possible to handle the speed of the acquisition.

2.3.2 Data acquisition system

The camera was connected with an high-resolution, high-speed PCI Express image acquisition device, the NI PCIe-1427. The shield has a pixel clock range from 20 MHz to 80 MHz, and it is able to process more than 200 MB s^{-1}. The image acquisition device was installed in a personal computer equipped with a 64 bit Microsoft® Windows® 7 Enterprise (SP1) operating system; 12 GB installed memory (RAM) and a processor Intel® Core™ i7-4770 CPU 3.40 GHz.
The computer was equipped with the Specim data recording application for hyper spectral image (HSI): Lumo Scanner. This application can control HSI and scanner, and store the data into the computer hard drive.
For the data elaboration was used a multi-paradigm numerical computing environment Matlab thanks to which all the algorithms were developed.

2.3.3 Robotic Manipulator

Robotic mechanisms are system of rigid bodies connected by joints (Siciliano and Khatib, 2008). The hyperspectral camera was mounted on a 6 degree of freedom manipulator (DOF) robotic manipulator Motoman MH5L. The manipulator and the hyperspectral camera were

physically integrated by a custom-made end-effector.
The manipulator has a payload of 5 kg with a repeatability of ±0.03 mm in reaching the position. The maximum speed reachable by the joints depends on which one is in movement and it vary from 270° s^{-1} to 720° s^{-1}.
To control the robotic manipulator kinematics an application was specially designed and developed. For the hyperspectral acquisition the software tool was thought to replicate and improve characteristics of the Lumo Scanner software. Specim software is able to control a servo motor which permit to establish a starting point and an ending point for the acquisition as well we implement in the custom-made application possibility to define a starting and an ending position for the scanning process. Furthermore, a manual movement with a defined angle to the right and to the left was implement. At the same time two *ex-novo* buttons were created to have a performing and accurate integration between the acquisition system and the manipulator: a robot homing button and an initial position one. The former permits to reach the homing position; the latter to reach the initial one from the manipulator.
An improvement for the human machine interface was made for the focusing button in which an integration between the Lumo Scanner software and the custom application was realized; furthermore, the possibility of defining the central position for the focusing function was integrated.

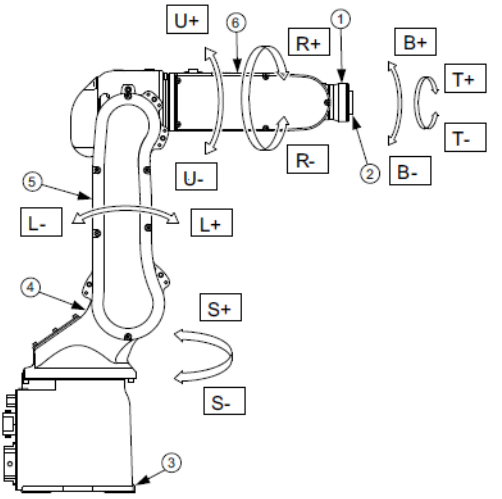

1	Wrist	4	Rotary head
2	Wrist flange	5	Lower arm (L-arm)
3	Robot base	6	Upper arm (U-arm)

(a) *Manipulator scheme*

(b) *Manipulator*

Figure 2.6: *The Motoman MH5L, the six DoF manipulator used during the experiment (Motoman, Germany)*

2.4 The first methodology developed: wavelengths of interest determination

2.4.1 ROI selection and spectra extrapolation

The first step for the analysis is the selection of the *region of interest* (ROI) from the hypercubes. During the experimentations two methods for the specta extrapolation were developed. The former fits with powdery mildew symptoms characteristics but, the latter fits with CGMMV symptoms but less with Powdery mildew ones.

Color code selection Contextually with the building of the hypercube the camera output includes a preview image. The file output is a classic three channels image; channels are customizable at will. For the ROIs selection a code of three numbers was used for each one of the classes analysed. The selection consists in painting the areas of interest by means of an imaging software tool (Paint.NET). During the selection the anti-aliasing system was disabled to have the certainty of a correct selection.

Spatial region selection The second methodology consists in the definition of four spatial coordinates in the spatial dimension (x, y) of the hypercube. The goal is to create a quadrilateral homogeneous region which is representative of the global condition of the leaf tissue.

The first method the selection is spatially limited and it doesn't cover a representative part of the leaf tissue leaving uncovered the study of CGMMV symptoms which are spread all around the leaf.

Regarding the second methodology exposed we can say that due to the manual selection of the region and the different leaf portion captured from the camera often the dimension of the region is variable among the classes and inside the classes considered. To overcome this inconvenient a sensitivity analysis will be presented on the window size.

2.4.2 Spectral normalization

Before each acquisition a white and a dark references were collected. The black reference was obtained by closing the shutter of the camera for 100 frames. White reference was acquired holding a white panel with 95% reflectance in front of the camera for at least 100 frames. The two reference were averaged along the y axis obtaining an average for the spatial dimension for all the 840 channels.

$$\text{Ref}_{j,z} = \frac{\sum_{i=1}^{n} \text{Ref}_{i,j,z}}{n} \tag{2.9}$$

where

Ref represents the dark or the white reference;

i is the x dimension of the hypercube which is dependant from the angle covered with the acquisition ($i = 1, 2, 3, \ldots, n$);

j is the y dimension of the hypercube, strictly connected whit the sensor characteristics;

z is dependant of the spectral sampling resolution of the hyperspectral camera.

The single reference spectrum after the selection of the correct portion is applied to the ROIs through the equation (2.2). To apply the correct portion of the spectrum is necessary to have the correspondence with the y axis of the sensor. This step is very important because it takes into account the sensor intrinsic characteristics: the electronic noise is present with different intensities along the sensor surface, contemporary also the sensor's sensibility vary along the surface influencing the white level which is the maximum signal obtainable without saturation.

In figure 2.7 there is as example the average for the white and the dark reference of the sensor. In particular we have the average for the single pixel of the dark/white intensity considering all the wavelengths. In reality during the experiment the two reference are applied

considering the spacial and spectral dimension of the hypercube (equation (2.9)).
The white reference (2.7a) shows a bell shape along the sensor spatial dimension: it means that we have a descending sensibility in the border of the sensor. For this reason, during the acquisition we decide to put the target canopy in the middle of the frame.
The dark reference (2.7b) obviously is proportionally very low if compared with the white one but it presents a shape which leaves inferred the division of the sensor in two halves with different sensibility.

2.4.3 Combinatorial wavelengths selection

The output generated by the hyperspectral camera cover 840 channels between visible and near infrared part of the spectrum, but for the development of a specific sensor we want to reduce this number as much as possible. To reach this purpose we decided to start selecting only 10% of the channels. The selection was made taking 1 channel at a step of 10. This approach permits to cover all the spectrum registered by the sensor.

The following statistical study was done among the channels selected but considering all the combination without repetition of two and three channels. For the more controversial case four wavelengths will be considered. The selection methodology is detailed in paragraph 2.1.8. To have an idea of the amount of the computing capacity required selecting two channels at a time of the 84 we have 3486 combinations; with three and four channels we have respectively ${}_{84}C_3 = 95284$ and ${}_{84}C_4 = 1929501$.

2.4.4 PCA & LDA

In order to establish a criterion of separation and understand how the variable are distributed in the space a supervised rule based on prin-

cipal component was developed (section 2.1.6). In more detail from the ROI selected a constant number of spectra for each hypercube was acquired. The spectral information was select randomly along the ROI area.
PCA was performed for all the combinations of wavelengths obtaining the principal component coefficients; the principal component scores and the variance explained by each principal component. To identify the best combination, the variance explained was used. In detail the best combination 2, 3 or 4 wavelengths is selected weather give us best variance explained respectively for the PC1, PC1 and PC2, and PC1 - PC2 - PC3. The PCs were not considered in their totality to avoid possible correspondences with other combinations in terms of variance explained.

In parallel with the principal component analysis also the linear discriminant analysis was used to study all the channel combinations. The specific channel combinations for the two classes are the predictors which are coupled with their class label. The main objective in this case is to perform a classification, and in the case in which a new observation is obtained we use the previous classification to label the predictor. As a statistical technique LDA is one of the most widely used classification procedures Hai and Wang (2006). The method maximizes the variance between categories and minimizes the variance within categories by means of a data projection from a high dimensional space to a low dimensional space (Zhang et al (2008); Wu et al (2002)).

The best combination is the one which give us the minimum resubstitution error which is the misclassification error i.e. the proportion of misclassified observation in the training set. To identify to which class the misclassified data belongs the confusion matrix will be presented.

At the end of this process we have two set of *wavelengths of inter-*

est, from the PCA and LDA study. In fact, from both PCA and LDA we obtain the best combination of two, three and four wavelengths obtaining the best results in terms of best variance explained and minimum misclassification error.

2.4.5 Deep window analysis

The next step is to extend the analysis and explore the neighbourhood of the wavelengths of interest. The objective of the *deep window analysis* is the investigation of the discriminant capability of the channels not considered in the previous step.
In detail the investigation started from the observation of the discriminant capability between the classes of all the hyperspectral channels considered individually. We note that some of the wavelengths selected by the first methodology derived from LDA, were very close to significant channels with a very low misclassification error: to explore the not covered portion of the spectrum a second step selection was performed at an higher spectral resolution: we decide to open a window around each one of the wavelengths of interest taking the five preceding and five subsequent channels of the wavelengths of interest. Considering for example the simplest case of two channel combination we will select 20 channels in the neighbourhood of the wavelengths of interest.

At this point we applied again the algorithm discussed up to here starting from the combination among the new channels selected passing to the LDA to arrive at the end to identify the *target channels* (two, three or four). Continuing with the example of two wavelengths we have 22 channels around the wavelengths of interest, all the combination of 2 channels were evaluated with PCA and LDA. Target channels are wavelengths at which we have the maximum discrimination between the groups, which is one of the objective of the study.

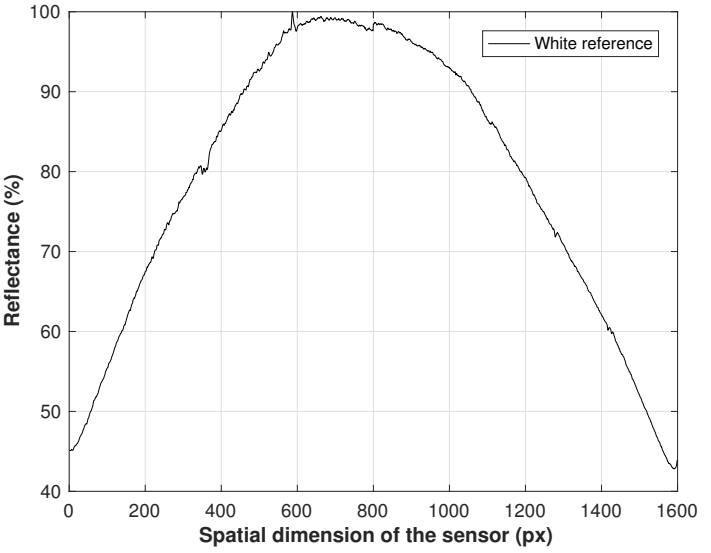

(a) *White reference spectrum*

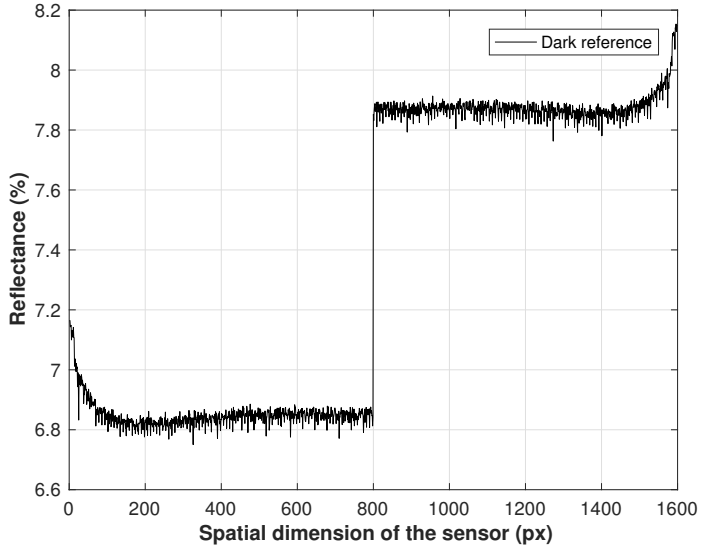

(b) *Dark reference spectrum*

Figure 2.7: *Average of the white and dark references for all the wavelengths*

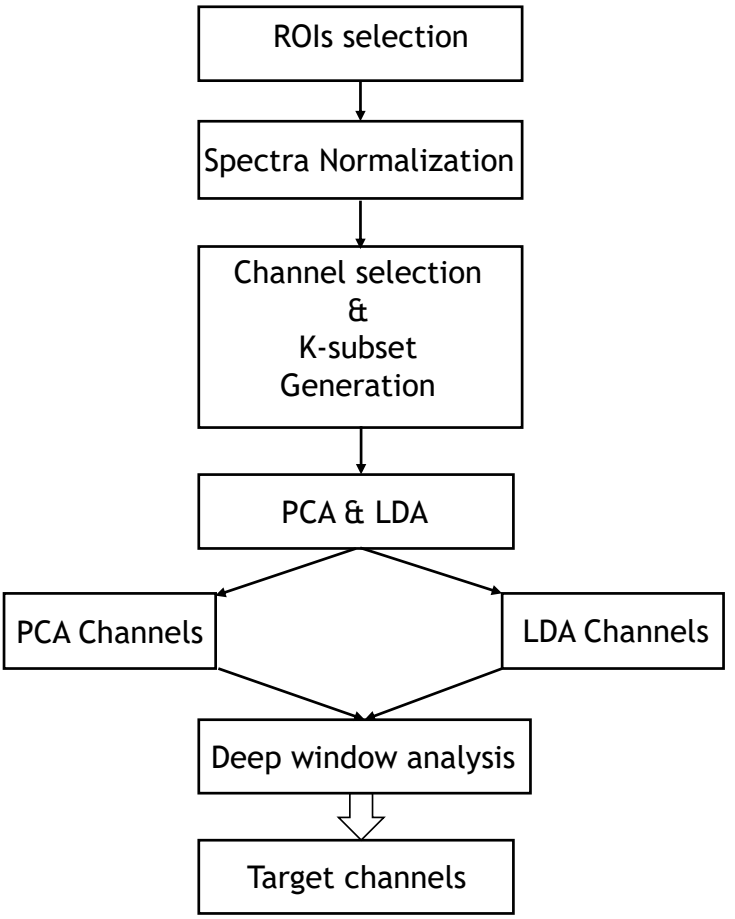

Figure 2.8: *Steps in determining the target channels according to the methodology exposed.*

2.5 The second methodology developed: moving window classifier

Starting from the experience of Schor et al (2016) a moving window filter was developed. The objective was to follow the symptoms characteristics of Plasmopara and CGMMV. We started from the observation that distortion symptomatology in CGMMV cause shadows in some hypercube channels. The intention is to check this peculiarity from a numerical point of view.

The moving window algorithm consists in a square window of customizable size which moves from right to left and from up to down with a step of 1 pixel along a defined area in the spatial dimension of the hypercube. To overcome the border problem of this neighbourhood operation the methodology described in section 2.1.4 was applied with the result of a smaller filtered image. At each step the coefficient of variation (CV) is calculated, generating an image (CV mask) composed of all the calculated CV.

$$CV = \frac{\sigma}{\mu}$$

where

σ is the standard deviation of the pixels inside the moving window;

μ is the mean of the pixel inside the moving window.

The CV of a moving window was calculated for all the 840 channels of the hypercube in a defined spacial region (ROI) and for different window sizes. We want observe the variation of light intensity inside a specific leaf area corrupted by the pathogen for a defined wavelength and comparing it with the healthy tissue.

Due to is difficult to analyse all the CV masks for the entire hypercube database we decide to condense the information inside each mask through indices. In detail for the entire mask we calculate separately a series of indices below summarized.

- average;
- median;
- standard deviation;
- coefficient of variation;
- dispersion index.

From each one of the indices we expect to obtain different informations strictly connected with the light intensity variation inside the region taken into account.

The dispersion index is a measure used to quantify whether a set of observed occurrences are clustered or dispersed compared to a standard statistical model.

$$D = \frac{\sigma^2}{\mu}$$

Different decision rules were implemented based on the examination of the indices calculated for each channel of the hypercubes for the classes selected. After the inspection in the different indices for the defined classes the index in which there is a clustering of the curves was chosen. Averaging the curves of the two groups it was calculated the absolute value of the difference between the two classes: channels of interest are the points in which there is the maximum distance among the two classes.
At the end of this analysis we have a set of rules: index, window size, channel of interest which applied to an unknown region are useful to select the data for the classification. Fixing the rules the linear discriminant analysis is used to quantify the classification capability of the defined points.

For this analysis the window size is one of the main parameter to choose. The window size is strictly connected with the symptoms characteristics and their amplitude. Supposing the acquisition is executed from 85 cm, considering the sensor structural characteristics and the optic used we have a spatial resolution of 0.17 mm px^{-1}. If we

have a symptom manifestation of 5 mm theoretically we will have a sharp contrast between healthy and symptomatic tissues for a window size smaller than 30 px if it is manifested for the specific wavelength. If the same symptom is 1 mm, a window size of 5 pixels is necessary to see differences inside the leaf tissue.

Using windows sizes greater than the disease symptoms can give us informations relative to the general state of the tissue, the presence of different colours, or small and distributed symptoms patches.
For the reasons exposed heads we decide to investigate the window sizes between 10 and 100 pixels by steps of 10 for a total amount of 10 window sizes.

2.6 Preliminary experiment on Powdery mildew

Plant material For the preliminary experiment 8 cucumber plants were infected with Powdery mildew etiological agent. The acquisitions with the camera were made from three different positions covering the entire canopy.

Experimental setup The acquisition of hypercubes in this preliminary experiment was conduct from a fixed position. The distance between the stem of the plant and the focus plan it was fixed at 75 cm.

Regarding the illumination two 500 W halogen lamps were used and positioned in the same plan of the camera lens. Lamps where directed to the plant with an angle of 45°compared to the camera plan. The distance between the two lamps was set in 75 cm to have a triangle in which in two extreme we found the illumination and in the other one the target.

In figure 2.9 there is the radiation spectrum of the halogen lamps used during the experiment. It is possible to see how the radiation covers all sensibility range of the camera. At the same time we can note that in the queues of the spectrum the radiation intensity is very low. The shape of the curve suggests that the leaf reflectance will be lower in the correspondent range with the possible formation of noise

in queues regions. The absorption pick at 730 nm is due to the light interaction with atmosphere.

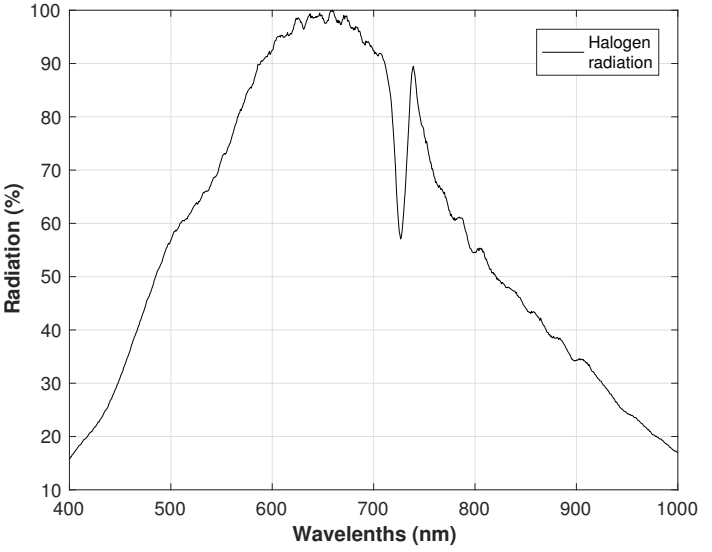

Figure 2.9: *Measured halogen light radiation along the sensor height.*

ROI selection and data normalization The ROI selection in the powdery mildew experiment follows the colour code procedure described in section 2.4.1. In particular, for each hyperspectral image of the training samples, two different classes were considered:

- symptomatic areas
- asymptomatic areas

not distinguishing the different symptoms in accordance with the degree of advancement of the disease, but trying to follow the evolution of the disease during a week.

The representative spectra selected allowed the construction of an artificial training image, which granted the use of a reduced and computationally less onerous amount of data.

After the selection of the different ROIs in the spatial region a software tool was conceived to read the correspondent spectra in z dimension of the hypercube and create a database in which the spectra are stored.

Considering the entire amount of spectra collected with the exposed method we have approx. 60000 spectra from each class. Due to the the nature of trial of this experiment the spectra were reduced to test the methodology developed (chapter 2). A constant ratio of spectra were collected randomly from the ROIs. The high number of data is the main limit to high computational time necessary for the analysis. In the definition of the ratio the base was the ROI amplitude (amount of spectra present in each region) and this was a weak point in this type of selection.

Before the database construction all the spectra were normalized following the procedure exposed in section 2.4.2.

2.6.1 Results and discussion

In relation to the preliminary experiment the analysis involved the method described in section 2.4 to prove the capability of the algorithm to determine the target wavelengths for disease symptoms recognition. Briefly the results will be presented. Regarding the principal component analysis, the best result in terms of variance explained for the two wavelengths combination algorithm are: 760 nm and 767 nm with 99.3% of variance explained. Applying the linear discriminant analysis to the variable selected with the PCA we obtain a misclassification error of 28.4%.

Considering the 3 channel combination algorithm the target wavelengths founded are: 396 nm, 417 nm and 760 nm. The variance explained for the selected channels is 96.3%. With LDA it was obtained a misclassification error of 28.8%.

Contemporary with the PCA, linear discriminant analysis was applied on all the combinations of 2, 3 and 4 wavelengths with the results exposed in table 2.1.

Looking at the disposition of the target wavelengths founded on figure 2.10, which represents the linear discriminant capability of each channel, it is possible to see how the best discrimination not always corresponds with the combination of channels with the minimum misclassification error. This point let understand that the interaction among the wavelengths are important more than the single discriminant capability.

Table 2.1: *LDA target channels for powdery mildew detection*

Combinations	Misclassification	Channels (nm)			
2	13,5%	543	871		
3	11,0%	612	869	874	
4	10,8%	542	613	750	923

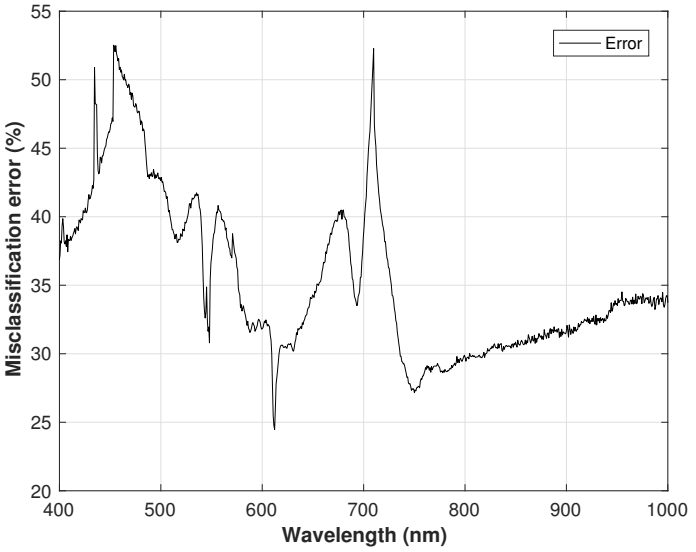

Figure 2.10: *Linear discriminant capability of each wavelength*

Prediction by day The equation founded applying the linear discriminant analysis was applied to predict the membership to one class or another of spectra randomly chosen inside the selected ROIs for each

day.
The average predicted error found is 15.5% for the two wavelengths LDA algorithm; 12.78% and 13% for the three and four wavelengths algorithm respectively.

Analysing these results showed that the predicted error is strictly connected with the number of spectra chosen to the formation of the discriminant model for each day. The spectra selection was made with a constant percentage not considering the amplitude of the ROI. This limitation will be overcome in CGMMV experiment due to the improved ROI selection method.

2.7 Cucumber green mottle mosaic virus detection

2.7.1 Materials and methods

Plant material During the experiment a plot of 100 cucumber plants was breed in greenhouse conditions. Cucumbers were acquired from Hishtil, a commercial nursery company, which graphs the cucumber plants with a pumpkin foot. Among the cultivars American types was chose for the importance in the fresh consumption.
Plants were fertigated proportionally with drippers 2-3 times per day with 5:3:8 NPK[2] fertilizer, allowing for 25 - 50% drainage. Irrigation water was planned to have total N, P, K concentrations of 120, 30, 150 mg l^{-1} respectively; electrical conductivity of water (EC) was 2.2 dS m^{-1}. The temperature was on an average of 25° to 35° during the day for the period of the experiment and 17° - 20° during the night. Plants were in a pest and disease free greenhouse where their healthy status was ascertained by visual inspections of a plant pathologist.

After the inoculation of the plants four classes were selected: healthy asymptomatic young leaves (HY), diseased symptomatic young leaves (DY), healthy asymptomatic old leaves (HO), diseased symptomatic old leaves (DO). In conformity with the development of the disease in the healthy classes (HY, HO) we do not have any colour variation or shape deformation. In contrast diseased classes are strictly connected with colour variation and shape deformation especially DY class. In DO the main symptoms regards almost colour variation.

For convention we decided to use the definition of old and young leaves based on how much time has passed from infection. Are considered old leaves the ones which were completely developed when the symptoms manifest themselves. Instead young leaves are growing during the disease manifestation.

[2] N = nitrogen; P = phosphorus and K = potassium

Experimental setup During this experiment the hyperspectral camera was mounted on the manipulator Motoman described in section 2.3.3 through an end-effector designed and build specifically for the experimentation. During the experiment the acquisition of hypercubes was done from distance between the leaf and the focus plan it was fixed at 85 cm, improving the old distance to meliorate the focus deepening.

Regarding the illumination two 500 W halogen lamps were used and positioned 14 cm ahead the camera lens to have a higher light intensity. Lamps where directed to the plant with an angle of 60° improving the preliminary experiment angle from 45°. The distance between the two lamps was set in 70 cm to have a rectangle triangle in which in two extreme we found the illumination and in the other one the target.

Regions of interest selection During the previous experiment on peronospora symptoms the selection was made by choosing a colour code with which masks were created. From the masks spectra were selected with a purpose made algorithm. This approach not permit to have an homogeneous selection to check the general status of the tissue. To overcome this problem a second methodology based on spatial region selection was implemented (section 2.4.1). For each class selected the CV indices were calculated for 24 samples images.

The amplitude of the region is depending on how wide is the leaf on the image. In any case the maximum possible area was covered. From each region an equal number of spectra were selected for the application of the target wavelengths determination (section 2.4). On the other hand, the application of the second methodology (section 2.5) was performed for all the wavelengths from 400 to 1000 nm.

Influence of the region area on the CV analysis The manual selection of the region inside the leaf with the second method of ROI selection presents a limit: it is not possible to have the same area among different images. Due to the high variability of the tissue covered with

the region selection a sensitivity test was conducted on different region sizes.

The purpose of the test is to verify how much the region area influence the coefficient of variation mask and the derived indices. In the database the smallest area selected is approx. 13000 px^2 while the greatest is ten times greater than the smallest. During the test for each class selected (HY, HO, DY, DO) we took the most extended ROI and create 10 sub-images reducing the original area. In detail the original region is proportionally reduced in ten steps from the original size to the smallest one present in the database. The evaluation of the CV mask is made for 5 channels distributed along the spectrum (466 nm, 546 nm, 612 nm, 711 nm, 839 nm) with five different window sizes (10 px, 20 px, 50 px, 70 px, 100 px) for each resized region.

The analysis starts with the study of the symptomatic old leaves (DO). The first index is the average of CV masks: reducing the area of the most extended hypercube in ten steps until it reach the area covered the less extended hypercube in the database the AVG index evaluation seems to be not influenced by the area. This behaviour is present for all the window sizes analysed (figure 2.11). Even if it is not showed the 100 px window size it is very similar to the 70 px window size. For higher window sizes in the CV mask creation the AVG index tend to grow more for smaller regions.

The same considerations can be done for the median index behaviour even if the variation for smaller area is greater than the average index. Different is the situation for the standard deviation index of the CV in which the 711 nm channel is influenced by the region width above the 70 px window size for smaller area. At 100 px window size all the wavelengths are influenced by the region width especially from the 7^{th} crop: the standard deviation index tends to descend.

Coefficient of variation index and dispersion index are both constant for window size smaller than 70 px after they tend to decrease.

The same considerations can be done for the symptomatic young leaves (DY) where the average CV index is constant for all the channels selected and all the window sizes evaluated for subsequent resized regions. The median index is perfectly comparable to the average index for all the cases analysed.

The standard deviation index is constant for window sizes smaller than 50 px, after that it starts to have a descending trend from the 5^{th} cropped region to the 10^{th}. The dispersion index is extremely influenced from the region width from the 6^{th} reduction already from a window size of 50 px. It is possible to do the same consideration for the coefficient of variation index where the variability of the index starts to be evident from the 7^{th} area reduction from 50 px window size.

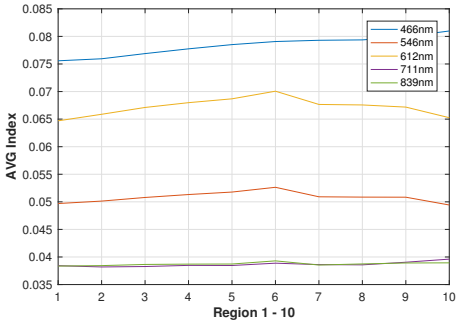

(a) *AVG index at 10 pixel window size*

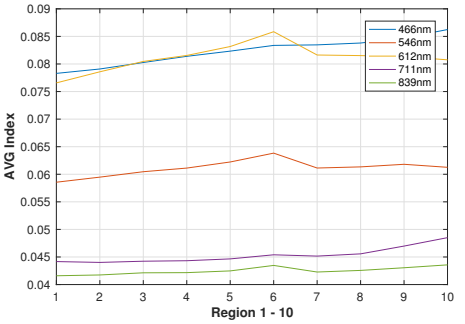

(b) *AVG index at 20 pixel window size*

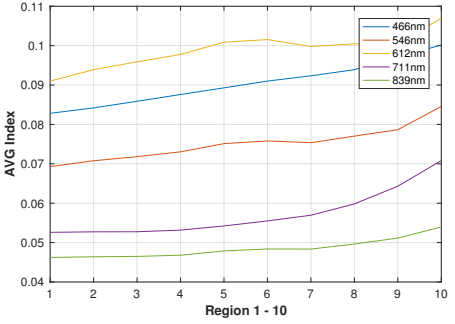

(c) *AVG index at 50 pixel window size*

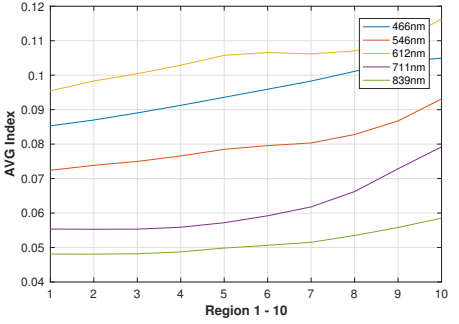

(d) *AVG index at 70 pixel window size*

Figure 2.11: *Sensitivity analysis on region area variation for different window size. In abscissa we have the ten different cropped regions form the most extended to the less extended. The average index is evaluated at five different wavelengths.*

Analysing the healthy old leaves it is possible to note a difference in the behaviour of the average index of CV which at 70 px window size for all the wavelengths analysed have a descending trend from the 8^{th} cropped region. At 100 px window size this trend is anticipated to 7^{th} reduction.

More constant is the median index which presents some variation only at 100 px window size for all the wavelengths with a bell shape from the 5^{th} to the 10^{th} region.

The standard deviation index is constant until the 50 px window size at the 6^{th} region in which for all the wavelengths considered there is a descending trend. As consequence the dispersion index and the standard deviation index are both influenced of the trend of the average and the standard deviation indices which start to be with a descending trend from a window size of 50 px at the 5^{th} area reduction.

Analysing the last class of healthy young leaves (HY) we have a very constant values for the average index for all the wavelengths and all the windows sizes. The same thing is about the median CV index.

Also for healthy young leaves the standard deviation index presents a descending trend from 50 px window size starting from the 7^{th} region. This trend is higher for windows size greater than 50 px. Coefficient of variation index and dispersion index will be influenced by this behaviour presenting the same descending trend. The 100 px windows size is the more influenced.

CV analysis on homogeneous panels One of the point of interest in the evaluation of the CV method (section 2.5) is the stability of the indices evaluation in a homogeneous region. This test represents the reference for the evaluation of the methodology.

In our analysis we decide to acquire the hypercube of three homogeneous coloured panels: white, dark and green. After the selection of a spatial region (ROI) inside the hypercubes the CV analysis is performed along the different ROIs for the same window sizes explored

in the main experiment.

In this section will be graphically presented only the results of the dark panel because for all the colours selected there is the same behaviour of the CV index analysis along all the wavelengths selected. The only discriminant among the different colours is the intensity of the generated curve. This behaviour is the first response and it was took in account and confirmed from the analysis due to the nature of the coefficient of variation which measures the amount of variability relative to the mean of a population.

Another consideration can be done on the figure 2.12 is the high intensity of CV value on the queues of the spectrum. It is possible to suppose the influence of the normalization on this behaviour. Observing the figure 2.7 on white and dark reference and considering the equation (2.2), dividing a number for a very low denominator the result tends to be very high. Reasonably this is the reason why we have high values of CV index in the queues of the graph.

In figure 2.12a we have the average of the CV mask for all the channels of the hyperspectral camera. It easy to note how there is the coincidence of the average CV index along all the spectrum for the whole set of window size analysed. The same trend is present also for the median index. At the same time it seems to exist an ascending trend of the intensity of CV index connected with the width of the moving window. Analysing the results, the same intensification of the CV index is present. In results the signal for greater window sizes often the signal tend to intensify.

Regarding the figure 2.12b the standard deviation index and in consequence all the derived indices (coefficient of variation and dispersion index) are influenced by the window size even if slightly. Among the windows applied the smallest ones are more influenced from the area covered: smaller regions present a higher variability than the wider ones. Reasonably the electronic noise influences this behaviour.

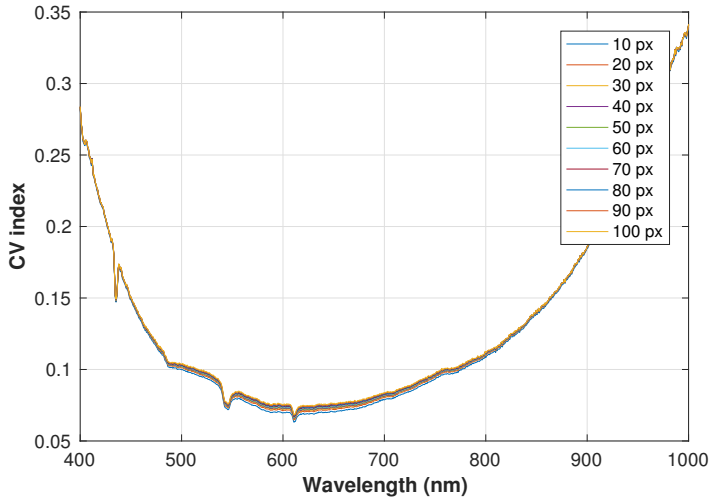

(a) *Average CV index*

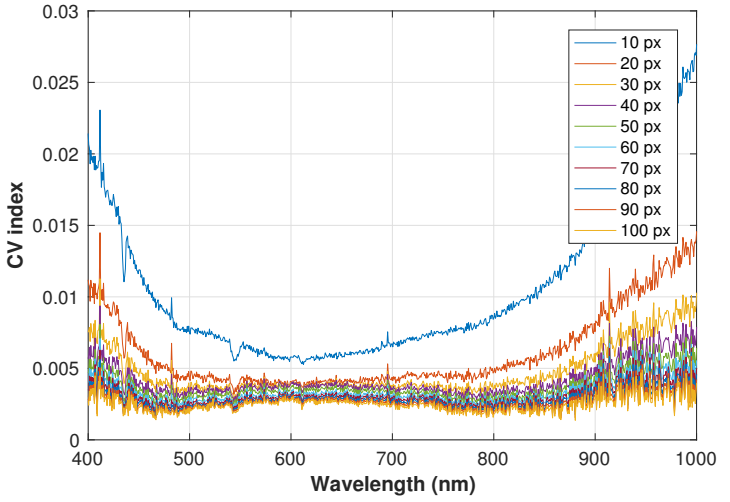

(b) *Standard deviation CV index*

Figure 2.12: *Results of the CV index evaluated on an homogeneous dark panel for the two main indices: average and standard deviation.*

2.8 Results

2.8.1 Young symptomatic leaves analysis

The first analysis is among young healthy leaves (HY) and young diseased ones (DY). In CGMMV young leaves are very influenced in their development in both shape deformations and colour mottling. How it was seen in figure 2.4 in young leaves colour variations are almost among light green and dark green. Considering the shape deformations in young leaves the magnitude of shape variation is the highest. In particular, we can have different types of alterations: bubbling tissue and contours disruptions due to different speed in tissue formation.

Channel combination The first step in this analysis is the definition of what are the channels of interest around which it possible to find the target channels. Starting from the two wavelengths combinations analysis we found as PCA channels of interest 396 nm and 672 nm. The variance explained for this combination is 99.92% for the first PC. How it is possible to observe the two classes have a distribution that overlaps. Applying the LDA on the selected channels we have a misclassification error of 25.5%. These two wavelengths are not able to discriminate between the groups, in fact from the linear discriminant analysis algorithm the channels which have the greater interest are 508 nm and 543 nm with a misclassification error of 17.44%.

Opening a window of 10 wavelengths around the LDA selected channels the classification has undergone a small improvement passing to 17%. The target channels in this classification are 508 nm and 546 nm. In figure 2.13 we have the representation PCA and LDA results. In figure 2.14 is represented the linear discriminant capability of each one of the 840 channels. There are low misclassification errors between 400 nm and 500 nm, around 550 nm; along the red-edge (650 - 750 nm) and after 950 nm. The linear discriminant analysis of all the combinations of three wavelengths among the 84 chose led to the definition of the following wavelengths of interest: 543 nm, 643 nm,

999 nm. The relative misclassification error is of 11.6%.

Considering the three channels combination algorithm the best variance explained among the data is with the following channel combination: 396 nm, 672 nm and 679 nm. The variance explained the first two PCs for the defined channels is 99.9%. Applying the LDA on this channel combination we have a misclassification error of 25.40%.

The next step was to open a spectral window around the wavelengths of interest applying the LDA to reduce the misclassification error. This analysis brought to the definition of the following target channels: 547 nm, 640 nm, and 1000 nm with a misclassification error of 11%.

Moving window classifier The second methodology have the aim to measure the variation of the light reflection inside a region. How explained in section 2.5 the coefficient of variation was chose how the index of the light variability inside the selected region.
In healthy young cucumber leaves tissues are homogeneous and when the leaf is observed at different camera channels it seems to be constant in the intensity inside the same leaf component. Young diseased leaf presents a bubbled tissue often with curvatures in the shape. Furthermore, sometimes the green mottle mosaic virus is the cause of perimeter disruptions with contour variations if compared with healthy asymptomatic leaves.

The algorithm was applied along the 840 channels of the camera for all the hypercubes collected during the experiment. The moving windows width evaluated are ten: from 10 to 100 pixels by steps of 10 pixels. To extract the informations from the masks generated by the algorithm for each channel five indices were evaluated: the average of the CV mask, the standard deviation of the CV mask, the coefficient of variation of the CV mask the dispersion index of the CV and the median value of the CV.

By leaf analysis. From a visual analysis of the distribution of the curves of the average of CV masks it is possible to divide the channels in four areas. The first is from 400 to 500 nm in which the signal is noisy and not intelligible. The second area goes from 500 to 700 nm in which the average of the CV masks for healthy leaves tend to stay under the diseased ones for a window size between 40 and 100 pixels, even if the values around the red-edge are not so clear. In the near infrared region between 700 and 950 nm there is the overlapping among the two groups. At the end of the spectrum (greater than 950 nm) healthy leaves tent to have a coefficient of variation of the light reflected average greater than diseased ones for all the window size analysed. As example an extract will be presented in figure 2.16.

The median value of the CV mask retraces almost the average CV with a differentiation among groups marked among 500 nm and 650 nm for all the windows sizes examined.

Looking at the standard deviation of the CV mask along the spectrum for the same group of diseased and healthy young leaves not considering the queues we have a high variability in the red edge region for both classes.
Different is the situation analysing the coefficient of variation of the CV masks in which the two classes are overlapped along all the spectrum and for all the window size analysed.

Analysing the dispersion index in which for all the windows sizes the standard deviation squared give more importance to the separation among the two groups is limited to the area among 550 nm and 700 nm in which the healthy leaves tend to overcome the diseased ones for all the windows size but especially for 40 and 50 pixel of width. A limited differentiation is also at the end of the spectrum over 950 nm. In the described region data are not clustered but dispersed.

Classification rules definition. Averaging all the leaves analysed by typology we obtain two different curves one for each class. To extrapolate some information, it was calculated the absolute value of the

difference between the two curves for all the windows sizes applied. In figure 2.17 is represented the difference at 60 pixels window size for the average of CV masks.
Considering the area of the spectrum selected with the previous observation for the average index of the CV mask it is possible to define four peaks of interest: 562 nm, 670 nm, 703 nm, 980 nm. In these channels for the selected window size there is the maximum distance between the two classes HY and DY.

Applying the same consideration to the median index for the two classes considered the region interested are the same of the average index.
Regarding the standard deviation and the explained graph the peak of the difference is in the red edge area around 670 nm at 10 pixels window size. For the same window size of the standard deviation index the dispersion index presents a peak at 671 nm. For the reasons previously exposed no considerations will be done for the CV.

2.8.2 Mature symptomatic leaves analysis

The second step of the investigation is the assessment of the difference between diseased old leaves and healthy old ones. The characteristics of the symptoms are different compared to young leaves due to a preponderant yellowing mottling and discolouration in old diseased leaves. Morphological deformations are limited whether the virus infects the plant when the leaf is already formed.

Channel combination study Applying the first methodology the principal component analysis gives us the following two wavelengths explaining the 99.9% of the variance among two channels: 396 nm and 672 nm. Computing the linear discriminant analysis on the selected channels we have misclassification error of 19%.

The other step is the evaluation of the PCA with the three channels algorithm. From the study three channels were selected with the 99.9% of the variance explained: 396 nm, 672 nm and 679 nm. The

LDA on this channel combination bring to the 19% of the misclassification error.

Observing the figure 2.19 we can see how the classification capability of each channel among the symptomatic and asymptomatic old leaves is various along the spectrum. Lower picks are between the range 400 nm and 500 nm. Around the red-edge zone between 650 and 750 nm. A decreasing of the misclassification error for the single channel is present after 820 nm. Applying the LDA with the two channels combination algorithm the selected channels fall around the range founded. In fact, the wavelengths of interest are at 501 and 543 nm with a classification error of 15.03%. Opening a spectral window around the selected channels it possible to improve the classification with a 14.6% error with the following channels: 503 nm 546 nm.

To improve the classification capability of the model we decide to perform a three channel combination algorithm. From the analysis of the 10% of the wavelengths the most important channels are 501 nm, 508 nm, and 549 nm with a misclassification error of 12.78%. After the deep spectral analysis, the target channels were defined as 503 nm, 505 nm and 546 nm with the and error of 12.44%. These wavelengths show that most of the difference between old diseased and asymptomatic leaves is around the cyan and green channels of the electromagnetic spectrum. It is possible to suppose that the selected channels are directly correlated with the characteristic yellow colour of the diseased old leaves.

Moving window classifier The second methodology have the aim to measure the variation of the light reflection inside a leaf region. For our classification we decide to consider old leaf symptoms the yellowed old leaves which do not present shape deformations.
The algorithm was applied along the 840 channels of the camera for all the hypercubes collected during the experiment in the class. The mov-

ing windows width evaluated also in this case are ten: from 10 to 100 pixels by steps of 10 pixels. The same five indices for the classification of the CV masks were used.

By leaf analysis. The first analysis is about the distribution of the curves of the average of CV masks for all the channels of interest. In the first part of the spectrum (400 to 500 nm) the signal is noisy and not intelligible. From 500 to 700 nm in which the average of the CV masks for healthy leaves tend to overlap the diseased ones for a window size between 40 and 100 pixels. It is interesting to note that the distribution of the diseased leaves has less variability. The differentiation between the two classes is marked in the red edge region especially at 80 pixels window size. In the near infrared region between 700 and 950 nm there is the overlapping among the two groups, only at the end of the spectrum (greater than 950 nm) healthy old leaves tend to have a coefficient of variation of the light reflected greater than diseased ones for all the window size analysed. In figure 2.21 is represented an extract of the average index for symptomatic old leaves (DO) and healthy asymptomatic old leaves (HO).

The median value of the CV mask retraces almost the average CV with but with a more pronounced distance between the two classes for a moving window greater than 80 pixels. The distance among the two classes is present also for value channels greater than 950 nm for all the window sizes analysed.

Looking at the standard deviation of the CV mask along the spectrum for the same group of diseased and healthy old leaves we have a high limited possibility of discrimination in the red edge region.
Different is the situation analysing the coefficient of variation of the CV masks in which the two classes are overlapped along all the channels and for all the window sizes analysed. The same consideration can be done analysing the dispersion index in which for all the windows sizes the separation among the two groups not possible.

Classification rules definition. Studying the absolute value of the difference between the two classes considered it is possible to define the rules which can be used for the correct classification of the selected region.
Considering the previous observation it is possible to define three peaks of interest: 546 nm, 671 nm, 980 nm. In these channels for window size of 80 pixels there is the maximum distance between the two classes HO and DO of the average index.

Applying the same consideration to the median index for the two classes considered the region interested are preponderant at 70 pixels window size at 546 nm, 671 nm and 980 nm.
Regarding the standard deviation the peak of the difference starts to be intelligible at 60 px window size in the red edge area around 670 nm. For the same window size of the standard deviation index the dispersion index presents a peak at 671 nm. For the reasons previously exposed no considerations will be done for the CV.

2.8.3 Overall discrimination of symptomatic leaves

The symptoms characteristics among young and old leaves for CGMMV depends on when the plant was infected. In our analysis are considered old leaves the ones which presents yellow mottling instead young leaves present green mottling and shape deformations. It's possible suppose the spectral differences between the groups will be limited to few regions. On the contrary relative more difference could be noted in the light reflection characteristics which will be investigated with the moving window classifier.

Channel combination study The application of the channel combination algorithm led to the definition of the following channels for the two wavelengths combination algorithm: 396 nm and 672 nm with a variance explained of 99.9% for the first PC. The two groups are almost overlapped: applying the LDA on the selected 2 channels we have a misclassification error of 45.6%.

Also the three channels combination algorithm led to an overlapping of the two groups with the 45.32% LDA misclassification error. The three wavelengths chose are 396 nm, 672 nm and 679 nm with the variance explained for the first two PC of 99.9%.

To obtain a better discrimination between the groups the linear discriminant analysis algorithm with the combination of two and four wavelengths. The discrimination with two channels reach a very high misclassification error 41%. Which is maintained also with the three channels combination algorithm (40%). The selected channels for the two algorithms are respectively are 515 nm and 672 nm for the two channels combination algorithm and 515 nm 672 nm and 679 nm. Opening a spectral window, the error it was reduced to 40% with the following two channels: 513 nm and 696 nm.

The error in LDA classification with two and three channels is very high for this reason the investigation continued with a four channel combination algorithm. The selected wavelengths are 672 nm, 694 nm, 716 nm, and 804 nm. With the selected four channels the error it was reduced only of 1% to 39%. From a deep spectral window analysis, it was obtained a very limited reduction of the misclassification error to 38% with the following wavelengths: 400 nm, 694 nm, 716 nm, 804 nm.

In figure 2.23 is represented the discriminant capability of each wavelength for the two classes DO and DY. The significant point is at 694 nm in which we have the minimum value of the misclassification error. With the interaction among different channels it is possible to reduce the error of the single wavelength in the red edge but in a perspective of development of a specific sensor one single channel results cheap and easy in management. At the same time, the misclassification error is very high and not effective for our purpose.

Moving window classifier Analysing the moving window classifier and considering the average CV index we have a different distribution of the index along the spectrum for the two classes. The signal tend to be very clustered and lower for diseased old leaves than symptomatic young ones for all the windows sizes inspected. As sample in figure 2.24 there is the average index at 50 pixels window size. Until 450 nm the signal is very noisy, after the different path for the two classes is clear with the diseased old leaves more uniform in the average of the reflected light if compared with diseased young leaves. This trend is constant for all the window sizes inspected and there is also a correspondence with the median CV index. The intensity of the signal appears more clustered from 40 pixels windows size.

Analysing the standard deviation index the disposition of the curves along the evaluated channels is constant with overlapping among the two classes for all the wavelengths. Some differentiation is present around 670 nm for windows size lower than 40 pixels.

Studying the dispersion index and the CV index also in this case there is an overlapping between the two groups for all the wavelengths and for all the windows size inspected.

Classification rules definition. The classification rule definition concerns only the average index of CV mask due to the characteristics previously exposed. In figure 2.25 it possible to observe the absolute value of the difference among the average of all the curves for the two classes considered at 50 pixels window size. The peaks in which there is the maximum difference are at 486 nm and at 670 nm.

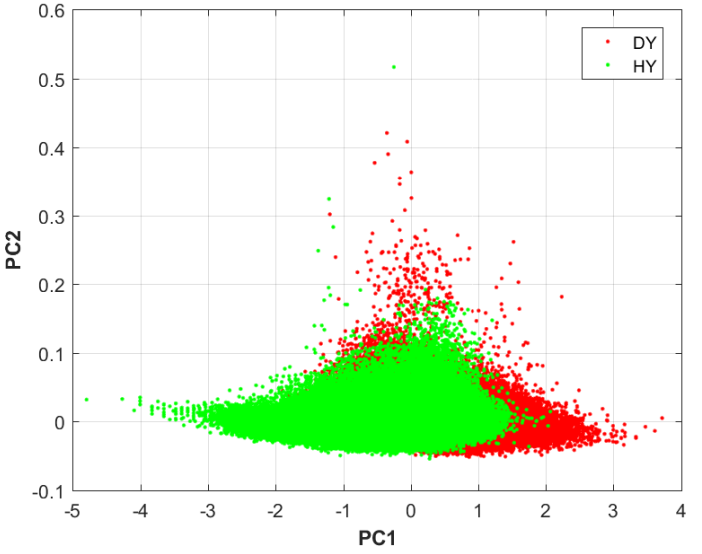

(a) *Two channels PCA*

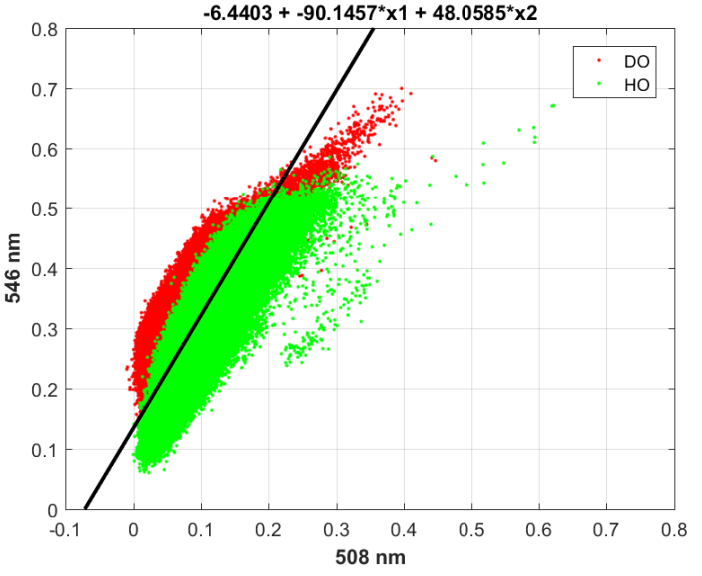

(b) *Two channels LDA*

Figure 2.13: *Results for the two wavelengths combination algorithm for PCA and LDA*

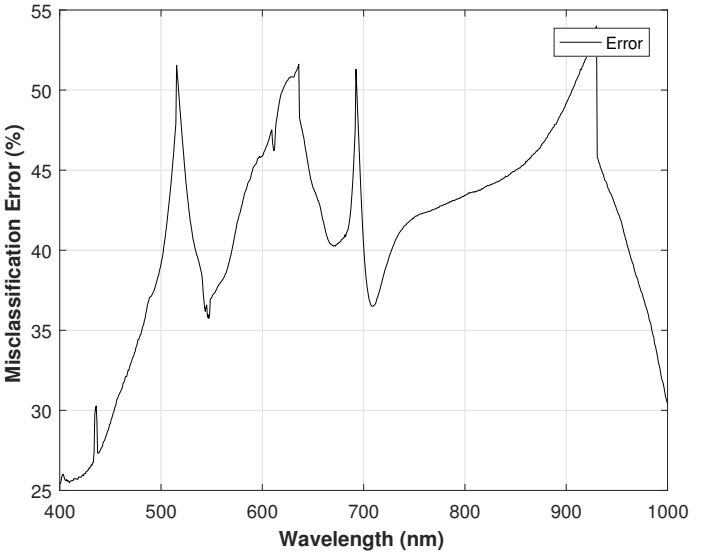

Figure 2.14: *Linear discriminant capability of each wavelength considering healthy and diseased young leaves.*

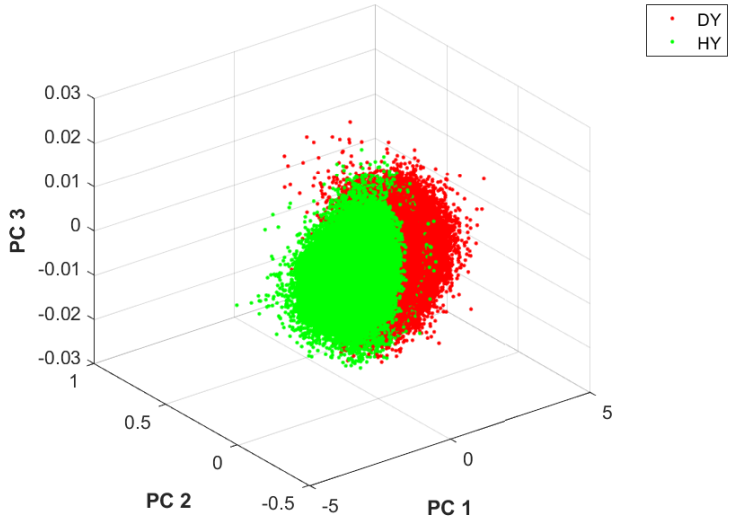

(a) *Two channels PCA*

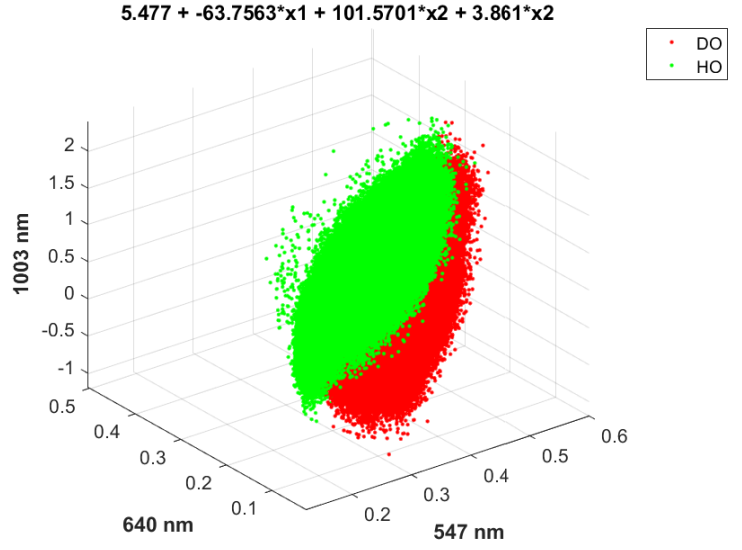

(b) *Two channels LDA*

Figure 2.15: *Results for the three wavelengths combination algorithm for PCA and LDA*

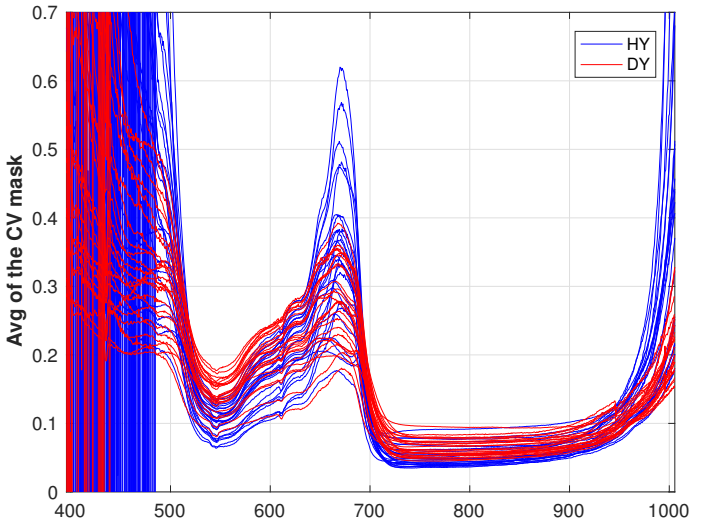

Figure 2.16: *Average of the CV mask along the spectrum for a 60 pixel moving window width comparing asymptomatic young leaves (HY) and symptomatic young leaves (DY).*

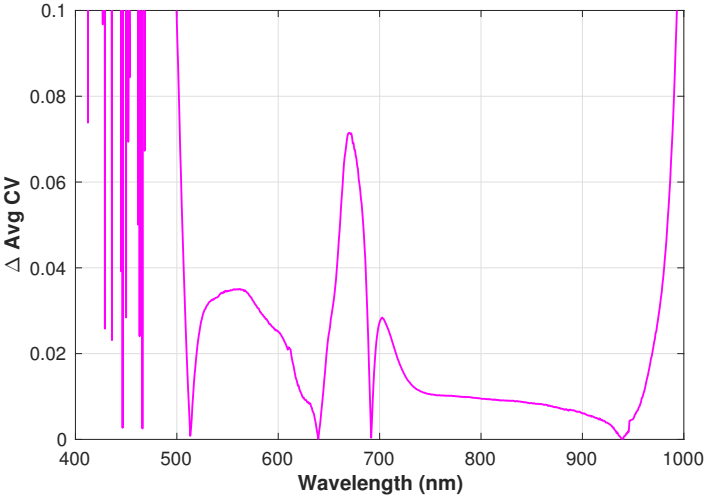

Figure 2.17: *Difference of the average of the CV mask along the spectrum for a 60 pixel moving window width comparing the average of the asymptomatic young leaves (HY) with the symptomatic young leaves (DY).*

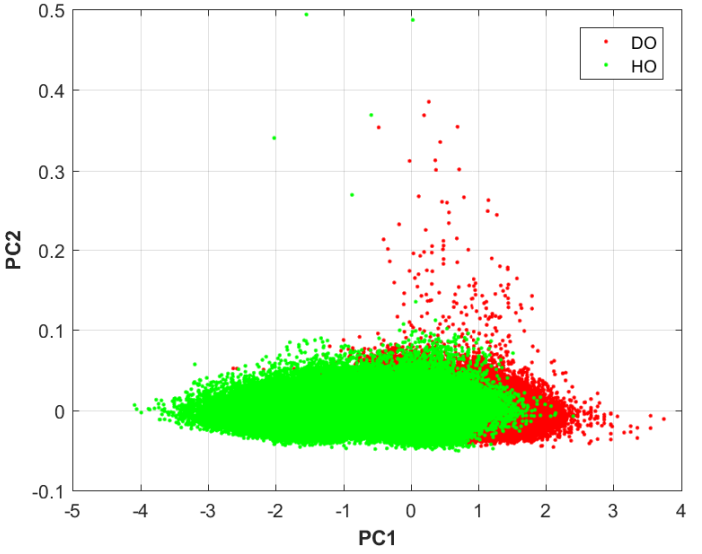

(a) *Two channels PCA*

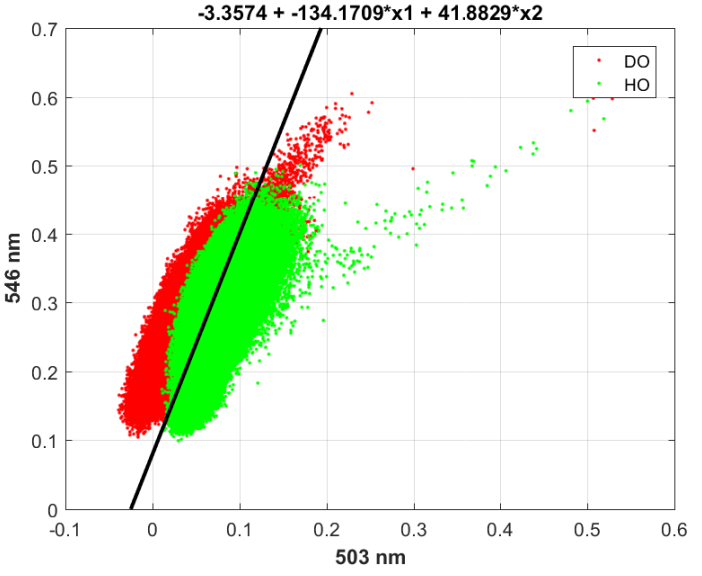

(b) *Two channels LDA*

Figure 2.18: *Results for the two wavelengths combination algorithm for PCA and LDA between symptomatic and asymptomatic old leaves.*

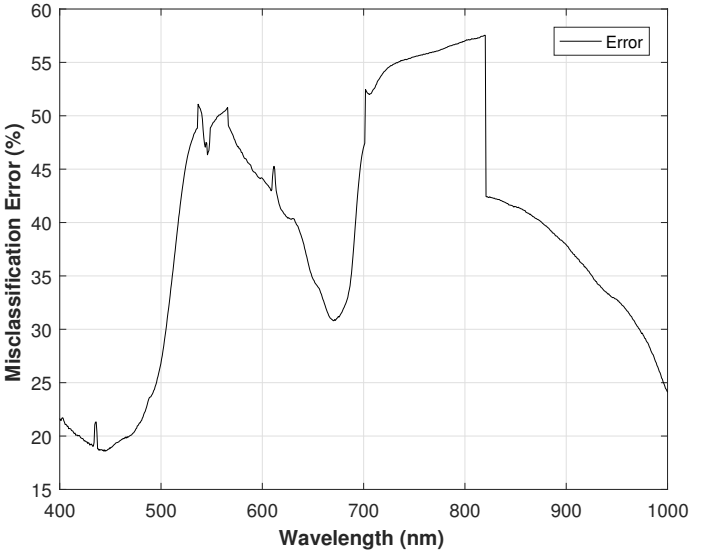

Figure 2.19: *Linear discriminant capability of each wavelength considering symptomatic and asymptomatic old leaves.*

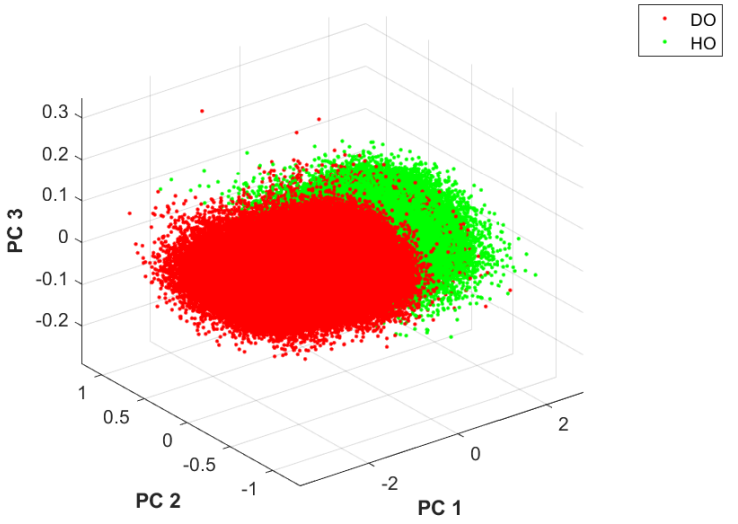

(a) *Two channels PCA*

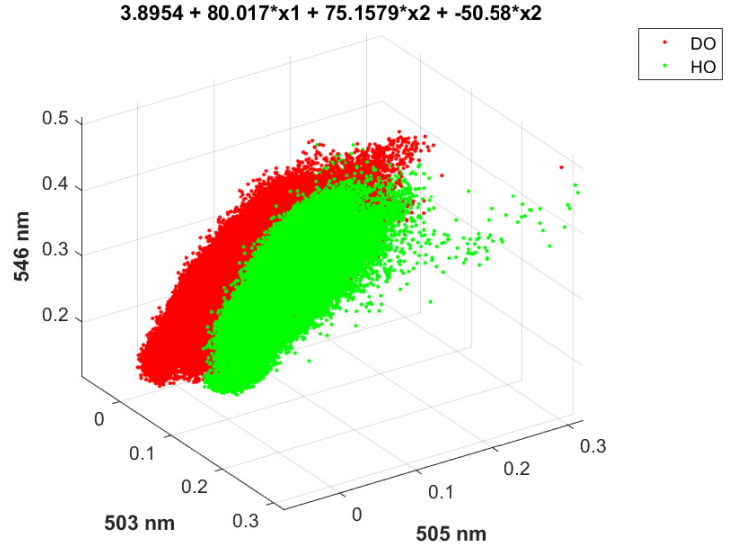

(b) *Two channels LDA*

Figure 2.20: *Results for the three wavelengths combination algorithm for PCA and LDA*

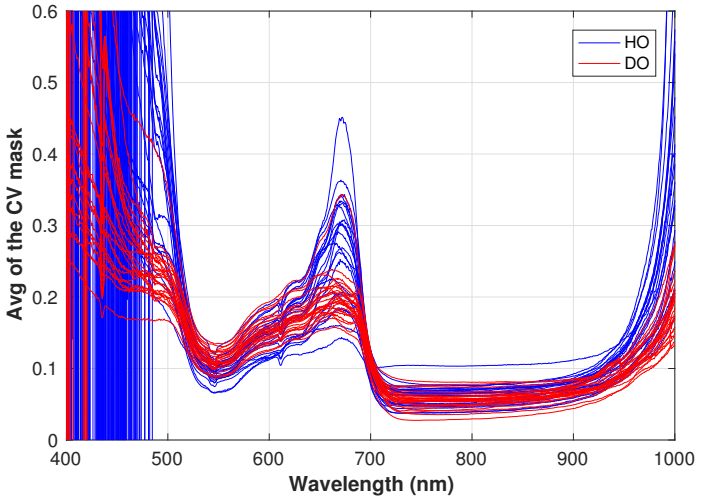

Figure 2.21: *Average of the CV mask along the spectrum for at 80 pixel moving window width comparing asymptomatic old leaves (HO) and symptomatic old leaves (DO).*

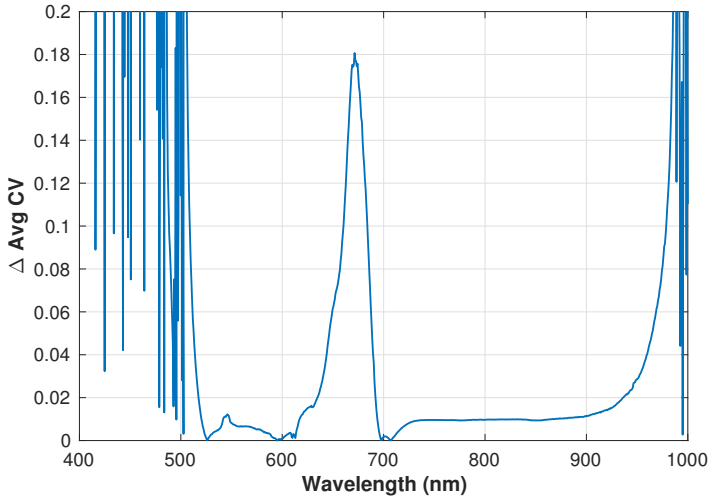

Figure 2.22: *Difference of the average of the CV mask along the spectrum for a 80 pixel moving window width comparing the average of the asymptomatic young leaves (HO) with the symptomatic young leaves (DO).*

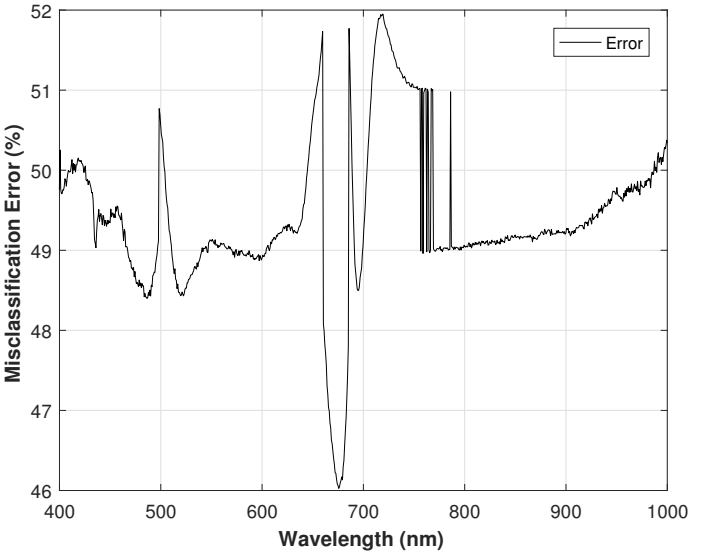

Figure 2.23: *Linear discriminant capability of each wavelength considering symptomatic old leaves (DO) and symptomatic young leaves (DY).*

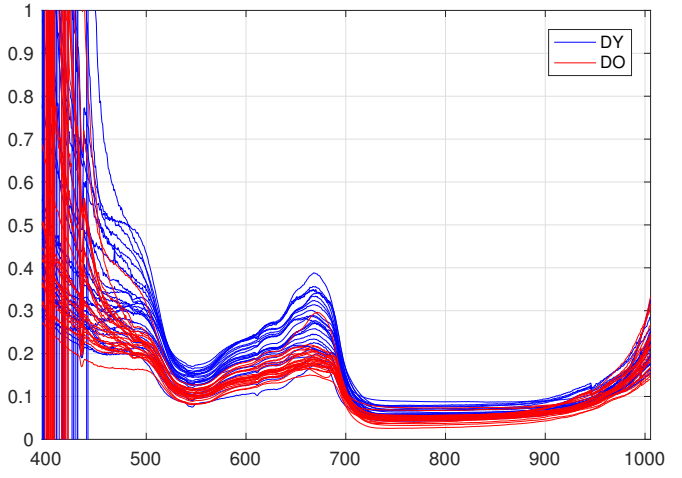

Figure 2.24: *Average of the CV mask along the spectrum for at 50 pixel moving window width comparing symptomatic old leaves (DO) and symptomatic young leaves (DY).*

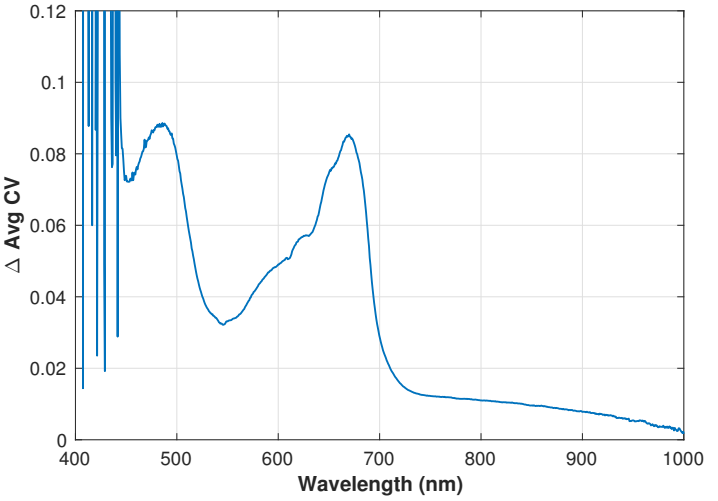

Figure 2.25: *Difference of the average of the CV mask along the spectrum for a 50 pixel moving window width comparing the average of the symptomatic young leaves (DY) with the symptomatic old leaves (DO).*

2.8.4 Discussion

The two methods discussed and applied to the CGMMV detection showed a great potentiality in plant disease detection. The reduction of the wavelengths is very important for the determination of the target channels thanks to which it is possible to develop a specific sensor for a defined disease. In table 2.2 are summarized the target wavelengths with the correspondence LDA misclassification error. For the identification of CGMMV symptoms in young leaves three channels were selected with a linear misclassification error of 11%.

The application of the first methodology comparing healthy old leaves with old leaves infected with CGMMV etiological agent led to the definition of three target channels with an error of 12% in the linear classification.

More complicated is the definition of a linear model for the classification of diseased young leaves and diseased old leaves. The target channels were extended to four and among the two million combination examined the misclassification error is of 39%.

Table 2.2: *Wavelengths of interest with the relative misclassification error for CGMMV symptoms identification in young leaves.*

	Two channels algorithm			Three channels algorithm				
	Wavelengths		Error	Wavelengths				Error
HY-DY	508	543	17%	547	640	1000		11%
HO-DO	396	672	19%	503	505	546		13%
DY-DO	513	696	40%	513	675	679		39%
				400	694	716	804	38%

In table 2.3 are summarized the main results in terms of misclassification error during the generation of the linear model for the three case studies analysed. Regarding the first classification between DY and HY the target wavelengths selected follow are between the green red and infrared part of the spectrum. The classification among the

DO and HO classes covers the violet, the red edge and the green part of the spectrum logically it is connected with the different photosynthesis ability of old symptomatic leaves in which the virus has a very high activity which influence the normal metabolism of the plant (section 2.2.2). Analysing the last classification, the correct identification is more difficult due to the presence of the disease symptoms in both classes but at the same time the leaves symptomatology is partially different. The best classification in this case was obtained with four wavelengths covering the entire spectrum. In fact the target channels register the light at 400 nm, 694 nm, 716 nm, and 804 nm which represent the violet, red-edge, and near infrared part of the spectrum. In figure 2.26 is represented the class prediction using the model developed with the four wavelengths algorithm. The classification of diseased symptomatic old leaves and young ones obtained greater results with the CV methodology.

Table 2.3: *Confusion matrix - LDA classification algorithm*

		Actual			
		Two channels LDA		Three channels LDA	
		HY	DY	HY	DY
	DY	16.23%	83.77%	11.47%	88.53%
	HY	82.38%	17.62%	89.02%	10.98%
		HO	DO	HO	DO
Predicted	DO	15.24%	84.76%	12.71%	87.29%
	HO	86.06%	13.94%	87.82%	12.18%
		DY	DO	DY*	DO*
	DO	60.55%	39.45%	62.64%	37.36%
	DY	41.44%	58.56%	39.65%	60.35%

* Referred to the four wavelengths LDA combination algorithm.

The developed methodology about the coefficient of variation is very promising for the measurement of the leaf-light interaction. CGMMV causes different symptoms like shape deformations, colour mottling

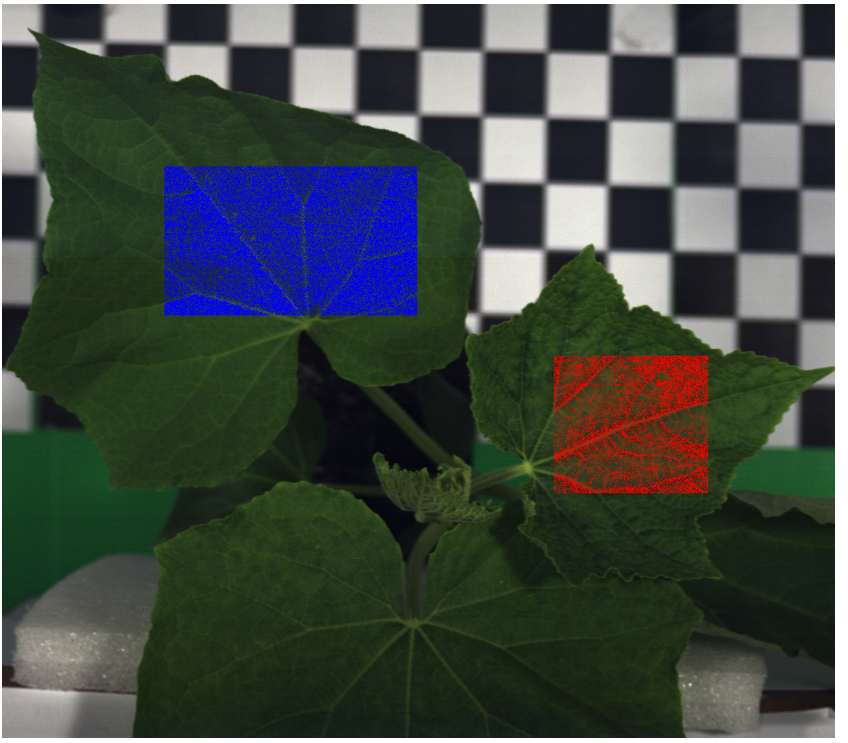

Figure 2.26: *Class prediction by single spatial coordinate of the symptomatic young leaf (DY, red) and symptomatic old leaves (DO, blue) through the linear model generated from the four wavelengths algorithm described in section 2.8.3.*

(green and yellow), bubbling tissue. It was demonstrated that specific wavelengths succeed in differentiating the symptoms both by a visual inspection and by the CV analysis of a region of interest took inside the symptomatic leaf.

In table 2.4 are summarized the predicted and actual percentage of the classification error of the linear discriminant analysis on the set of rules defined with the CV indices analysis. The set of rules in the CV methodology is the combination of index applied on the single CV mask for each channel, the moving window size and the corresponded selected channels in which there is the maximum distance between the two classes considered.

The different linear models evaluated present strengths and weak-

nesses points but they are not able to reach the combinatorial spectral analysis methodology. Nevertheless, good results were reached, but surprisingly the CV index analysis led to a greater discrimination comparing DO and DY leaves.

Even if the methods proposed seems to be able to reach the prefixed purposes, further analysis must be implemented for the study of the CV masks indices. Furthermore, for an effective application the study of the disease will need an improvement of the variability of the sample and development of a cross-validation study to have stronger results in terms of reliability.

Table 2.4: *Confusion matrix - CV classification algorithm*

Set of rules				Classification		
Index	Window size (pixel)	Selected channel (nm)	Class	Actual		Error (%)
				HY	DY	
Average	50×50	652	HY	60%	40%	42%
			DY	44%	56%	
		670	HY	68%	32%	30%
			DY	28%	72%	
		703	HY	72%	28%	28%
			DY	28%	72%	
		980	HY	64%	36%	26%
			DY	16%	84%	
Standard dev.	10×10	670	HY	68%	32%	24%
			DY	16%	84%	
Dispersion	10×10	671	HY	64%	36%	28%
			DY	20%	80%	
				HO	DO	
Average	80×80	546	HO	80%	20%	26%
			DO	32%	68%	
		671	HO	60%	40%	22%
			DO	4%	96%	
		980	HO	60%	40%	28%
			DO	16%	84%	
Median	70×70	546	HO	80%	20%	24%
			DO	28%	72%	
		671	HO	60%	40%	20%
			DO	0%	100%	
		980	HO	48%	52%	32%
			DO	12%	88%	
				DO	DY	
Average	50×50	486	DO	96%	4%	18%
			DY	32%	68%	
		670	DO	96%	4%	16%
			DY	28%	72%	

CHAPTER 3

Technical-economic analysis in crop protection equipment at increasing technological levels

Plant protection products (PPPs), commonly referred as pesticides, play a crucial role in securing worldwide food and feed production, especially in high-intensive agricultural areas. On the other hand pesticides use and misuses represent a major public concern about impact of agriculture on environment of food products.

To address these concerns, the reduction of pesticides use is one the main objectives of the policy actions related to agriculture sustainability. For example, this is the strategic theme of the framework directive 2009/128/EC, which proscribes to the state member of European Union action plans for reducing the dependence of agriculture on pes-

ticides.
These objectives can be reached through the implementation of different and complementary approaches, including: rotation of crops and selection of resistant varieties; crop management techniques; planning of appropriate scouting practices; introduction of thresholds for triggering protection treatments; application of biocides and beneficial organisms.
A primary contribution can also come from the technological advances in the equipment used to carry out the protection treatments. This can play a fundamental role in allowing improved capability of pesticide deposition on the plant, and in particular by enabling the practical implementation of precision spraying, i.e. the possibility of varying the amount of pesticide distribution across the field according to the site-specific characteristics of the crop, in opposition to a uniform application of treatments to the fields.
At this point of the dissertation the economic sustainability in adopting advanced system for disease management will be investigated. The analysis is conducted on specialty crops which are high value crops and are considered to be the first field of application of new technologies.

3.1 Theoretical background

3.1.1 Machine performance

In order to contextualize the theoretical basis for the study it will presented the main standards for the agricultural machinery management. The importance of this aspects is given by possibility to provide those who manage agricultural machinery operations assistance in determine optimum practices.
Optimum farm machinery management occurs when the economic performance of the total machine system has been maximized. The performance of a machine system is profitable only when it can add value to products and processes beyond the system's cost of operation.

Field capacity The economic performance of a machinery system is measured in terms of dollars per unit of output (ha h^{-1}; € ha^{-1}; etc.). To summarize the three components of economic performance are:

1. Machine performance;
2. Power performance;
3. Operator performance.

Referring to ASABE Standards (2013) field efficiency is the ratio between the productivity of a machine under field conditions and the theoretical maximum productivity. Considering the field efficiency accounts for failure to utilize the theoretical operating with of the machine; time lost because of operator capability and habits and operating policy; and field characteristics. It is very important to underline that field efficiency is not a constant for a particular machine, but varies with the size and shape of the field, pattern of field operation, crop yield, moisture and crop conditions. A rate of machine performance is reported in terms of quantity per time and represents the machine capacity. To evaluate the effective field capacity C_a (ha h^{-1}) we have to take in account:

s is field speed, km h^{-1};

w is the working width, m, (i.e. the inter-row distance);

E_f is field efficiency, decimal.

$$C_a = \frac{swE_f}{10} \tag{3.1}$$

where: E_f accounts the incidence of idle time on working time.
The term *theoretical field capacity* is used to describe the field capacity when the field efficiency is equal to 1.0, i.e., theoretical field capacity is achieved when the machine is using 100% of its width without interruption for turns or other idle time.

Material capacity is expressed as:

$$C_m = \frac{swyE_f}{10}$$

Where

C_m is material capacity, t h^{-1};

s is the field speed, km h^{-1}

w is the working width, m;

E_f is field efficiency, decimal;

y is unit yield of the field, t ha.

Part of the performance of the machinery is the transporting of materials. Harvesting machinery gather and process grain and forage; seeding machines distribute seeds and fertilizers; atomizers distribute pesticides. In this contest it is possible to talk of *material efficiency*. In the case in which the quality of the transported product is influenced by the machine the most realistic measure of material efficiency must be the reduction of the value of a material after being handled by a machine compared to the value it would have with no material losses or deterioration.

Theoretical capacity Field efficiency decreases with increases in theoretical capacity. One can feel intuitively that a minute wasted with a large machine represents more loss in potential production than the same minute loss with a smaller machine (Hunt and Wilson, 2015). Field capacity we saw depends on the travel speed: increasing the field speed will decrease the actual working time required. At the same time, if time losses remain the same the field efficiency will be less: it is better not use slow speeds to keep the numerical value of field efficiency high. Field speeds may be limited for the following factors:

- overloading the machine's functional units;

- inability of the operator to control the machine accurately;
- loss of function and structural damage to machine due to rough ground surface.

Another point which we took in account during the technical economic analysis is the machine manoeuvrability. Of course machine used inside the speciality crop field are designed to permit them to make short turns at the end of the rows. Nevertheless, considerable time is necessary to manoeuvre the machine. The turning radius of implements is an important factor affecting the time lost in end travel and at corners.
Field pattern permit to improve the field efficiency, of course the pattern depends on the size and shape of the field. The main objective in establishing an efficiency pattern is to minimize the amount of field travel. In fact, nonworking turns, the travel distance in a turn and the amount of nonworking travel in the interior of a field are all valuable time and energy which can be avoided or should be eliminated.

Considering the field efficiency we can say that is represented by the ratio between the productivity of a machine under field conditions and the theoretical maximum productivity. Field efficiency accounts for failure to utilize the theoretical operating width of the machine; field efficiency is not a constant for a particular machine, but varies with the size and shape of the field, pattern of field operation, crop yield, crop moisture, and other conditions. If we want to summarize the majority of the time lost in the field is given by:

- turning and idle travel;
- materials handling;
- cleaning clogged equipment;
- machine adjustment;
- lubrication and refuelling

Field efficiencies are not constant values for a specific machine but vary widely. The theoretical time (τ_t, h) required to perform a given field operation varies inversely with the theoretical field capacity and can be calculated using the following equation:

$$\tau_t = \frac{A}{C_{at}} \tag{3.2}$$

where

C_{at} is the theoretical field capacity, ha h^{-1};

A is the area to be processed, ha.

The actual time required to perform the operation will be increased by a factor dependant on overlapping, time required for turning on the ends of the field, time required for loading or unloading materials, etc. Such time losses lower the field efficiency below 100%.

$$E_f = \frac{\tau_t}{\tau_e + \tau_h + \tau_a} \tag{3.3}$$

where

τ_e = τ_t / w

w = fraction of implement width actually used

τ_a = time losses that are proportional to area, h

τ_h = time losses that are not proportional to area, h

τ_a-type losses are for example unclogging of spray nozzles, adding filling fertilizer or seed boxes, or filling spray tanks. Regarding τ_h-type losses are proportional to effective operating time, τ_e; including rest stops, adjusting equipment, and idle travel at field ends if such travel is at normal operating speed. τ_h concerns the field shape; it can have less importance compared to τ_e if we are working in a narrow field.

Operator performance

The way in which the machine is managed inside the field is one of the component of the economic performance of a machine system. Today electronic devices are used to five more information to the operator. Automation of machine guidance functions has been an interest for agricultural researcher since the beginning of agricultural mechanization.
Precision agriculture has contributed in advance vehicle guidance firstly in terms of providing position information that is required for vehicle guidance. Secondly, precision agriculture has placed the notion of vehicle automation within the conceptual boundary of equipment manufacturers and agricultural producers.
Automatic guidance in tractor present into the market permit to avoid te human operator for steering, an operator of such a tractor or machine might still be needed for detecting contingencies and making decisions Srivastava et al (2006).

3.1.2 Machinery costs

In a farm like in any other economic activity costs have a great influence on profit. For farmers who don't have control on product price the revenue is fixed and profit depends only on the cost.
Machinery costs are divided in costs of ownership and operation as well as penalties for lack of timeliness. Usually ownership costs are called also fixed costs or overhead costs due to their amount is not dependent of the use of the machine itself. Conversely operating costs are strictly dependant of the time in which the machine is used. The sum of operative costs and ownership costs are defined total machine costs. Total per-hectare cost is calculated by dividing the total annual cost by the area covered by the machine during the year.
Per-hectare ownership costs vary inversely with the amount of annual use of the machine. Therefore, a certain minimum amount of work must be available to justify purchase of a machine and, the more work

available, the larger the ownership costs that can be economically justified.

Ownership costs Ownership costs include depreciation of the machine, interest on the investment, and cost of taxes, insurance and housing of the machine.
Depreciation is often the largest cost of farm machinery (Srivastava et al, 2006), measures the amount by which the value of a machine deceases with the passage of time whether used or not. The actual total depreciation can be never be known until the equipment has been sold (ASABE Standards, 2013). To estimate the depreciation at the end of each year the value of a machine is compared with its value at the start of the year (fig. 3.1). The difference is the amount in depreciation. The estimated values of aged farm machines are established at farm sales, at specialized machinery auctions, and by farm equipment dealers through use of guides. There are significant variations due to make and models.
The machine's value at the end of its life (V_{end}, €) is given by:

$$V_{end} = V_0(1 - D_r)^l \tag{3.4}$$

where:

V_0 is the value of the new machine, €;

D_r is the depreciation rate, %;

l is the effective life of the machinery, year.

Factors of depreciation:

Physical obsolescence: The parts of the machine become worn whit use and cannot perform as effectively as previously. These parts are the economically irreparable mechanism in a machine (ex. machine frame);

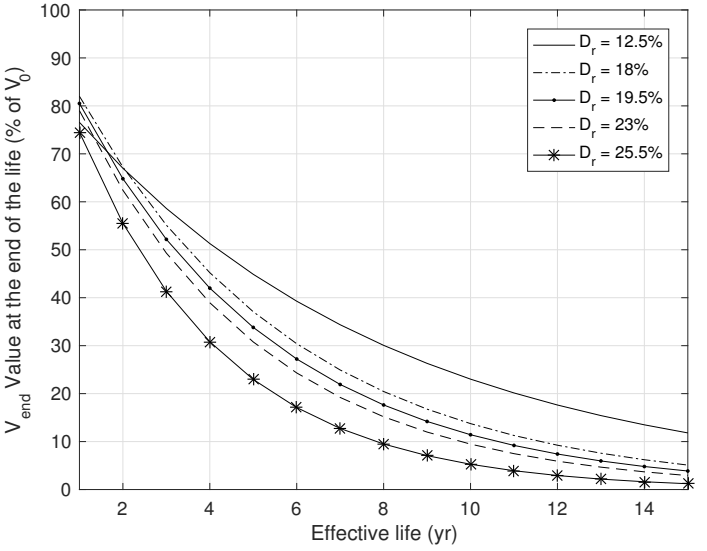

Figure 3.1: *Estimation of V_{end} in function of the effective life of the machinery (l), and of the depreciation rate (D_r)*

Operative costs growth: The expense of operating the machine at its original performance increases as more power, labour, and repair costs for the same unit of output are required;

Economic obsolescence: A new, more efficient machine or practice become available. The existing machine may be functionally adequate but because of new technology it is uneconomic to continue to operate it.

Farm characteristic: The size of the enterprise is changed and the existing machine's capacity is not proportionally adequate.

The main concepts which we have to take in account in machine economic management are: the physical life, accounting life, and economic life. The physical life ends when a machine cannot be repaired due to the absence of repair parts or irreparable part failures. The accounting life is the predicted life of a machine based on survey use of existing machines and from the design life for new machines. Usually

the accounting life is expressed in hours so we can calculate the predicted life in years by dividing the wear-out life by the annual use of the machine itself.
The economic life is very important and is defined as the length of time from purchase of a machine to that point where is more economic to replace with a second machine than to continue with the first. It's very important to underline that at this time a machine may still have considerable service life but for an economic analysis it must be replaceable. In the case in which the machine is sold the price paid by the second owner will determine the depreciation cost to the first owner.

The interest on investment in a farm machine is included in operational cost estimates. Nominal interest rates include expected inflaction and the time value of money invested in the machinery it they were not invested. Due to the trend of depreciation the amount will be variable each year. Considering ASABE Standards (2013), a method for determining the capital costs of ownership which includes the time value of money makes use of a Capital Recovery Factor, (CRF). The investment in the machine is multiplied by the proper CRF to give a series of equal payments over the life of the machine which includes both the cost of depreciation and interest.

$$R = (P - S)\left[\frac{\left(\frac{i}{q}\right)\left(1+\frac{i}{q}\right)^{nq}}{\left(1+\frac{i}{q}\right)^{nq}-1}\right] + \frac{Si}{q} \tag{3.5}$$

where:

R is one of a series of equal payments due at the end of each compounding period, q times per year;

P is principal amount;

i is interest rate as compounded q times per year;

n is life of the investment in years;

S is savage value.

Other expenses are considered taxes, insurance and machinery shelter. Due to the high variability of this expenses they were evaluated as a percentage (1.5 - 2%) of equipment initial value V_0. In detail we have:

- taxes 1%;
- housing 0.75%;
- insurance 0.25%;

To evaluate the total annual ownership costs ASABE Standards (2013) propose to multiply the purchase price of the machine by the ownership cost percentage which can be calculated with the following equation:

$$C_o = 100\left[\frac{1 - S_v}{L} + \frac{1 + S_v}{2}i + K_2\right] \tag{3.6}$$

where:

C_o is the ownership cost percentage;

S_v is salvage value factor of machine at end of machine life, decimal;

L il machine life, yr;

i is interest rate, decimal;

K_2 is ownership cost factor for taxes, housing, and insurance.

Costs of operation

Costs for operation vary directly with the amount of use and are often called variable costs. This types of costs are associated whit the use of machine. They include the costs of labour, fuel and oil, and repair and maintenance.
Variable costs may be greater than ownership costs, for some high-use

machines. The actual estimation of variable costs is usually based on hours of use of the machinery. The cost of the operator is relatively easy to estimate, it is not possible tell the same think for repair and maintenance factor.

Repair and maintenance costs (C_{rm}, € h^{-1}) are the expenditures for parts and labour for installing replacement parts after a part failure and reconditioning renewable parts as a result of wear these costs are highly variable depending on the care provided by the manager of the machine but tend to increase with the size and complexity of the machinery and the with the purchase price of the equipment itself (see figure 3.2).

$$C_{rm} = RF1 \frac{(E_l\ AWt)^{k-1}}{Ph_l^k} V_0 \tag{3.7}$$

where:

V_0 is the value of the new machine, €;

E_l is the economic life, year;

Ph_l is the estimated physical life, h.

$RF1$ is the fraction of V_0 which is needed to cover C_{rm} along l;

k is a coefficient which define the intensity of variation of the hourly C_{rm} costs. Higher values are for machinery which have low hourly costs of use (tractors, 1.9), lower values are for equipment with high hourly cost for low intensity in use (sprayer, 1.3)

To predict the fuel consumption for a specific operation it is necessary to determine the total tractor power for the executing operation and the specific fuel consumption of the tractor cs_t (g kWh^{-1}).

$$cs_t = cs_{min} \left[2 - \left(2 - \frac{\lambda}{\lambda_0} \right) \frac{\lambda}{\lambda_0} \right]$$

where:

cs_{min} is the minimum specific fuel consumption (220 g kWh^{-1});

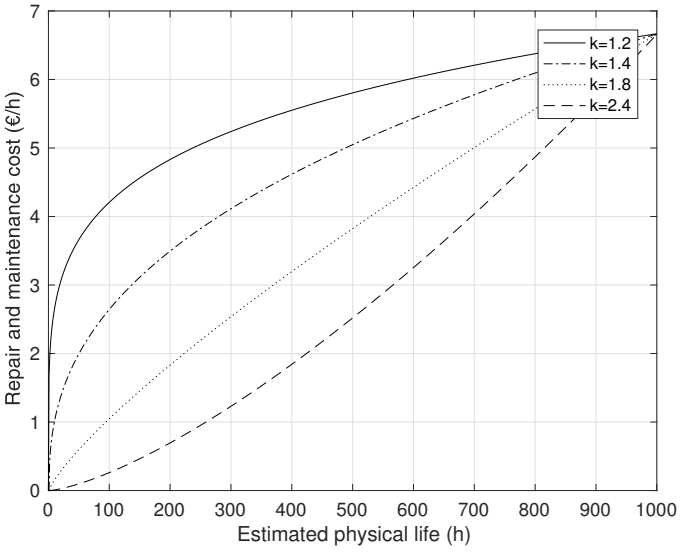

Figure 3.2: *Maintenance and repair cost variation at different k coefficients (V_0 = 100000 €; RF = 0.8; Ph_l = 12000 h; E_l = 12 yr)*

λ is the average engine load, decimal;

λ_0 is the engine load in which there is the minimum specific fuel consumption.

Engine oil consumption is based on 100 h oil change intervals, and is defined as the volume per hour of engine crankcase oil replaced at the manufacturer's recommended change interval. ASABE Standards (2013) help in estimating the oil consumption (l h^{-1}) considering different motor types:

Gasoline	$0.000566\ P_n + 0.02487$
Diesel	$0.00059\ P_n + 0.02169$
LPG (liquefied petroleum gas)	$000041\ P_n + 0.02$

For our purpose we calculate the lubricant costs amount with the

following equation

$$C_{oil} = 0.0004956\ P_n + 0.01822$$

where P_n is the power of the tractor (kW) and the values expressed are empirical data. C_{oil} is expressed in kg h^{-1}.
Regarding the labour cost should be determined from alternative opportunities for use of time when the operator coincide with the owner of the farm, but for a hired operator a constant hourly rate is appropriate.

3.1.3 Machinery selection and replacement

The chose of the appropriate field capacity for a machine is a very important issue. The final purpose for the farm operator is to have the maximization of profit with the optimal capacity. There is a positive correlation between the per-hectare machinery costs and the farm size because the land area is fixed and larger machine cost more than the small machines. Timeliness is an important factor in almost all the farm operations. In this sense the larger machines are able to complete the work quickly but are more expensive than the smaller one. In situation like orchard or vineyard the influence of the type of farming is the bottleneck for the machine dimension. Timeliness costs rise sharply when machines are too small to complete the work in a timely manner (Srivastava et al, 2006).

Mathematically, the field capacity giving least total cost for an individual machine can be determined by combining all of the cost equations into one equation and differentiating with respect to field capacity.

$$C_{aopt} = \sqrt{\frac{A}{C_{os}K_p}\left[L_c + T_{fc} + \frac{K_\tau AYV}{\lambda_o TPwd}\right]} \tag{3.8}$$

where:

C_{aopt} is the optimum field capacity, ha h^{-1};

L_c is the labour cost, € h^{-1}

K_p unit price function

A value for T_{fc} can be determined by using the following equation:

$$T_{fc} = \frac{C_o}{\tau_{At}} \tag{3.9}$$

where:

T_{fc} is the amount charged to machine for tractor use, € h^{-1}

C_o is the annual ownership cost of tractor

τ_{At} total annual use of tractor, h yr^{-1}

When the machine life is finished due to the economic life is over or the physical life reached the limit the equipment have to be replaced. How previously mentioned a machine can finish its life also due to the repair parts are no longer available or when the replacement can produce a greater profit.
Usually processing machines (balers, combines, atomizers, etc.) becomes obsolete faster than tractors. The substitution is essential when the frequency of breakdowns become so large to represent a problem executing the works. Large economic penalties can result when field work is delayed and an unreliable machine can cause delays.

To resume machines, have to be replaced when:

- Accidents have damaged the implement beyond repair;
- Field capacity of the machine is inadequate because of an increase in the scope of the operation
- a new machine or farm practice makes the old machine obsolete
- anticipated costs for operating the old machine exceed those for a replacement machine

Time of replacement decision depends on the accumulated costs over a period of years (Hunt and Wilson, 2015). The incidence of the cost is very high during the first year because a real marketplace depreciation obtained from the estimated value method. After the first period the incidence of fixed cost drop and raise the value of repair and maintenance. The optimum replacement time is at crossing point since the accumulated cost curve (fixed cost and variable costs) is at a minimum and is expected to rise after that point.
To predict when a machine has to be replaced is necessary to know an average expected use of the machine per each year to have an idea of the annual fixed cost and annual variable costs. Replacement time is the point at which accumulated costs divided by accumulated use is minimum. Of course the best method to predict the optimum replacement time is based on marketplace remain value previously exposed (see equation (3.4)).

The very important factor today is the determination of the obsolescence which increase at each year at a constant rate. An obsolescence factor can be defined as the rate of drop in machine value with time as desirable new features are added to new models. An obsolescence factor, ObF, can be estimated. Supposing a machine of 15000 € with a straight line depreciation. If the economic life of the machine is 20 years but for us it become worthless after 10 years, the cost of obsolescence would be € 7500/10 i.e. 750 € yr^{-1}.

3.1.4 Sensitivity analysis

For our study we took in account also the sensitivity analysis of a model. The output of this technique aims to quantify the relative importance of each input model parameter in determining the value of an assigned output variable (Homma and Saltelli, 1996). Many techniques are developed around the sensitivity analysis, and they can be classified in two main branches: local S.A., and global S.A.

Local sensitivity analysis looks at the modification of the model

output to small changes in the model inputs. The slope, or derivative, of the model response in a very small neighbourhood is used to estimate the local sensitivity of a function.

$$\frac{\delta y}{\delta x}|x_0$$

where x_0 specifies the neighbourhood in which the local sensitivity is to be estimated and δ represents the small change or partial derivative on the function.
Local S.A. can be very quick and informative method of understanding how model output responds to its uncertain factors but only for small factor changes and so does not directly provide the sensitivity of the model response over the whole of the range of uncertainty.

Global S.A. focuses on the output uncertainty over the entire range of values of the input parameters. The values of input are in a range specific for each parameter. S.A. can then help to identify key parameters whose uncertainty affect most the output, helping in establish research priorities. At the same time the opposite problem it is possible to investigate the interrelationship between system description and different scales (Petropoulos and Srivastava, 2016).
In an uncertainty setting, this means have a function $Y = f(X)$ whit n uncertain factors $X = \{X_1, X_2, \ldots, X_n\}$ and we want to understand how the uncertainty in X leads to uncertainty in Y and, in particular, how the individual elements of X, lead to uncertainty in Y across the range of G_i which represents the uncertainty distribution.
One-at-a-time sensitivity analysis methods are a way of testing the effect of perturbation of uncertain model factors on the model one at a time (Daniel, 1973). This approach was used during the technical-economic analysis.

3.1.5 Social-economic impact of automation

How previous explained (paragraph 1.1) one the objective of the study is the exploration of the possibility of the introduction of completely autonomous machinery in precision pest management. It seems interesting to understand how automation is changing the human role in production, services, organizations and innovation. All these changes are going to alter also the society stratifications, human values, requirement in skills and individual conscience. Automation means all kinds of activities perfected by machines and not by the intervention of direct human control. How it is easy to understand this definition can cause a series of concerns regarding the human factor in the development. The concept, which give us an idea about the question is the man-machine paradox because the human role in all kinds of automation is a continuously emerging constituent of man-machine symbiosis, with feedback to the same (Nof, 2009).

Due to the diffusion of automated systems in everyday life it is very difficult to separate the progress of the technology from general trends and usage. It is enough to think that about 70% of all the aircraft function are related to automation and the limit is related only to humans rather than to technology. What is important to understand is that the crucial point is the changing of human roles due to mechanization-automatization processes. Trying to compare the impact of automation in the society we have to think about the end of slavery and the consequent development of mechanization or about the acquisition of equal right for women during the past century. The most important effect is a direct consequence of the statement that the human being is not a draught animal anymore, and this is represented in the role of physical power.

The introduction of automation in agricultural activities implies effects in the production function of the company and it has an effect on

costs flexibility. The transformation of a labour-intensive process into a capital-intensive one implies the modification of cost structure of the enterprise by increasing the capital cost while reducing the labour costs.
Let the total cost C_T be defined by the cost of the three factors, namely intermediate goods, labour, and capital respectively

$$C_T = p_X X + wL + c_K K \tag{3.10}$$

where

p_X is the unitary cost of the intermediate goods;

X quantity of intermediate goods;

L quantity of labour;

w unitary cost of labour;

K denotes the quantity of capital;

c_K denotes the unitary cost of capital

Referring total cost to the production Q, the cost per production unit c can be stated assuming constant capital value in the short term

$$c = \frac{C_T}{Q} \tag{3.11}$$

On the contrary, in capital-intensive systems, the presence of large amounts of automation induces the following effects:

1. Labour productivity λ_A surely greater than that which could be obtained in labor-intensive system ($\lambda_A > \lambda_X^*$);

2. A salary w_A that dows not require incentives to obtain optimum efforts from workers, but which implies an additional cost with respect to the minimum salary fixed by the market ($w_A \lessgtr w_E^*$), in order to select and train personnel

3. A positive correlation between labour productivity and production quantity, owing to the presence of qualified personnel who the enterprise does not like to substitute, even in the presence of temporary reductions of demand from the final product market

$$\lambda_A = \lambda_A(Q), \quad \delta\lambda_A/\delta Q > 0, \quad \delta^2\lambda_A/\delta Q^2 = 0 \tag{3.12}$$

4. A significantly greater cost of capital, due to the higher cost of automated machinery, than that of a labor-intensive process ($c_{KA} > c_K$), even for the same useful life and same rate of interest of the loan.

According to these statements, the unitary cost in capital intensive system can be stated as

$$c_A = p_X\beta + w_A/\lambda_A(Q) + c_{KA}K/Q \tag{3.13}$$

Denoting by profit per product unit π the difference between sale price and cost

$$\pi = p - c \tag{3.14}$$

The relative advantage of automation D, can be evaluated by the following condition

$$D = \pi_A - \pi \tag{3.15}$$

Except in extreme situations of large underutilization of production capacity, the inequality $w_E^*/\lambda_L^* > w_A/\lambda_A(Q)$ denotes the necessity condition that assures that automated production techniques can be economically efficient. In this case, the greater cost of capital can be counterbalanced by greater benefits in terms of labor cost per product unit.

The result shows that automation could be riskier than labour-intensive methods, since production variations induced by demand fluctuations could reverse the benefits.

Automation in economic activities is characterized by dominance of capital dynamics over the biological dynamics of human labour. Automation plays a positive role in reducing costs related to both labor control, and supervisors employed to assure the highest possible utilization of personnel. In spite of this positive effect there is a greater rigidity of the cost structure: some variable cost change into fixed costs. This induces a greater variance of profit in relation to production volumes and a higher risk of automation in respect to labour-intensive systems (Ravazzi and Villa, 2009).

3.2 Analysed scenarios and applied methodology

3.2.1 The considered crops and the adopted protection protocols

In this work two speciality crops were considered as case studies: grapevine (*Vitis vinifera*) and apple orchard (*Malus domestica*), two of the most diffused crops worldwide. To define a general protection protocol of these specific crops, we focused on the most relevant and frequent diseases found in the intensive production areas of Central-Southern Europe, and we relied on the typical crop protection strategy generally adopted in these areas.

To conduct the technical-economic analysis is necessary to preliminary define the main crop management and protection parameters adopted: number of treatments per season, time available to carry out the treatments, used active ingredients (AI) and their costs, application rates, and row distance in orchards.

The quantification of the number of treatment executed in one productive season, the costs and the application rate of pesticides most diffused and the machine field speed were referred to best practices adopted in this region.

All technical data are based on technical literature review (Anon, 2016a; Bohren et al, 2016a,b; Anon, 2016d,e,b) and personal communications from crop protection experts advisers and growers.

Grapevine scenario

Under the considered pedoclimatic conditions, the most diffused and important diseases in grapevine are due to the pathogenic fungi *Botrytis cinerea* (grey mold), *Plasmopara viticola* (downy mildew) and *Erysiphe necator* (powdery mildew) (Brewer and Milgroom, 2010; Williamson et al, 2007). Usually the protection against the last two pathogens is conducted within the same treatment, and it consists on average of 10 to 15 fungicide applications per season. On the other hand, *B. cinerea* typically requires 1 to 3 specific treatments per season.
The available time to carry out an effective protection treatment is largely depending on local specific condition. Nevertheless, a reasonable range might be considered between 2 and 4 days. In our analysis a conservative value of 2 days was assumed for all the diseases considered.
Fungicide active ingredients typically used to protect vineyards from downy and powdery mildew are *fosetil aluminium, ditihocarbamate, cyazofamid, sulfur, penconazol* and few others; while for grey mold *pyrimethanil, boscalid, fluopyram* and others specialised fungicide are used.

The cost range for different active ingredients is varying with diseases. An average cost of 10 to 35 € kg^{-1} and of 25 - 50 € kg^{-1} is typical for powdery mildew and downy mildew respectively. Against grey mold, the AI costs ranges from 80 and 120 € kg^{-1}.
A certain variability can be also found in AI application rates: for downy mildew and powdery mildew application rates of 3.5 to 7 kg ha^{-1} and from 1 - 3.5 kg ha^{-1} are adopted. For grey mold the adopted AI application rates ranges from 0.8 - 2 kg ha^{-1} and, as a particular feature, it must be noted that for this treatments the spraying equipment is set to only target on a limited (50 - 70 cm) band of the canopy height corresponding to the so called "cluster belt" where all the berry bunches grows.
Based on this general framework and considering a typical inter-row

distance of 2.3 m in vineyard, we assumed the parameters detailed in table 3.1 as representative for grapevine protection scenario. The treatments against powdery and downy mildew are all referred as TRG1 treatments group. On the other hand, due to the specificity of protection treatments against grey mold, their operative characteristics are separately referred as TRG2 treatments group.

Apple scenario

Under the considered pedoclimatic conditions the most diffused and important diseases in apple crop are due to the pathogenic fungi *Venturia inaequalis* (apple scab) and *Podosphaera leucotricha* (powdery mildew) (Williams and Kuc, 1969). Usually the protection against the two pathogens is conducted within the same treatment. The number of application is largely depending on local whether conditions and can typically range from 15 to 32 fungicide applications per season.
Also the time available to carry out an effective protection treatment strictly depends on local specific conditions. A reasonable range might be considered between 2 and 4 days. In our analysis a conservative value of 2 days was assumed for all the diseases taken in consideration.
Fungicide active ingredients typically used to protect apple orchards from apple scab and powdery mildew vary from the traditional and relatively inexpensive *copper oxychloride* to high-priced *cyprodinil*. Other active ingredients that are used in protection protocols are *bupirimate, dithianon, pirimetanil*.
The cost range for these active ingredients varies on average 20 to 50 € kg^{-1}.
A certain variability can be also found in the application rates varying from 1 kg ha^{-1} to 5 kg ha^{-1} per treatment.
Based on this general framework and considering a typical inter-row distance of 3 m in apple orchard, we assumed the parameters detailed in table 3.1 as representative for the apple protection scenario. All the treatments on apple are referred as a common TRA treatments group.

Table 3.1: *Protection treatment parameters considered for the technical-economic analysis.*

	Grapevine		Apple
	TRG1[(a)]	TRG2[(b)]	TRA[(c)]
Number of treatments (n yr^{-1})	13	2	25
Available time (d tr^{-1})	2	2	2
AI cost (€ kg^{-1})	18	90	32
AI application rate (kg ha^{-1})	5	1	1.5

[(a)] TRG1 refers to protection treatments on grapevine against powdery and downy mildew
[(b)] TRG2 refers to protection treatments on grapevine against grey mold
[(c)] TRA refers to all the protection treatments on apple

3.2.2 The different spraying equipment considered

Technological characteristics of the spraying equipment

In this analysis three different spraying equipment, hereafter referred as L0, L1 and L2 (figure 3.3), were considered. These types of machines are characterised by the adoption of different technological levels which enable increasing capability of adapting the application rate and the spraying pattern to the site-specific canopy characteristics. As consequence, we assume for each technological level an associated saving in pesticide application, without any negative effect on crop protection efficiency.
Machines characteristics are defined in accordance with actual models present in the market, or with latest evidences from literature when more advanced equipment is considered. To conduct economic analysis of machinery, average market prices were adopted whenever possible. In contrast, when considering higher level of automation nowadays proposed only as prototypes, machinery cost was estimated by using current costs of technological components and including a raw assessment of industrial development cost.

The main characteristics of the different technological levels of the spraying equipment are described in the following:

L0 refers to state-of-the-art equipment, i.e. the conventional tractor-coupled air-blast sprayer used for vineyard and orchard crop protection. The spray application to the crop is conducted at a constant flow-rate which, in turn, corresponds to a homogeneous application rate, provided that field speed is kept constant during the treatment. The application accuracy of this equipment highly relies on: 1) the calibration of spraying patterns; 2) the calibration of the air-flow carrier pattern; 3) the homogeneity of canopy shape and volume across all the orchard/vineyard plots. In real field situation this generally leads to an AI over-application where the canopy volume is lower, and to AI deficiency when it is higher (Gil et al, 2013).

In our analysis, L0 represents the equipment reference level against which the possible cost and benefits of more advanced technologies are quantified.

L1 refers to an air-blast sprayer equipped with: 1) a sensing systems (e.g. ultrasonic sensors) able to detect the canopy presence in the sprayed area; 2) a control system which can correspondingly switch on or off each single nozzle in real time during the treatment.

Therefore L1 is assumed to be capable of distributing pesticides only in presence of canopy, while some or all the nozzles are switched off when vegetation is not present (e.g. canopy gaps, heterogeneity in plant size, raw turnings etc.).

Examples of such spraying equipment can be found in Balsari and Tamagnone (1998); Moltó et al (2001); Downey and Giles (2005). The use of this typology of machines allowed significant reported savings when compared to a corresponding homogeneous application rate (i.e. obtained with L0 equipment). The obtained savings depends on the operative conditions, and they

Table 3.2: *Agrochemical savings assumed in this study for L1 and L2 technological levels compared to L0.*

	Grapevine		Apple
	TRG1	TRG2	TRA
L0	0%	0%	0%
L1	20%	10%	20%
L2	35%	20%	35%

range from about 10%, when treating vineyard with rather homogeneous managed canopy, up to more than 35% for young olive trees exhibiting large gaps between single plants vegetation.

L2 refers to air-blast sprayer equipped with: 1) an advanced sensing system (e.g. LIDAR sensors or time of flight 3D cameras) able to detect the shape and volume of the sprayed canopy; 2) a control system which correspondingly vary the flow-rate sprayed by each single nozzle proportionally to the vegetation target; furthermore, actuators are controlled to real-time adjust the nozzles and air-deflectors geometry in order to adapt the air-carried spraying pattern to the canopy characteristics. Examples of similar equipment are described by Solanelles et al (2006); Escolà et al (2007); Balsari et al (2009); Gil et al (2013); Escolà et al (2013). The reported savings obtained with these advanced prototypes are in a range of 25% to 45%, depending on the specific considered conditions.

Based on the results reported in scientific literature, for technological level L1 and L2 we assumed savings in agrochemicals compared to L0, as indicated in table 3.2. These savings are related to grapevine and apple crops protection protocols, and imply no reductions in protection efficiency when compared to conventional treatments.

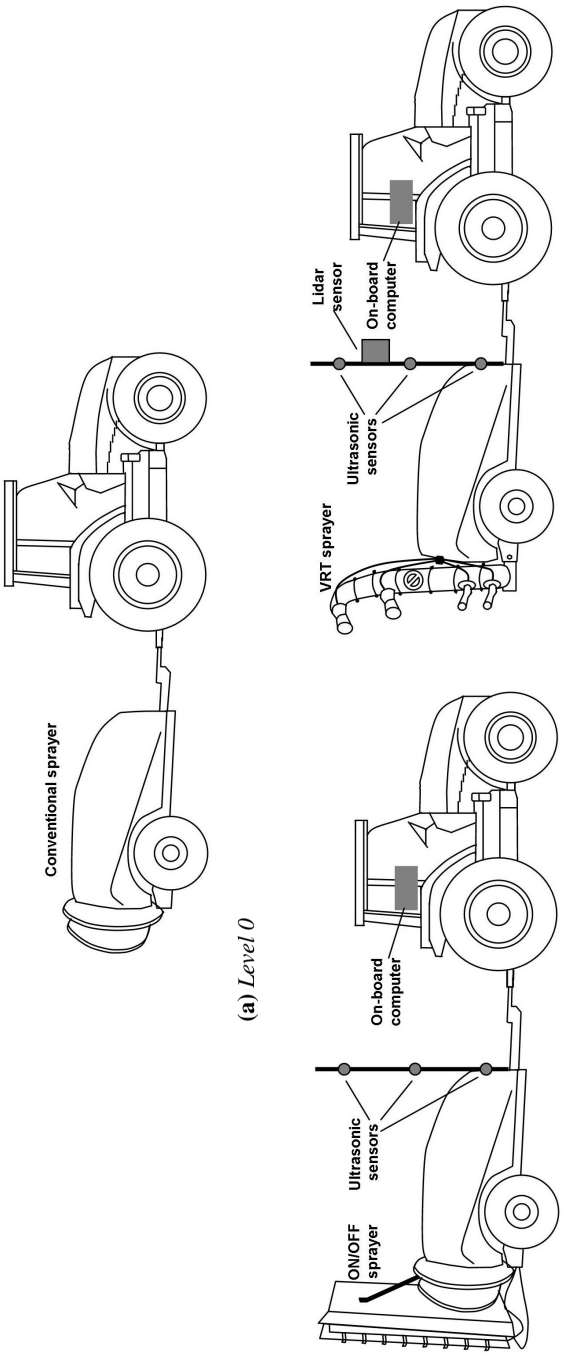

(a) *Level 0* **(b)** *Level 1* **(c)** *Level 2*

Figure 3.3: *Schematic representation of the three considered typology of spraying equipment at increasing technological level.*

Operative characteristics of spraying equipment

In order to compare the profitability of the L1 and L2 technological levels compared to L0, it is necessary to compute their corresponding field capacity (3.1).
Regarding the field capacity among other parameter it depends on the travel speed, which is a very important parameter due is limited by the characteristics of the equipment used, but essentially from the type of operation conducted. A good operator test and judge the crop and soil conditions and then operate as fast as possible.
In the analysis it was define a field speed (table 3.3) adequate to the condition of fields in the soils in the geographic region considered and acceptable for the spraying operation according to the references (Hunt and Wilson, 2015; ASABE Standards, 2013; Srivastava et al, 2006).
For spraying operation, idle time is mainly the time for turns and for tank fillings. In our analysis we assumed an incidence of turns conservatively equal to 15% of spraying time. This is due to in orchards and vineyards usually small machines are used which are able to cover a narrow angle easily.
In the analysis we suppose fields with a shape optimized for the operations, it means that in fields we have the minimization of: nonworking turns, the travel distance in a turn, and the amount of nonworking travel inside the field.
The same consideration of optimal field structure was done considering the filling time, it was supposed a standard distance from the source of water for all the farm sizes selected. Filling time, thanks to spray savings obtained with L1 and L2 technological levels, is considered proportionally decreasing in association with L0, L1 and L2 equipment respectively.
In detail, filling time was assumed 25% of spraying time for L0, while this value was reduced according to savings (table 3.2) for L1 and L2 equipment. This leads to the following expression for the field effi-

ciency of the spraying equipment:

$$E_f = \frac{1}{1 + \tau_t + \tau_f \left(1 - S\right)} \tag{3.16}$$

where:

E_f is the field efficiency, decimal;

τ_t is the turning time incidence, decimal (in our case 0.15);

τ_f is the filling time incidence, decimal (in our case 0.25);

S is the specific degree of savings in agrochemicals for each technological levels, decimal.

Given the field speed s (set at 6 km h^{-1} for all the three equipment), and substituting E_f as resulting in Equation (3.16), is then possible to obtain the equipment effective field capacity by Equation (3.1).
Another important consideration is the definition of the number of machinery necessary to perform the operation in an tolerable time. Considering to have a defined area A (ha) after the evaluation of the effective field capacity of the machine (ha h^{-1}) we can calculate how many hours a single tractor sprayer combination needs to cover the field. At the same time the biological characteristics of the disease to be treated is the bottle neck which define how much time there is for treating the field, dividing the result of the previous division for the time available for the treatment (t_a). Whether the hours founded exceed the turn shift which is available for the treatment there is the obligation to add another tractor-sprayer combination to the farm. Summarizing considering a growing farm area A (ha), and setting the time available for field work each day (G) at 11 h d^{-1}, it follows that the number of sprayer-tractor equipment units (N_u) necessary to execute the treatment in the available time t_a (d tr^{-1}) according to the specific protection parameters defined in table 3.1, is:

$$\lceil N_u \rceil = \frac{A}{C_a \, t_a \, G} \tag{3.17}$$

Table 3.3: *Technical parameters related to different technological levels of spraying equipment.*

	Tractor	Sprayer
	L0 - L1 - L2	L0 - L1 - L2
Engine power (kW)	50	-
Average engine load (%)	65	-
Field speed (km h^{-1})	6	6
Tank volume (dm^3)	-	1500
Time available each day (h d^{-1})	11	11

where $\lceil x \rceil$ represents the ceil function which map a real number to the largest integer greater than or equal to the value x.
The technical parameters related to the considered equipment at different technological levels are reported in table 3.3. The amount of power and the amount of energy required for performing various farm tasks are neither precise nor constant, but we can estimate field operation energy for any given farm from the performance of an existing implements. Draft and power are important in selecting tractors and implements because tractors must be large enough to supply power requirement for the field operation.
In the analysis the power has been chosen in accordance with the sprayer requirements and tabled values (ASABE Standards, 2013; Srivastava et al, 2006).

3.2.3 Economic analysis of spraying equipment

The economic analysis was applied to vineyard/orchard hypothetical farms with a growing area A varying from 5 ha to 200 ha. The analysis considered the investment and operating costs of the three types of spraying equipment and the pesticide costs used for protection treatments.

Spraying equipment costs

In order to evaluate the costs of the considered spraying equipment, the methodology defined by ASABE Standards (2013) was applied. This approach accounts for ownership costs (including depreciation rate, interest rate for the machinery investment, taxes, housing and insurance) and operating costs (including labour, fuel and lubricants, repair and maintenance). Table 3.4 summarises the economic parameters used for applying the ASABE methodology.

In order to compute the operating costs of the equipment, the annual

Table 3.4: *Economic parameters related to different technological levels of spraying equipment.*

	Tractor	Sprayer
	L0 - L1 - L2	L0 - L1 - L2
Purchase price ('000 €)	50	12 - 24 - 40
Economic life (yr)	12	6
Depreciation rate (%)	12.5	18
Estimated life (h)	12000	2000
Repair and maintenance factor (%)	80	60
Labour cost (€ h^{-1})	20	-
Annual interest rate (%)	3.5	3.5

work time (AWt, h yr^{-1}) was obtained as:

$$AWt = n_{tr} \frac{A}{N_u \, C_a} \tag{3.18}$$

where:

n_{tr} is the number of annual treatments associated to the protection protocol (table3.1)

AWt value is extremely important because it gives us a forecasting of the real life of the equipment. For example, supposing we have in one case AWt equal to 500 h yr^{-1} and our sprayer has 2000 h of estimated

life, with an economic life of 6 years. In this case the nominal AWt_n limit for the equipment is given by the ratio $2000/6 = 333.3\ h$ which is greater than our needs. In this case the physical life is a limit because $2000/500 = 4$ year. It means that we have to replace our sprayer within the fourth year of usage. Inversely supposing a $AWt = 250$ in this case the economic life will be the limit for the replacement of the equipment.
The cost of the tractors used during the analysis were taken from the price list of the machines present in the market for all the level of automation studied (L0, L1, L2). The price is variable in base of the manufacturer, the intrinsic characteristics of the machines, and also the reference market (Europe/USA/Asia). In this sense the varibility is in the order of ±10000 €. The final tractor cost was harmonized for all the levels to 50000 €.

Considering now the cost of sprayer utilized in L0 we took the price lists of the major manufacturer companies present in the market. The price lists were taken in account considering the technological characteristics of the equipment and the operating parameters used in the analysis. For L0 sprayer system the average price list found it was 12400 €, which was rounded to 12000 € during the simulation. The standard deviation of the price stood around ±5400 €.
Considering the sprayer in L1 the machine is still not present in the market but they exist in form of manufacturer prototypes. Sprayers present in the market have systems to control the flow rate in base of the machine speed advancement in the field. By a comparison of the characteristics and a raw estimation of the components hypothesized (see table 3.5) we estimate the total cost of the sprayer in L1 in 24000 €. In fact, on total component cost is necessary to add a perceptual for the manufacturing and of engineering that we quantify in approx. 40% of total cost. Supposing the use of 6 ultrasonic sensors in L1 equally distributed in both sides of the machine we quantify the raw cost of sensors in 2500 €.

Table 3.5: *Estimation of the development cost of L2 equipment on the hypothesized component.*

	L1 Components cost (€)	L2 Components cost (€)
Sensors	2500	7000
VRT system	3000	6000
Controller	4000	5000
Base platform	10000	10000
Total	17500	28000

The situation is completely different in the L2 case due to the absence both in market and as manufacturer prototype of spraying equipment with the characteristics presented in section 3.2.2. For this reason, the main strategy to estimate the purchase price of the machine was the consultation of the hypothesized machine's components price list and an estimation of the industrial development cost. In table 3.5 are summarized the main components of the L2 equipment with the associated price. Supposing the use of advanced sensors like time of flight cameras or LiDAR sensors the total amount of sensor cost was estimated in 7000 €. Also in this case we add a perceptual for the manufacturing and of engineering that we quantify in approx. 40% of total cost.

To estimate the value of the equipment at the end of its life (V_{end}, see equation (3.4)) in the analysis we use a uniform rate applied each year to the annual remaining value of the machine, it means that the depreciation amount is different for each year of the machine's life. The sprayer for the structural characteristics and the intense use it is subjected it will be a depreciation rate higher than the tractor which present few intensive used components.
In section 3.1.2 it is described how the annual use of the equipment influences the operative costs which are for definition variable costs. The amount relative to the operating costs are added to the fixed costs described above to arrive at the annual cost for a machine operation.

Referring to real farm practice and timeliness needs, we assumed that the tractor coupled to the sprayer is solely employed for protection operations. In detail operating costs include the repair and maintenance cost, labour costs, fuel and oil consumption.
The average engine load, necessary to quantify fuel and oil consumption, is assumed to be 65%. The cost for fuel and lubricant it was found in the range of 9 € h^{-1}.
Lubricant consumption is based on 100 h oil change intervals. The consumption rate of oil ranges from 0.0378 to 0.0946 L h^{-1} depending upon the volume of the engine's crankcase capacity.
The last component of operating cost is the labour cost, which vary with the geographic location. In the analysis we tried to select a median value for the labour hourly cost (see table 3.4).

Treatment costs

In order to compare the treatment cost (APC) and corresponding benefit of the different technological levels, it is necessary to compute the total costs of used pesticides basing on their unitary cost (AI_p in € kg^{-1}), the application rate (AI_{ar} in kg ha^{-1}) and the number of annual treatments (n_{tr}) associated to the protection protocol (table 3.1). Thanks to the savings (S, decimal) associated with the specific technologies (table 3.2), the costs for the treatments conducted using equipment L1 and L2 were decreased correspondingly.

$$APC = n_{tr}\ AI_{ar}\ (1 - S)\ AI_p \tag{3.19}$$

Total costs of protection treatments

The annual total costs per hectare associated to the use of the three typologies of equipment were computed by adding ownership, operating and pesticide costs:

$$ATC = \frac{AOC + AWt\ OC + APC}{A} \tag{3.20}$$

where

AOC are the annual ownership costs of the equipment, € yr^{-1};

OC are the annual operating costs of the equipment, € h^{-1};

AWt is the annual work time, h yr^{-1};

APC is the annual protection costs, €;

A is the vineyard/orchard area, ha.

3.2.4 Advanced robotic level as perspective scenario

In a speculation about perspective developments of crop protection equipment, we hypothesized the introduction of an advanced robotic platform (hereafter referred as equipment of technological level L3) able to carry out autonomous protection treatments, and to target the spraying of pesticide only where needed by the crop, namely on disease foci and on buffer canopy regions around the infected areas. The effect of this hypothesis is that is possible to ignore the labour cost in the formation of operative costs. At the same time we expect high expenses relative to the automation system.
The robotic platform L3 is assumed to be equipped with a disease detection system (e.g. based on multi-spectral or hyperspectral sensors) and an on-board intelligent classifier, possibly connected with a remote assisting information system. The robot actuators are assumed to perform localised spraying spots onto the identified targets and modulated application on buffer areas, according to the severity of the symptoms and the risks of infection's spreading.
A possible example of such an advanced approach was explored with the CROPS robotic platform (www.crops-robot.eu). Starting from the experimental results by Oberti et al (2016), even if very partial, in our analysis we hypothesized that for both treatments on grapevine and apple crops the robotic technology corresponding to this perspective scenario L3 can enable pesticide saving of 75%, as compared to the

reference scenario L0. Also in this case, the savings are assumed to be obtained without negatively affecting the protection capability of the selective treatments.

Inherently this selective approach, it is the fact that not all the crop area is covered by periodical treatments conducted on a regular basis. Therefore, to guarantee an effective crop protection, the robotic platform must be able to monitor every point of the vineyard/orchard within a safe time interval, so that when an infection focus emerges it can be selectively treated at a conveniently early stage of development. In our analysis, we set this revisit time t_R at 3 days, i.e. the time interval needed by the robot for a complete monitoring of the whole crop area.

Furthermore due to the fully autonomous operation capability of technological level L3, the robotic platform is assumed to work on average of 20 h d^{-1}. Finally, in consideration of the needed capability of operating at high spatial resolution, we considered an average field speed of 1.2 km h^{-1}.

The conditions described cause a change in the evaluation of the treatment costs (equation (3.19)), in particular the number of annual treatments cannot be considered the same of other levels studied. Supposing the machine working all day long we have a productive period (P_p) of approx. 130 days per year, during this time span the machine constantly is looking for disease in the field also without effectively spraying the canopy. In this context the annual number of passes (n_p) in the field is given by the following equation

$$n_p = \frac{P_p}{t_R}$$

Given these parameters, summarized in table 3.6a, the number of robotic platforms needed to manage a given farm area was computed with equation (3.17). In table 3.6b are reported the economic parameters used in the analysis.

The volume of the tank in the robotic platform was dimensioned in

Table 3.6: *Technical - economic parameters associated to the robotic level (L3).*

(a) *Technical parameters*

	Robot
	L3
Engine power (kW)	20
Average engine load (%)	80
Field speed (km h^{-1})	1.2
Tank volume (dm^3)	250
Work time available each day (h d^{-1})	20

(b) *Economic parameters*

	Robot
	L3
Purchase price ('000 €)	-*
Economic life (yr)	6
Depreciation rate (%)	12.5
Estimated life (h)	10000
Repair and maintenance factor (%)	100
Annual interest rate (%)	3.5

* To be determined by the analysis

accordance with the theoretical daily needs. Looking at the most intensive scenario represented by the apple orchard with 25 applications per year, the total brew applied is around 35 m^3 which, considering savings in order of 75%, for the entire productive season it will be used only approx. 26 m^3. How previously explained considering P_p equal to 130 we have that the average total daily amount of liquid material applied is expected in 200 dm^3. Conservatively the dimension of the tank was increase of 25% in comparison with the expected daily amount of liquid material to overcome peak demand.

The aim of the study of the robotic level L3 is to quantify the maximum purchase cost of the robotic platform, which could be balanced

by the enabled savings of pesticide, as compared to the amount needed by the equipment at lower technological levels. To reach this purpose a simple algorithm was developed, which is based on iterative comparison of total annual costs among L3 and other levels: increasing the price of the platform from 0 to 1 million euros, when L3 cost line (5 to 200 ha) overcomes the cost line respectively of L0, L1, and L2 the platform price for the specific point is recorded.

3.2.5 Sensitivity analysis

A sensitivity analysis was conducted in order to estimate how the uncertainty on the considered parameters could affect the output of the technical-economic analysis of equipment at different technological levels. The sensitivity analysis is defined as the study of how uncertainty in the output of a model can be attributed to different sources of uncertainty in the model input. Mathematically, the sensitivity of the cost function with respect to certain parameters is equal to the partial derivative of the cost function with respect to those parameters. Our analysis is defined as local sensitivity analysis, and refers the fact that all derivatives are taken at a single point. Local sensitivity analysis is a one-at-a-time (OAT) technique. OAT techiniques analyze the effect of one parameter on the cost function at a time, keeping the other parameters fixed (Saltelli et al, 2008).
The sensitivity analysis was evaluated by including the parameters shown in table 3.7 with the corresponding range of variation considered. All the parameters ranges were taken in according with the real variability of the data. An high variability was found in the pesticides market prices, and in the number of treatments, which at the moment are strictly connected to the weather condition. Considering the technical-economic parameters an high varibility is present also in the market prices of the machinery which for the sprayer is strictly connected with its estimated life.
The results are computed only for a farm area of 30 ha (a representative average size farm), and are quantified in term of change in total cost

Table 3.7: *Parameters and corresponding range considered in the sensitivity analysis.*

(a) *Ranges of the protection protocols*

	Grapevine				Apple	
	TRG1		TRG2		TRA	
	Min	Max	Min	Max	Min	Max
Number of treatments (n yr^{-1})	10	15	1	3	15	32
AI application rate*(kg ha^{-1})	4	7	0.5	1.5	1	2
AI cost (€ kg^{-1})	10	25	80	120	20	40

* Savings were maintained constant (table 3.2) through different technological levels

(b) *Ranges of the technical-economic parameters*

	Grapevine - Apple		
	Levels	Min	Max
Sprayer purchase price ('000 €)	L0	10	15
	L1	20	30
	L2	35	45
Tractor purchase price ('000 €)	All	35	65
Sprayer estimated life (h)	All	1500	2500
Field speed (km h^{-1})	All	3	10

(%), as compared to those obtained with input parameters above specified in sections 3.2.1 to 3.2.3, and used for the technical-economic analysis.

3.3 Results and discussion

3.3.1 Comparison among different levels of automation

Grapevine

Equipment costs

Figure 3.5a shows the annual equipment cost per hectare computed for the different technological levels in the vineyard scenario.
Each curve exhibits the expected hyperbolic trend for increasing vineyard area. For areas smaller than 15 ha the equipment cost varies dramatically with vineyard size, while above this threshold the cost is much less dependent on the area.
Sharp cost edges appear in correspondence of the area requiring an additional tractor-sprayer unit to execute the treatment in the available time t_a. For all the three levels, the first edge (from one to two tractor-sprayer units) occurs at around 22 ha. For larger areas, the transition edges tend to slightly shift among technological levels. This is due to the higher field efficiency of L1 and L2 equipment linked to lower filling time than L0 obtained by corresponding savings in spraying.
As a comparative index among levels, the equipment cost for a medium sized farm with an area of 30 ha was computed. This cost resulted to increase with the technological level, namely it was 922 € ha^{-1} yr^{-1} for L0; 1101 € ha^{-1} yr^{-1} for L1; and 1340 € ha^{-1} yr^{-1} for L2, respectively.
From an analysis of the composition of the equipment cost in vineyard scenario it is interesting to see the trend of the incidence of variable costs on total equipment cost. To remember that composition of variable cost is given by tractor fuel and oil consumption, maintenance of both sprayer and tractor, and labour cost.
In figure 3.4a the L0 variable costs incidence is around 50% and 60% on total equipment cost (figure 3.5a). For area smaller than 40 ha instead we have high variability on the incidence, from 15% to 60%. From a comparison with other levels we can see a reduction in the im-

portance of variable costs to the formation of the total equipment cost, even if the shape of the trend is almost the same compared to L0 we have an incidence of 55% and 50% respectively for L1 and L2.
Another consideration is the inverse trend of the curves of equipment cost composition (figure 3.4) among the acquisition of a new tractor sprayer combination, if compared with the equipment cost in figure 3.5a. The saw shape of the curve is the opposite, and it is due to before the acquisition of new equipment the use of the machine become more and more intense reaching the area threshold for the acquisition of a new tractor-sprayer combination.

Total cost

The annual cost per hectare associated to pesticides used in protection treatment was obviously found to be independent from the vineyard area: for L0 the total treatment cost was 1350 € ha^{-1} yr^{-1}; for L1 1098 € ha^{-1} yr^{-1}; and 905 € ha^{-1} yr^{-1} for L2.
Figure 3.5b shows the total annual cost per hectare, computed by adding equipment and pesticide costs, of protection treatments in vineyard, conducted with the equipment at different technological levels. The plotted curves show that for worked area smaller than 10 ha, L0 is the most profitable option among the considered equipment, with relative cost savings of about 1% - 5% compared to L1, and of about 3% - 18% compared to L2.
For area larger than 10 ha, L1 becomes more profitable than L0, with cost savings limited to 5% compared to L0. It must be noticed that this advantage pattern is strongly changes around the curve edges, i.e. the transition farm area corresponding to the introduction of an additional tractor-sprayer unit (edge effect).
Interestingly, the more advanced and expensive equipment L2 becomes the best option for vineyards with area larger than 100 ha approx., it possible to affirm that there is a coincidence between L1 and L2 curves. Given these results, it was possible to evaluate the amount of savings in agrochemicals which would make profitable the adoption

of equipment of higher levels L1 and L2 instead of current machinery L0. Two examples of vineyard size were considered to this aim: a small farm with an area of 10 ha and a large farm of 150 ha.
For the small farm case, equipment L1 would become more convenient than L0 if the associated savings were higher than 18% (instead of the 15% assumed) for pesticides used in treatments TRG1, and higher than 9% (assumed 10%) for TRG2. For the more expensive equipment L2, these savings should reach at least 43% (instead of the assumed 35%) and 21.5% (instead of the assumed 20%) for TRG1 and TRG2 respectively.
For the large farm case, equipment L1 would be more convenient than L0 even if the associated savings were just higher than 10% for TRG1 and 5% for TRG2, respectively. While for L2, these thresholds resulted to be 25% and 12.5% respectively.

Sensitivity analysis

The main results of sensitivity analysis for vineyard scenario are summarised in figure 3.7a. It shows the change (in percent) of total cost due to the variation of a single input parameter, keeping constant all the others. The data show that changes in the input economic parameters (table 3.7b except field speed) resulted in a limited impact (less than ±5%) on the total cost for all the three technological levels L0, L1, L2.
On the contrary, the field speed (and in turn the spraying work rate) appears to have the largest impact in the sensitivity analysis for all technological levels. This is due, on one hand, to the obvious changes in operational costs linked to variations in work time. Additionally, a major effect on costs is also associated with the number of tractor-sprayer units needed to cover the farm area, which is directly related to the machine work rate.
Furthermore, the main protection protocol parameters (table 3.7a) had a significant influence on the computed final cost. Approximately the variation of AI cost, application rate, and number of treatments influ-

enced the total cost from -18% to +15%, (figure 3.7a).
From a comparison among the levels it is possible to note the growing incidence of field speed in the formation of total cost, also sprayer cost and sprayer life have more incidence in the formation of total cost. At the same time, it is possible to see the reduction of the impact of treatment related variables with the growth of automation among levels. From a comparison among the two scenarios, grapevine and apple orchard the variation on total cost is more consistent in the latter (see paragraph 3.3.1).
It is important to notice that even if the incidence of machinery parameters is growing with the automation level at 30 ha the total cost is lower for L1 and L2.

Apple

Equipment costs

Figure 3.6a shows the annual equipment cost per hectare computed for the different technological levels in apple orchard scenario. Also in this case, for areas smaller than 15 ha the equipment cost varies dramatically with orchard size, while above this threshold the cost is much less dependent on the area. Again sharp cost edges appear in correspondence of the transition area where introduction of an additional tractor-sprayer unit is needed.
As a comparative index among levels, the equipment cost for a reference farm of 35 ha resulted to increase with the technological level: namely, for L0 the cost resulted 1094 € ha^{-1} yr^{-1}; for L1 1257 € ha^{-1} yr^{-1}, and for L2 1480 € ha^{-1} yr^{-1}. Analysing the composition of variable costs, we have that (figure 3.4b) the L0 variable costs incidence is around 60% and 70% on total equipment cost (figure 3.6a). These values are higher than vineyard scenario and it is due to apple orchard is more intensive in terms of number of treatments per year. The incidence of variable cost is lower for L1 and L2 but always above 50%. Only before 30 ha the variability is very high.

The inverse trend of the curves of equipment cost composition (figure 3.4) among the acquisition of a new tractor sprayer combination is also in apple orchard case very sharp. The use of the machine become more and more intense reaching the limit crop area in which another tractor sprayer combination is necessary.

Total cost

The annual cost per hectare associated to pesticides used in apple orchard protection resulted to be: 1200 € ha^{-1} yr^{-1} for L0, 960 € ha^{-1} yr^{-1} for L1, and 780 € ha^{-1} yr^{-1} for L2.
Figure 3.6b shows the total annual cost per hectare of protection treatments in apple orchard conducted with the equipment at different technological levels. The curves show that in this case L0 is the most profitable option for area smaller than 9 ha. The relative cost savings range about 1% - 7% compared to L1, and from 14 ha of about 2% - 20% compared to L2.
For area larger than 17 ha, L1 becomes more profitable than equipment L0 and L2, with relative cost savings limited to less than 1.5% when compared to L0, and 2% - 4% when compared with L2.
Differently from the vineyard case, in this scenario equipment L2 never resulted the most profitable option compared to L1. This is related, on one hand, to the lower costs of agrochemicals considered in the apple protection protocol; on the other to the significantly higher number of annual treatments which implies a greater weight of use of equipment in determining the total cost.
It must be noticed that this general pattern of relative cost advantage among equipment levels, is distorted around the curve edges (edge effect).
Concerning the computed savings in pesticides making the adoption of equipment of higher levels more profitable than L0, two orchard sizes were considered as examples. In the case of small farm area (10 ha), equipment L1 would become profitable instead of L0, if the associated savings were higher than 20% (instead of the 15% assumed) for agro-

chemicals used in treatment TRA. For L2 the savings should be higher than 47% (instead of 30%).
For the large farm (150 ha) case, equipment L1 would be more convenient than L0 with savings higher than 12% (instead of 15%), while L2 should enable savings higher than 28% (instead of 30%) to become profitable compared to L0.

Sensitivity analysis

The sensitivity analysis for apple orchard scenario (figure 3.7b) led to similar results obtained for vineyard. Changes in purchase cost of tractor and sprayer, and life of the operating machine, resulted to have a limited impact (less than ±5% approx.) on the total cost for all the three technological levels L0, L1, L2. For the same reasons mentioned for vineyard, also in this case the field speed had the largest impact for all technological levels. Changes in agrochemical cost and in application rate resulted in corresponding variations of total cost approximately from -16% to +13% as compared to those obtained with input parameters adopted in the technical-economic analysis. On the other hand, the total costs resulted significantly influenced (from -30% to more than +20%) by the annual number of treatments, since these involve a lower or higher use of machines associated to operative costs.
From a comparison among the different levels we can see a growing importance of machine parameters with the growth of automation level. Considering the field speed, we have 60% more impact comparing L0 and L2. The sprayer cost impact is growing more than 120%. Almost constant is the impact of the tractor cost. These trends are due to the greater economic value of machines for growing automation levels.
Considering the treatment variables we have a lost of importance for the number of treatments the pesticides costs and their rate. Of course it this condition is due to the savings that we have for growing level of automation.
Also in apple orchard even if the incidence of the variation of the

equipment parameters in the formation of total cost is higher, we have at 30 ha convenience to adopt an automated machinery.

3.3.2 Future perspectives: advanced robotic level

Thanks to the potential savings in pesticides that were assumed to be enabled by the robotic platform L3, the analysis allowed to compute the maximum purchase cost ensuring the profitability of robot technology on the spraying equipment at lower technological levels. This profitability threshold is equal to the purchase cost originating the minimum total cost shown by curves in figure 3.5b and 3.6b for vineyard and apple orchard, respectively.
For whatever farm size, in the grapevine scenario this purchase cost resulted to be around 49600 €, while for apple orchard is 67300 €.
With the technical economic parameters carefully chosen in defining the scenario explored by this analysis, the resulting price range appears to be far from any sustainable development and industrial production cost, making the application of the robotic platform L3 quite unrealistic. Indeed, even assuming extreme savings in used agrochemicals, the profitability of L3 is not reachable at a current technology cost.

Platform purchase cost investigation

It becomes not so important trying to improve the field speed in the robotic level for obtaining an higher platform purchase price, due to it seems to be high enough to this type of technology; but how we can see in figure 3.8 trying to change the physical estimated life (Ph_l) the purchase cost value is influenced. In both vineyard and apple orchard scenarios we get the maximum purchase cost for the platform at 12000 of physical life. The median value for all the crop area considered in vineyard scenario is: 20509 € at Ph_l = 3000 h; 30600 € at Ph_l = 5000 h; 38900 € at Ph_l = 7000 h; and 61900 € at Ph_l = 12000 h.
Higher values are obtainable in apple orchard scenario in which we have: 28462 € at Ph_l = 3000 h; 42700 € at Ph_l = 5000 h; 59100 € at

Ph_l = 7000 h; and 86650 € at Ph_l = 12000 h.
An front of an improvement of 3 times of the physical estimated life the advance of the platform purchase cost is limited to twice for both scenarios. It is interesting to notice that in apple orchard scenario the margin of improvement in the platform purchase cost is higher: this aspect is due to this is a very high intensity scenario more subjected to be treated. Also in the maximum physical life value used the platform purchase cost is limited for the industrial development of this type of machinery even if in apple orchard for Ph_l = 12000 h we reach 86650 €.

We can suppose the ability of the platform to maintain a level of savings higher than 75% setted. Due to how it possible to see in the literature exposed in the section 1.5 higher savings are reachable. If we suppose saving in the order of 85% economical margins are still very low with the median of platform purchase price for all the crop areas limited to 65900 € if compared with L0 in apple orchard scenario and 535600 € in comparison with vineyard one. Only improving the field speed from 1.2 km h^{-1} to 1.5 km h^{-1} and leaving the platform physical life to 12000 h with very high savings we can reach a platform purchase cost of 121800 € in the more intensive scenario (median of all the crop area comparing with L0). But develop a machine with such characteristics is far from to be possible, remaining a pure speculation about the future.

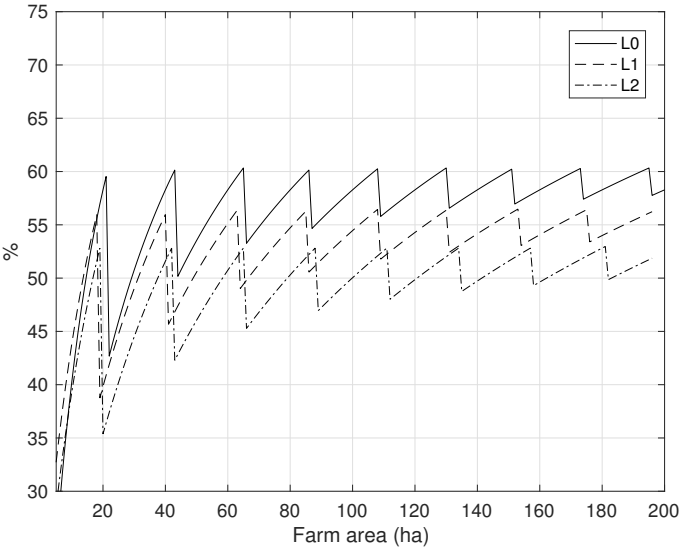

(a) *Vineyard variable cost incidence on total equipment cost*

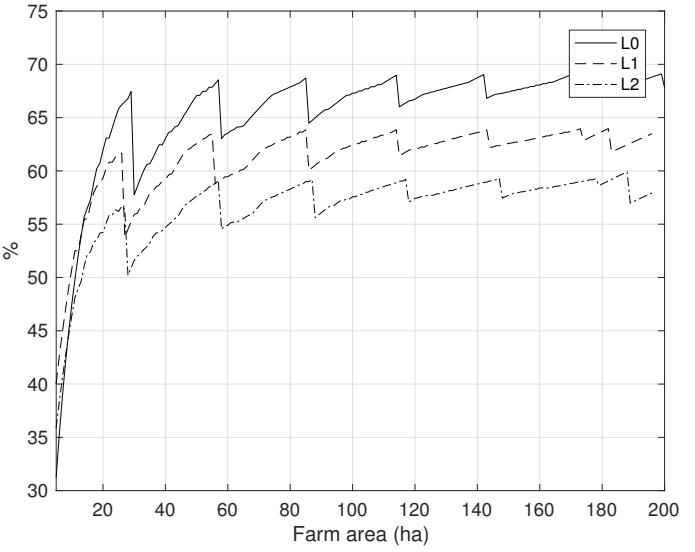

(b) *Apple variable cost incidence on total equipment cost*

Figure 3.4: *Variable cost weight on total equipment cost for vineyard (a) and apple orchard (b).*

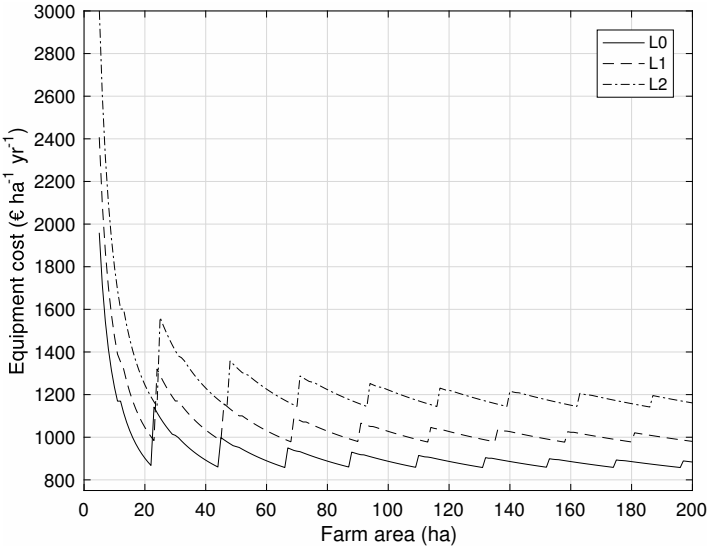

(a) *Equipment costs*

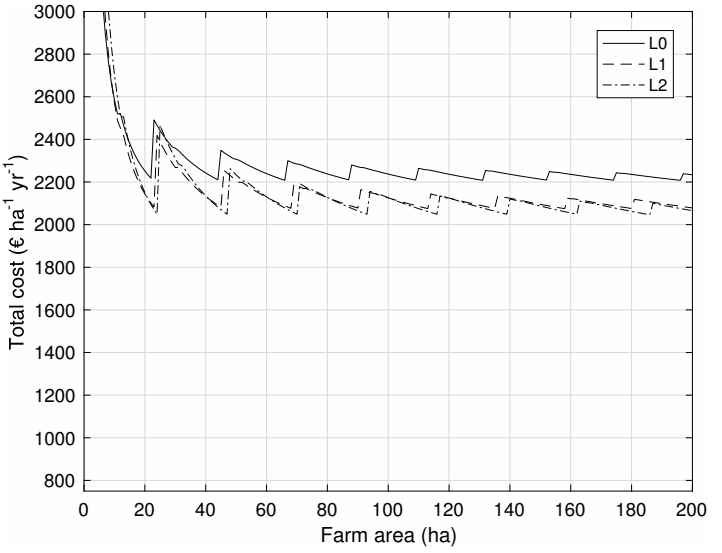

(b) *Total annual costs*

Figure 3.5: *Vineyard: (a) annual equipment costs per hectare and (b) total annual costs per hectare in different farm area for rising technological levels.*

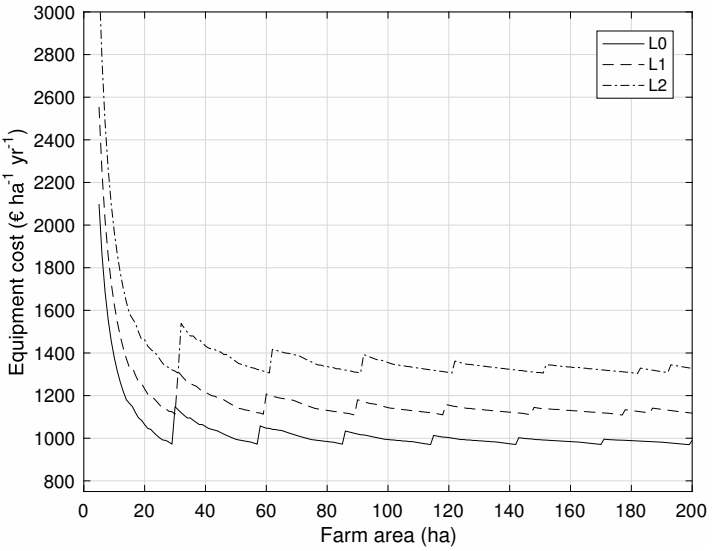

(a) *Equipment costs*

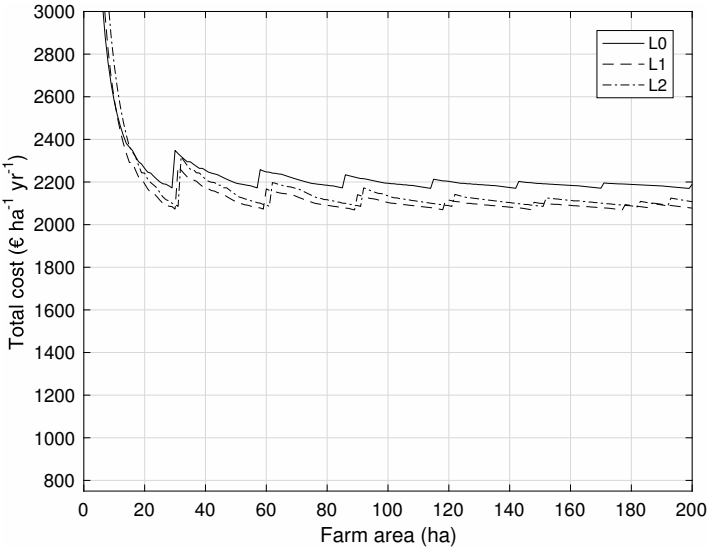

(b) *Total annual costs*

Figure 3.6: *Apple orchard: (a) annual equipment costs per hectare and (b) total annual costs per hectare in different farm area for rising technological levels.*

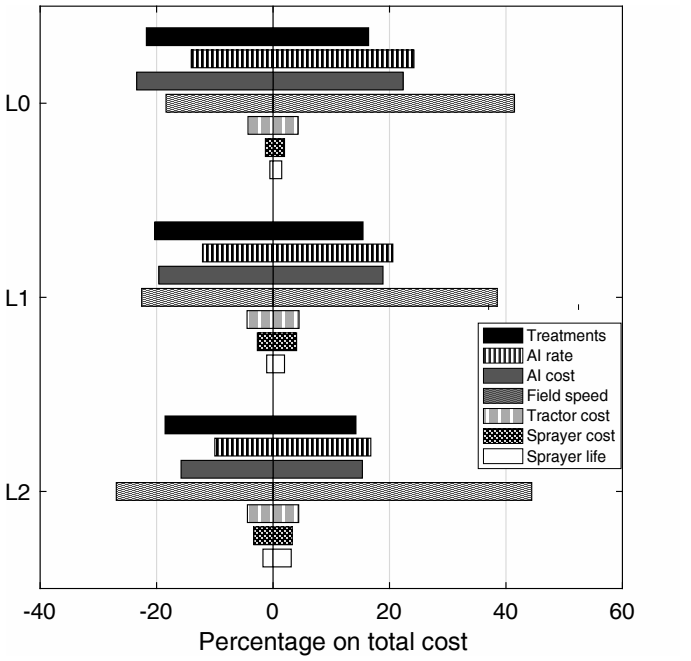

(a) *Vineyard*

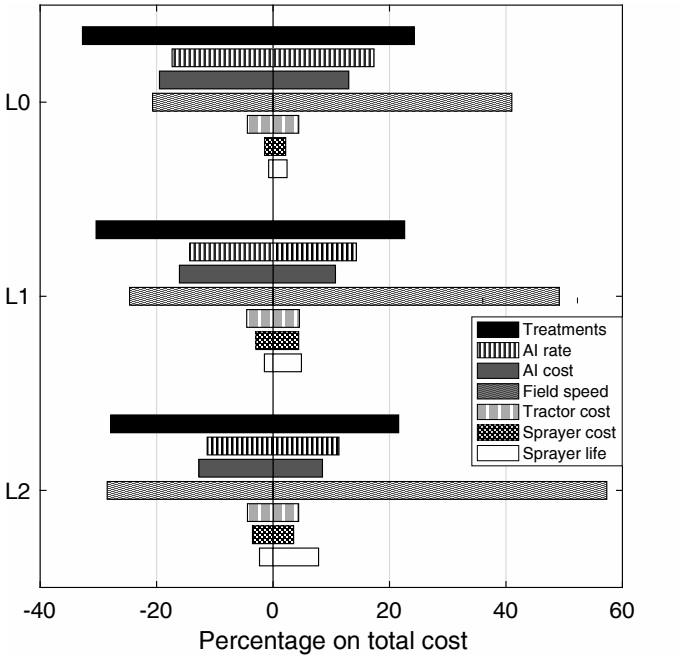

(b) *Apple orchard*

Figure 3.7: *Sensitivity analysis: percentage variation of the total annual costs in vineyard (a) and apple orchard (b), for variables considered.*

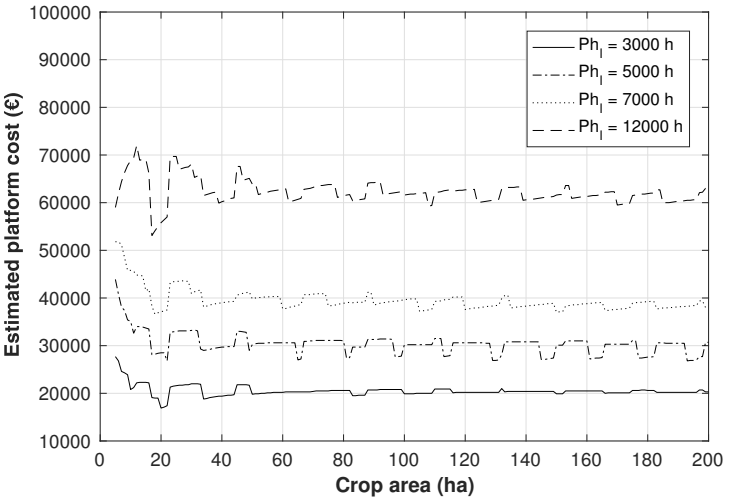

(a) *Vineyard*

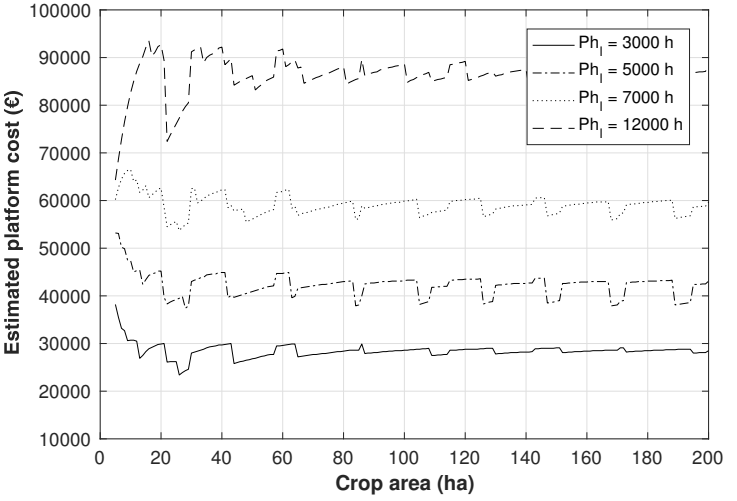

(b) *Apple orchard*

Figure 3.8: *Platform purchase cost variation in accordance with the estimated physical life (Ph_l) in vineyard (a) and apple orchard (b).*

3.4 Machine substitution effect

The whole analysis made it was done smoothing the *substitution effect* of the equipment between two subsequent acquisitions of a new machine-tractor combination at growing crop area. To explain the concept we are going to analyse the apple orchard scenario.
In apple orchards the machine is used intensely at specific crop areas due to the high number of hours which are necessary each year to conduct the treatments. The extreme use of the equipment, especially for the sprayer, is a limiting factor to the physical life of the machine.
The sprayer, especially in the apple orchard scenario, is subjected to a fast physical obsolescence which does not permit to the machine to reach the economic life limit of the machine itself (in our case 6 years, table 3.4). For example, let consider the case L0 in apple orchard at 62 ha. The nominal maximum hours AWt_n for the sprayer is given by the ratio Ph_l/E_l = 2000/6 = 333.3 h. Comparing with the annual hours which are necessary to execute the operation (approx. 402 h) we have a real life (Sp_l) of the sprayer equal to

$$\lfloor Sp_l \rfloor = \frac{Ph_l}{H_{yr}} = \frac{2000}{402} = 4 \text{ yr}$$

where H_{yr} represents the annual hours necessary to execute the treatments and the $\lfloor x \rfloor$ symbol represents the floor function which map a real number to the largest integer less than or equal to the value x.

In detail we can look at the figure 3.9, in which is represented apple orchard equipment cost presenting the substitution effect. How it is possible to see in figure 3.9a the acquisition of a new tractor-sprayer combination is respectively at 57 ha, 59 ha, and 61 ha for L0, L1, and L2: the peaks here are given by the necessity to cover a larger field area in the available time we have impose for the treatment (table 3.1). Going ahead along the abscissa axis we encounter other peaks at 62 ha, 65 ha and at 66 ha, respectively for L0, L1, and L2. This shape defor-

mation is due to the substitution effect previously exposed. The cost of the sprayer is divided for a smaller sprayer life. In L2 the peak overcome even the peak at 61 ha, which regards the acquisition of a new tractor-sprayer combination.
In figure 3.9c it is possible to observe the trend of the calculated life or real life of the machine. In correspondence of the points listed above there is a decreasing in sprayer life from 5 to 4 years. Of course the increasing of the annual working hours is constant and parallel with the crop area covered (figure 3.9b).

In figure 3.9a it possible to observe a series of peaks also at the end of the graph between 75 ha and 90 ha. The correspondence of the peaks here is with the reduction of the life of the sprayer from 4 to 3 years (very intense use of the equipment). Only the acquisition of a new tractor-sprayer combination is able to push up the life of the sprayer from 3 to 4 years. This effect is due to the repartition of the annual working hours necessary to cover the field among more equipment units.
The substitution effect is an artifice present in the evaluation of the equipment cost in this analysis derives exclusively from the sprayer and not from the tractor which has a very high physical life (1000 h yr^{-1}).

It is very interesting to note how the substitution effect is reflected on the variable cost weight on total cost. Considering the same portion of the graph on figure 3.10 we have the variable cost weight on total equipment cost for the apple orchard scenario.
When the life of the sprayer is reducing from to 4 or 3 years there is a step down in the curves. This step down is due to the reduction of economic life factor in repair and maintenance cost equation (3.7).

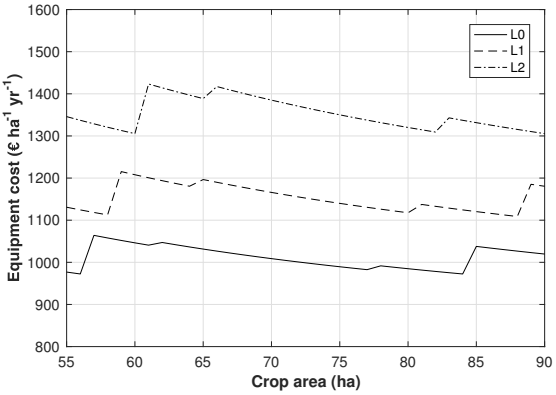

(a) *Not smoothed equipment cost in apple orchard between 55 ha and 90 ha*

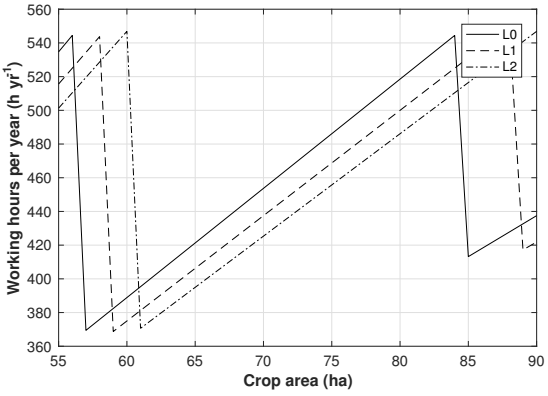

(b) *Annual working hours per year in apple orchard*

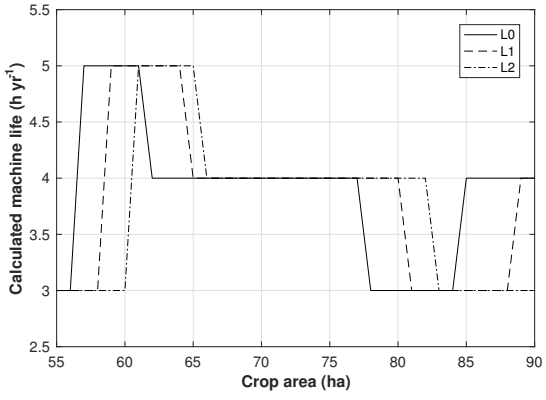

(c) *Real life of the sprayer*

Figure 3.9: *Detail of the substitution effect on apple orchard equipment cost*

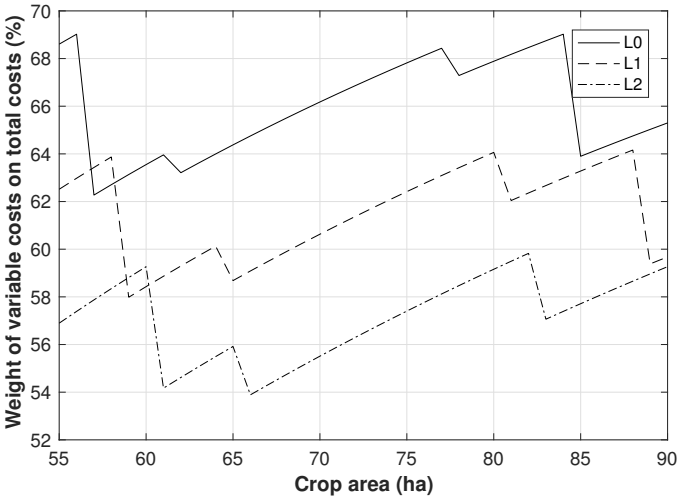

Figure 3.10: *Substitution effect: weight of the variable costs on total equipment cost in apple orchard scenario.*

3.5 Conclusions

A technical-economic analysis was conducted on three different technological levels of spraying equipment for speciality crops (grapevine and apple) which were assumed to enable correspondingly increasing levels of reduction in distributed pesticide, without negatively affecting the biological efficacy. Fungicide treatments against major fungal diseases in vineyard and apple-orchard were considered, and the annual total costs of protection treatments (costs of equipment and pesticide) when operating with a conventional air-blast sprayer (referred as technological level L0), with an on-off nozzle switching sprayer (L1) and with a canopy-optimised distribution sprayer (L2), were evaluated.
Within the assumptions made, the results of the analysis highlighted that:

- for a given worked area, the equipment cost raised with technological level, as expected; the obtained values for a reference vineyard/orchard farm of 30 ha increased from 944 € ha^{-1} yr^{-1} to 1316 € ha^{-1} yr^{-1}, respectively for L0 and L2 in grapevine case, and from 1107 € ha^{-1} yr^{-1}; to 1518 € ha^{-1} yr^{-1}, respectively for L0 and L2 in apple case;
- thanks to pesticide savings enabled by the different level of precision spraying technologies, the annual cost of pesticide per hectare decreased from 1350 € ha^{-1} yr^{-1} to 905 € ha^{-1} yr^{-1}, respectively for L0 and L2 in grapevine case, and from 1200 € ha^{-1} yr^{-1} to 780 € ha^{-1} yr^{-1}, respectively for L0 and L2 in apple case;
- in term of annual total costs of protection treatments, on grapevine the conventional sprayer L0 resulted the most profitable option for vineyard area smaller than 10 ha; from 10 ha to approx. 100 ha L1 was the best option, while above 100 ha the more advanced equipment L2 resulted the best choice;
- the perceptual of variable costs in equipment cost is always above the 50% for L0, L1, and L2 in apple orchard scenario resulting

the most work intense. In vineyard we have the same situation compared to apple orchard for L0 and L1. In L2 this trend is not so sharp due to the high cost of the sprayer equipment;

- on apple, the lowest total costs of protection treatments for orchard area smaller than 17 ha were obtained with L0; above 17 ha L1 was the best option, while L2 never resulted profitable compared to L0 and L1;
- both for grapevine and apple cases, the sensitivity analysis put in evidence that the uncertainty on equipment economic parameters had a limited impact on the total costs of protection; on the contrary, the uncertainty on protection parameters had an evident influence on the computed final costs: on average the range of variation of AI price, application rate, and number of treatments influenced the total cost from about -20% to +15% and from about -30% to +20%, on grapevine and apple respectively;
- the variation of sprayer field speed, which is not inherent to the precision spraying technologies considered in this study, appears to have the largest costs impact in the sensitivity analysis for all technological levels;
- for the estimation of the equipment cost in an agricultural farm it is important take in account the *substitution effect* described in section 3.4. This effect can give artifices and oscillations in the evaluation that can be misleading for the real equipment management.

Finally, in a speculation on possible perspectives of precision spraying in speciality crops, the analysis was addressed to the case of an autonomous robotic platform able to selectively target the pesticide on diseased areas. The obtained results indicated that:

- the purchase price that would make profitable the robotic platform, thanks to the assumed pesticide and labour savings over

sprayers at technological levels L0, L1 and L2, was unrealistically lower than current industrial cost;

- regardless the area of the vineyard/orchard considered, for the grapevine scenario the robot purchase cost threshold resulted around 54700 €, while for apple scenario was 66500 €.
- within the assumptions made in this study, the results indicate that cost profit cannot be the only driver for possible adoption, in the very next future, of autonomous intelligent platforms for advanced precision spraying in speciality crops;
- varying the physical life of the platform, improving the components characteristics, it is possible to speculate on the final price of the platform which in the best case of 12000 h of physical life reach 86650 € in vineyard scenario and 121800 € in apple rchard resulting the most work-intensive crop.

Bibliography

Agrios GN (2005) Plant pathology, vol 5. Elsevier Academic Press Burlington, MA

Aleixos N, Blasco J, Navarron F, Moltó E (2002) Multispectral inspection of citrus in real-time using machine vision and digital signal processors. Computers and electronics in agriculture 33(2):121–137

Andreatta S (1998) Agrochemical exposure and farmworker health in the caribbean: a local/global perspective. Human Organization 57(3):350–358

Anon (2009) Directive 2009/128/EC of the european parliament establishing a framework for community action to achieve sustainable use of pesticides. Official Journal of European Union L309:71–86

Anon (2013) Infographic: Pesticide planet. Science 341(6147):730–731, DOI 10.1126/science.341.6147.730, URL http://science.sciencemag.org/content/341/6147/730, http://science.sciencemag.org/content/341/6147/730.full.pdf

Anon (2016a) Bullettins viticoles. URL `http://www.agrometeo.ch/fr/bulletins-viticoles`

Anon (2016b) Le guide ARBO du sud-ouest PFI et BIO. L'action agricole 106

Anon (2016c) Nasa's imagine the universe. `http://imagine.gsfc.nasa.gov/science/toolbox/emspectrum1.html`, accessed: 2016-11-07

Anon (2016d) Supplemento difesa della vite - gestione della peronospora. suppl. i. L'Informatore agrario 10

Anon (2016e) Vigneto e fruttero. L'Informatore agrario Suppl I 10

Arngren M (2011) Hyperspectral nir camera. Technical University of Denmark, Department of Informatics and Mathematical Modeling Technical Note, ver 1

ASABE Standards (2013) EP496.3 FEB2006 Agricultural machinery management Ed. 54^{Th}. St. Joseph Mich. - ASABE

Balsari P, Tamagnone M (1998) An ultrasonic airblast sprayer. In: Proceedings of the International Conference on Agricultural Engineering AgEng, pp 585–586

Balsari P, Doruchowski G, Marucco P, Tamagnone M, Van De Zande J, Wenneker M (2008) A system for adjusting the spray application to the target characteristics. Agricultural Engineering International: CIGR Journal 10:1–11

Balsari P, Marucco P, Tamagnone M, et al (2009) A crop identification system (cis) to optimise pesticide applications in orchards. Journal of Horticultural Science and Biotechnology ISAFRUIT Special Issue 113:116

Batte M, Ehsani M (2006) The economics of precision guidance with auto-boom control for farmer-owned agricultural sprayers. Com-

puters and Electronics in Agriculture 53(1):28–44, DOI 10.1016/j.compag.2006.03.004

Belasque Jr J, Gasparoto M, Marcassa LG (2008) Detection of mechanical and disease stresses in citrus plants by fluorescence spectroscopy. Applied Optics 47(11):1922–1926

Bennett AL, Pannell DJ (1998) Economic evaluation of a weed-activated sprayer for herbicide application to patchy weed populations. Australian Journal of Agricultural and Resource Economics 42(4):389–408, DOI 10.1111/1467-8489.00059, URL http://dx.doi.org/10.1111/1467-8489.00059

Berge T, Goldberg S, Kaspersen K, Netland J (2012) Towards machine vision based site-specific weed management in cereals. Computers and Electronics in Agriculture 81:79 – 86, DOI http://dx.doi.org/10.1016/j.compag.2011.11.004, URL http://www.sciencedirect.com/science/article/pii/S0168169911002602

Bodria L, Fiala M, Oberti R, Naldi E (2002) Chlorophyll fluorescence sensing for early detection of crop?s diseases symptoms. In: 2002 ASAE Annual Meeting, American Society of Agricultural and Biological Engineers, p 1

Bohren C, Debruis PH, Kuske S, Linder C, Naef A (2016a) Index phytosanitaire pour la viticulture 2016. Revue suisse de viticulture arboriculture horticulture Suppl I 48(1):1–16

Bohren C, Debruis PH, Kuske S, Linder C, Naef A (2016b) Index phytosanitaire pour la viticulture 2016. Revue suisse de viticulture arboriculture horticulture Suppl II 48(1):1–16

Bravo C (2006) Automatic foliar disease detection in winter wheat. PhD thesis, Katholieke Universiteit Leuven

Bravo C, Moshou D, West J, McCartney A, Ramon H (2003) Early disease detection in wheat fields using spectral reflectance. Biosystems Engineering 84(2):137–145

Brereton R (2009) Chemometrics for pattern recognition. John Wiley & Sons

Brewer MT, Milgroom MG (2010) Phylogeography and population structure of the grape powdery mildew fungus, Erysiphe necator, from diverse Vitis species. BMC evolutionary biology 10(1):268, DOI 10.1186/1471-2148-10-268, URL `http://www.biomedcentral.com/1471-2148/10/268`

Brualdi RA (1977) Introductory combinatorics. Learning 4(5):6

Campbell L, Cooke A (1997) The indirect effects of pesticides on birds. RSPB Conservation Review (United Kingdom)

Camps-Valls G, Bruzzone L, et al (2009) Kernel methods for remote sensing data analysis, vol 2. Wiley Online Library

Cerović ZG, Samson G, Morales Iribas F, Tremblay N, Moya I (1999) Ultraviolet-induced fluorescence for plant monitoring: present state and prospects

Christensen S, Søgaard HT, Kudsk P, Nørrmark M, Lund I, Nadimi ES, Jørgensen R (2009) Site-specific weed control technologies. Weed Research 49(3):233–241, DOI 10.1111/j.1365-3180.2009.00696.x, URL `http://dx.doi.org/10.1111/j.1365-3180.2009.00696.x`

Daley PF (1995) Chlorophyll fluorescence analysis and imaging in plant stress and disease. Canadian journal of plant pathology 17(2):167–173

Dammer KH, Adamek R (2012) Sensor-Based Insecticide Spraying to Control Cereal Aphids and Preserve Lady Beetles.

Agronomy Journal 104(6):1694, DOI 10.2134/agronj2012.0021, URL https://www.agronomy.org/publications/aj/abstracts/104/6/1694

Dammer KH, Ehlert D (2006) Variable-rate fungicide spraying in cereals using a plant cover sensor. Precision Agriculture 7(2):137–148, DOI 10.1007/s11119-006-9005-x, URL http://dx.doi.org/10.1007/s11119-006-9005-x

Daniel C (1973) One-at-a-time plans. Journal of the American Statistical Association 68(342):353–360, DOI 10.1080/01621459.1973.10482433, URL http://www.tandfonline.com/doi/abs/10.1080/01621459.1973.10482433, http://www.tandfonline.com/doi/pdf/10.1080/01621459.1973.10482433

Dennis MJ (2003) Human rights in 2002: The annual sessions of the un commission on human rights and the economic and social council. The American Journal of International Law 97(2):364–386

Downey D, Giles D (2005) Reducing orchard spray rates and ground deposit by using tree sensors and sprayer control. Ann Rev Ag Eng 4:229–36

Duda RO, Hart PE, et al (1973) Pattern classification and scene analysis, vol 3. Wiley New York

Ehlert D, Horn HJ, Adamek R (2008) Measuring crop biomass density by laser triangulation. Computers and electronics in agriculture 61(2):117–125

Esau T, Zaman Q, Groulx D, Corscadden K, Chang Y, Schumann A, Havard P (2016) Economic analysis for smart sprayer application in wild blueberry fields. Precision Agriculture (in press), DOI 10.1007/s11119-016-9447-8, URL http://dx.doi.org/10.1007/s11119-016-9447-8

Esau TJ, Zaman QU, Chang YK, Schumann AW, Percival DC, Farooque AA (2014) Spot-application of fungicide for wild blueberry using an automated prototype variable rate sprayer. Precision Agriculture 15(2):147–161, DOI 10.1007/s11119-013-9319-4, URL http://dx.doi.org/10.1007/s11119-013-9319-4

Escolà A, Camp F, Solanelles F, Llorens J, Planas S, Rosell J, Gràcia F, Gil E, Stafford J (2007) Variable dose rate sprayer prototype for tree crops based on sensor measured canopy characteristics. In: Precision agriculture '07, Papers presented at the 6th European Conference on Precision Agriculture, Skiathos, Greece, 3-6 June, 2007., Wageningen Academic Publishers, pp 563–571, URL http://www.cabdirect.org/abstracts/20073176117.html?freeview=true

Escolà A, Rosell-Polo J, Planas S, Gil E, Pomar J, Camp F, Llorens J, Solanelles F (2013) Variable rate sprayer. part 1–orchard prototype: Design, implementation and validation. Computers and electronics in agriculture 95:122–135

Everhart SE, Askew A, Seymour L, Scherm H (2013) Spatio-temporal patterns of pre-harvest brown rot epidemics within individual peach tree canopies. European Journal of Plant Pathology 135(3):499–508, DOI 10.1007/s10658-012-0113-3, URL http://dx.doi.org/10.1007/s10658-012-0113-3

FAO (2013) FAO Statistical Yearbook. World Food and Agriculture

FAO (2016a) FAOSTAT, Accessed 20/10/2016. URL http://faostat3.fao.org

FAO (2016b) Submission and evaluation of pesticide residues data for the estimation of maximum residue levels in food and feed. Food and agriculture organization of the United Nations

Fauvel M, Tarabalka Y, Benediktsson JA, Chanussot J, Tilton JC (2013) Advances in Spectral-Spatial Classification of Hyperspec-

tral Images. Proceedings of the IEEE 101(3):652–675, DOI 10.1109/JPROC.2012.2197589, URL http://ieeexplore.ieee.org/articleDetails.jsp?arnumber=6297992

Fenner K, Canonica S, Wackett LP, Elsner M (2013) Evaluating pesticide degradation in the environment: Blind spots and emerging opportunities. Science 341(6147):752–758, DOI 10.1126/science.1236281, URL http://science.sciencemag.org/content/341/6147/752, http://science.sciencemag.org/content/341/6147/752.full.pdf

Fisher RA (1936) The use of multiple measurements in taxonomic problems. Annals of Eugenics 7(2):179–188, DOI 10.1111/j.1469-1809.1936.tb02137.x, URL http://dx.doi.org/10.1111/j.1469-1809.1936.tb02137.x

Gerhards R, Sökefeld M, Timmermann C, Kühbauch W, Williams MM (2002) Site-specific weed control in maize, sugar beet, winter wheat, and winter barley. Precision Agriculture 3(1):25–35, DOI 10.1023/A:1013370019448, URL http://dx.doi.org/10.1023/A:1013370019448

Gil E, Escolà A, Rosell J, Planas S, Val L (2007) Variable rate application of plant protection products in vineyard using ultrasonic sensors. Crop Protection 26(8):1287 – 1297, DOI http://dx.doi.org/10.1016/j.cropro.2006.11.003, URL http://www.sciencedirect.com/science/article/pii/S0261219406003528

Gil E, Llorens J, Llop J, Fàbregas X, Escolà A, Rosell-Polo J (2013) Variable rate sprayer. Part 2 Ű Vineyard prototype: Design, implementation, and validation. Computers and Electronics in Agriculture 95(0):136–150, DOI 10.1016/j.compag.2013.02.010, URL http://www.sciencedirect.com/science/article/pii/S0168169913000495

Giles D, Delwiche M, Dodd R (1989) Sprayer control by sensing orchard crop characteristics: Orchard architecture and spray liquid savings. Journal of Agricultural Engineering Research 43:271–289

Giles DK, Delwiche M, Dodd R (1987) Control of orchard spraying based on electronic sensing of spray target characteristics. American Society of Agricultural Engineers (USA)

Giles DK, Delwiche MJ, Dodd RB (1988) Electronic measurement of tree canopy volume. Transactions of the ASAE 31(1):264–272

Gonzalez RC, Woods RE (2008) Digital image processing. Prentice hall Upper Saddle River, NJ, USA

Gonzalez RC, Woods RE, Eddins SL (2003) Digital Image Processing Using MATLAB. Prentice-Hall, Inc., Upper Saddle River, NJ, USA

Gowen A, O'Donnell C, Cullen P, Downey G, Frias J (2007) Hyperspectral imaging–an emerging process analytical tool for food quality and safety control. Trends in Food Science & Technology 18(12):590–598

Hai Z, Wang J (2006) Electronic nose and data analysis for detection of maize oil adulteration in sesame oil. Sensors and Actuators B: Chemical 119(2):449–455

Ham J, Chen Y, Crawford MM, Ghosh J (2005) Investigation of the random forest framework for classification of hyperspectral data. IEEE Transactions on Geoscience and Remote Sensing 43(3):492–501

Heege HJ (2015) Precision in crop farming. Springer

Homma T, Saltelli A (1996) Importance measures in global sensitivity analysis of nonlinear models. Reliability Engineering & System Safety 52(1):1–17

Huang JF, Apan A (2006) Detection of sclerotinia rot disease on celery using hyperspectral data and partial least squares regression. Journal of Spatial Science 51(2):129–142

Huang W, Lamb DW, Niu Z, Zhang Y, Liu L, Wang J (2007) Identification of yellow rust in wheat using in-situ spectral reflectance measurements and airborne hyperspectral imaging. Precision Agriculture 8(4-5):187–197

Hunt D, Wilson D (2015) Farm power and machinery management. Waveland Press

Hvistendahl M (2013) In rural asia, locking up poisons to prevent suicides. Science 341(6147):738–739, DOI 10.1126/science.341.6147.738, URL http://science.sciencemag.org/content/341/6147/738, http://science.sciencemag.org/content/341/6147/738.full.pdf

INRA (2016) Erysiphe cichoracearum - French National Institute for Agricultural Research. URL http://www7.inra.fr/hyp3/images/6032042.jpg

Jahn OL (1979) Penetration of photosynthetically active radiation as a measurement of canopy density 01 citrus trees. J Amer Soc Hort Sci 104(4):557–560

Jeyaratnam J (1990) Acute pesticide poisoning in asia: the problem and its prevention. In: Impact of pesticide use on health in developing countries. Proceedings of a symposium held in Ottawa, Canada, pp 17–20

Jimenez LO, Landgrebe DA (1998) Supervised classification in high-dimensional space: geometrical, statistical, and asymptotical properties of multivariate data. IEEE Transactions on Systems, Man, and Cybernetics, Part C (Applications and Reviews) 28(1):39–54

Khot LR, Ehsani R, Albrigo G, Larbi PA, Landers A, Campoy J, Wellington C (2012) Air-assisted sprayer adapted for precision horticulture: Spray patterns and deposition assessments in small-sized citrus canopies. Biosystems Engineering 113(1):76 – 85, DOI http://dx.doi.org/10.1016/j.biosystemseng.2012.06.008, URL http://www.sciencedirect.com/science/article/pii/S1537511012001031

Landgrebe DA (2005) Signal theory methods in multispectral remote sensing, vol 29. John Wiley & Sons

Larbi PA, Ehsani R, Salyani M, Maja JM, Mishra A, Neto JC (2013) Multispectral-based leaf detection system for spot sprayer application to control citrus psyllids. Biosystems Engineering 116(4):509 – 517, DOI http://dx.doi.org/10.1016/j.biosystemseng.2013.10.011, URL http://www.sciencedirect.com/science/article/pii/S1537511013001712

Larson JA, Velandia MM, Buschermohle MJ, Westlund SM (2016) Effect of field geometry on profitability of automatic section control for chemical application equipment. Precision Agriculture 17(1):18–35, DOI 10.1007/s11119-015-9404-y, URL http://dx.doi.org/10.1007/s11119-015-9404-y

Lee H, Kim MS, Lim HS, Park E, Lee WH, Cho BK (2016) Detection of cucumber green mottle mosaic virus-infected watermelon seeds using a near-infrared (NIR) hyperspectral imaging system: Application to seeds of the ?Sambok Honey? cultivar. Biosystems Engineering 148:138–147, DOI 10.1016/j.biosystemseng.2016.05.014

Lee W, Alchanatis V, Yang C, Hirafuji M, Moshou D, Li C (2010) Sensing technologies for precision specialty crop production. Computers and Electronics in Agriculture 74(1):2–33, DOI 10.1016/j.compag.2010.08.005, URL http://www.scopus.com/inward/record.url?eid=2-s2.0-77956906919{&}partnerID=tZOtx3y1

Li Y, Xia C, Lee J (2009) Vision-based pest detection and automatic spray of greenhouse plant. In: 2009 IEEE International Symposium on Industrial Electronics, pp 920–925, DOI 10.1109/ISIE.2009.5218251

Mahlein AK, Steiner U, Dehne HW, Oerke EC (2010) Spectral signatures of sugar beet leaves for the detection and differentiation of diseases. Precision Agriculture 11(4):413–431

Malaj E, von der Ohe PC, Grote M, Kühne R, Mondy CP, Usseglio-Polatera P, Brack W, Schäfer RB (2014) Organic chemicals jeopardize the health of freshwater ecosystems on the continental scale. Proceedings of the National Academy of Sciences 111(26):9549–9554, DOI 10.1073/pnas.1321082111, URL `http://www.pnas.org/content/111/26/9549.abstract`, `http://www.pnas.org/content/111/26/9549.full.pdf`

Malneršič A, Hočevar M, Širok B, Marchi M, Tirelli P, Oberti R (2012) Close range precision spraying airflow/plant interaction. In: Proceedings of the first international conference on robotics and associated high-technologies and equipment for agriculture, Pisa University Press, pp 107–112

Malthus TJ, Madeira AC (1993) High resolution spectroradiometry: spectral reflectance of field bean leaves infected by botrytis fabae. Remote Sensing of Environment 45(1):107–116

Marrs R, Frost A, Plant R (1991) Effects of herbicide spray drift on selected species of nature conservation interest: the effects of plant age and surrounding vegetation structure. Environmental Pollution 69(2-3):223–235

Más FR, Zhang Q, Hansen AC (2010) Mechatronics and intelligent systems for off-road vehicles. Springer Science & Business Media

Mascarelli A (2013) Growing up with pesticides. Science 341(6147):740–741, DOI 10.1126/science.341.6147.740,

URL http://science.sciencemag.org/content/341/6147/740, http://science.sciencemag.org/content/341/6147/740.full.pdf

McCartney H, Fitt BD (1998) Dispersal of foliar fungal plant pathogens: mechanisms, gradients and spatial patterns. In: The epidemiology of plant diseases, Springer, pp 138–160

Miller P (2003) Patch spraying: future role of electronics in limiting pesticide use. Pest management science 59(5):566–574, DOI 10.1002/ps.653, URL http://dx.doi.org/10.1002/ps.653http://onlinelibrary.wiley.com/doi/10.1002/ps.653/full

Miller P, Lane A, Wheeler H, et al (2000) Matching the application of fungicides to crop canopy characteristics. In: The BCPC Conference: Pests and diseases, Volume 2. Proceedings of an international conference held at the Brighton Hilton Metropole Hotel, Brighton, UK, 13-16 November 2000., British Crop Protection Council, pp 629–636

Mnzava N, Ngwerume F (2004) Plant resources of tropical africa: Vegetables prota foundation. Backhury's publishers, Leiden Netherlands/CTA Wageningen 2:191–195

Moltó E, Martiť n B, Gutiérrez A (2001) Pesticide loss reduction by automatic adaptation of spraying on globular trees. Journal of Agricultural Engineering Research 78(1):35–41, DOI 10.1006/jaer.2000.0622, URL http://www.sciencedirect.com/science/article/pii/S002186340090622X

Moshou D, Bravo C, West J, Wahlen S, McCartney A, Ramon H (2004) Automatic detection of ?yellow rust?in wheat using reflectance measurements and neural networks. Computers and electronics in agriculture 44(3):173–188

Nelson R, Krabill W, Tonelli J (1988) Estimating forest biomass and volume using airborne laser data. Remote sensing of environment 24(2):247–267

Nilsson M (1996) Estimation of tree heights and stand volume using an airborne lidar system. Remote Sensing of Environment 56(1):1–7

Nof S (2009) Springer Handbook of Automation. Springer Handbook of Automation, Springer Berlin Heidelberg, URL https://books.google.it/books?id=2v_91vSCIK0C

Nordmeyer H (2006) Patchy weed distribution and site-specific weed control in winter cereals. Precision Agriculture 7(3):219–231, DOI 10.1007/s11119-006-9015-8, URL http://dx.doi.org/10.1007/s11119-006-9015-8

Oberti R, Tirelli P, Marchi M, Calcante A, Iriti M, Borghese A (2012) Automatic disease detection in grapevine under field conditions. In: Proceedings of the first international conference on robotics and associated high-technologies and equipment for agriculture, Pisa University Press, pp 101–106

Oberti R, Marchi M, Tirelli P, Calcante A, Iriti M, Hočevar M, Baur J, Pfaff J, Schütz C, Ulbrich H (2013) Selective spraying of grapevine?s diseases by a modular agricultural robot. Journal of agricultural engineering 44(2s)

Oberti R, Marchi M, Tirelli P, Calcante A, Iriti M, Tona E, Hočevar M, Baur J, Pfaff J, Schütz C, Ulbrich H (2016) Selective spraying of grapevines for disease control using a modular agricultural robot. Biosystems Engineering DOI 10.1016/j.biosystemseng.2015.12.004, URL http://www.sciencedirect.com/science/article/pii/S1537511015001865

Oerke EC (2006) Crop losses to pests. The Journal of Agricultural Science 144(1):31–43, DOI 10.1017/

S0021859605005708, URL https://www.cambridge.org/core/article/crop-losses-to-pests/AD61661AD6D503577B3E73F2787FE7B2

Oerke EC, Schonbeck H, F Weber A, Rainey W, Jorgensen S, SN Jorgensen L, Runge C, Lotterman R, E Creason J, Urbina N, et al (1994) Crop production and crop protection: estimated losses in major food and cash crops. F01 16, IICA, Bogotá (Colombia)

Organization WH, et al (1990) Public health impact of pesticides used in agriculture

Osterman A, Gode?a T, Ho?evar M, ?irok B, Stopar M (2013) Real-time positioning algorithm for variable-geometry air-assisted orchard sprayer. Computers and Electronics in Agriculture 98:175 – 182, DOI http://dx.doi.org/10.1016/j.compag.2013.08.013, URL http://www.sciencedirect.com/science/article/pii/S0168169913001919

Paice M, Miller P, Bodle J (1995) An Experimental Sprayer for the Spatially Selective Application of Herbicides. Journal of Agricultural Engineering Research 60(2):107–116, DOI 10.1006/jaer.1995.1005

Pascal B (2011) Traité du triangle arithmétique. Éd. les Caractères d'Ulysse

PCA (2016) Cucumber green mottle mosaic virus on cucumbers. URL http://www.protectedcroppingaustralia.com

Peterson RB, Aylor DE (1995) Chlorophyll fluorescence induction in leaves of phaseolus vulgaris infected with bean rust (uromyces appendiculatus). Plant physiology 108(1):163–171

Petropoulos G, Srivastava PK (2016) Sensitivity Analysis in Earth Observation Modelling

Quigley M, Conley K, Gerkey B, Faust J, Foote T, Leibs J, Wheeler R, Ng AY (2009) Ros: an open-source robot operating system. In: ICRA workshop on open source software, Kobe, Japan, vol 3, p 5

Ratle F, Camps-Valls G, Weston J (2010) Semisupervised neural networks for efficient hyperspectral image classification. IEEE Transactions on Geoscience and Remote Sensing 48(5):2271–2282

Ravazzi P, Villa A (2009) Economic aspects of automation. In: Springer Handbook of Automation, Springer, pp 93–116

Riar DS, Ball DA, Yenish JP, Burke IC (2011) Light-activated, sensor-controlled sprayer provides effective postemergence control of broadleaf weeds in fallow. Weed Technology 25(3):447–453, DOI 10.1614/WT-D-10-00013.1, URL http://dx.doi.org/10.1614/WT-D-10-00013.1

Rola A (1989) Pesticides, health risks and farm productivity: a Philippine experience. URL http://agris.fao.org/agris-search/search.do?recordID=PH19910113458{#}.WAsc6u-LlO0.mendeley

Saltelli A, Ratto M, Andres T, Campolongo F, Cariboni J, Gatelli D, Saisana M, Tarantola S (2008) Global sensitivity analysis: the primer. John Wiley & Sons

Sankaran S, Mishra A, Ehsani R, Davis C (2010) A review of advanced techniques for detecting plant diseases. Computers and Electronics in Agriculture 72(1):1 – 13, DOI http://dx.doi.org/10.1016/j.compag.2010.02.007, URL http://www.sciencedirect.com/science/article/pii/S0168169910000438

Savary S, Ficke A, Aubertot JN, Hollier C (2012) Crop losses due to diseases and their implications for global food production losses and food security. Food Security 4(4):519–537, DOI 10.1007/s12571-012-0200-5, URL http://dx.doi.org/10.1007/s12571-012-0200-5

Schor N, Bechar A, Ignat T, Dombrovsky A, Elad Y, Berman S (2016) Robotic disease detection in greenhouses: Combined detection of powdery mildew and tomato spotted wilt virus. IEEE Robotics and Automation Letters 1(1):354–360, DOI 10.1109/LRA.2016.2518214

Siciliano B, Khatib O (2008) Springer handbook of robotics. Springer Science & Business Media

Slaughter DC, Giles DK, Tauzer C (1999) Precision Offset Spray System for Roadway Shoulder Weed Control. http://dxdoiorg/101061/(ASCE)0733-947X(1999)125:4(364) DOI 10.1061/(ASCE)0733-947X(1999)125:4(364)

Solanelles F, Escolà A, Planas S, Rosell J, Camp F, Gràcia F (2006) An electronic control system for pesticide application proportional to the canopy width of tree crops. Biosystems engineering 95(4):473–481

Gonzalez-de Soto M, Emmi L, Perez-Ruiz M, Aguera J, Gonzalez-de Santos P (2016) Autonomous systems for precise sprayingă?ăevaluation of a robotised patch sprayer. Biosystems Engineering 146:165 – 182, DOI http://dx.doi.org/10.1016/j.biosystemseng.2015.12.018, URL http://www.sciencedirect.com/science/article/pii/S153751101500197X, special Issue: Advances in Robotic Agriculture for Crops

Spósito MB, Amorim L, Bassanezi RB, Filho AB, Hau B (2008) Spatial pattern of black spot incidence within citrus trees related to disease severity and pathogen dispersal. Plant Pathology 57(1):103–108, DOI 10.1111/j.1365-3059.2007.01705.x, URL http://dx.doi.org/10.1111/j.1365-3059.2007.01705.x

Srivastava A, Goering C, Rohrbach R, Buckmaster D (2006) Engineer-

ing principles of agricultural machines. american society of agricultural and biological engineers. ST Josef, Michigan, USA

Stoate C, Boatman N, Borralho R, Carvalho CR, De Snoo G, Eden P (2001) Ecological impacts of arable intensification in europe. Journal of environmental management 63(4):337–365

Timmermann C, Gerhards R, Kühbauch W (2003) The economic impact of site-specific weed control. Precision Agriculture 4(3):249–260, DOI 10.1023/A:1024988022674, URL http://dx.doi.org/10.1023/A:1024988022674

Tirelli P (2011) Adaptive processing architecture of multi-sensor signals for low-impact treatments of plant diseased. PhD thesis, Università degli Studi di Milano

Tukey JW (1977) Exploratory data analysis. Reading, Mass.

Tumbo S, Salyani M, Whitney JD, Wheaton T, Miller W (2002) Investigation of laser and ultrasonic ranging sensors for measurements of citrus canopy volume. Applied Engineering in Agriculture 18(3):367

Turrell FM, Garber MJ, Jones WW, Cooper WC, Young R (1969) Growth equations and curves for citrus trees. University of Calif.

USDA (2016) Cucumber green mottle mosaic virus on cucumbers. URL https://www.rd.usda.gov/ks

Van De Zande J, Achten V, Schepers H, Van Der Lans A, Michielsen J, Stallinga H, Van Velde P (2009) Plant-specific and canopy density spraying to control fungal diseases in bed-grown crops. In: ECPA (ed) Proc. 7th European Conference on Precision Agriculture

Vani S, Varma A, et al (1993) Properties of cucumber green mottle mosaic virus isolated from water of river jamuna. Indian Phytopathology 46(2):118–122

Vieri M, Lisci R, Rimediotti M, Sarri D (2012) The innovative RHEA airblast sprayer for tree crop treatment. In: Proceedings of the First International Conference on Robotics and Associated High Technologies and Equipment for Agriculture (RHEA 2012), Pisa, Italy, September, pp 19–21

Vieri M, Lisci R, Rimediotti M, Sarri D (2013) The rhea-project robot for tree crops pesticide application. Journal of Agricultural Engineering 44(s1):e71

Waard M, Georgopoulos S, Hollomon D, Ishii H, Leroux P, Ragsdale N, Schwinn F (1993) Chemical control of plant diseases: problems and prospects. Annual review of phytopathology 31(1):403–421

Waggoner PE, , Aylor DE (2000) Epidemiology: A science of patterns. Annual Review of Phytopathology 38(1):71–94, DOI 10.1146/annurev.phyto.38.1.71, URL http://dx.doi.org/10.1146/annurev.phyto.38.1.71, pMID: 11701837, http://dx.doi.org/10.1146/annurev.phyto.38.1.71

Wei J, Salyani M (2004) Development of a laser scanner for measuring tree canopy characteristics. American Society of Agricultural and Biological Engineers, p 1

Welbaum GE (2015) Vegetable production and practices. CABI

Wellington C, Campoy J, Khot L, Ehsani R (2012) Orchard tree modelling for advanced sprayer control and automatic tree inventory. In: IEEE/RSJ International Conference on Intelligent Robots and Systems (IROS) Workshop on Agricultural Robotics, pp 5–6

West JS, Bravo C, Oberti R, Lemaire D, Moshou D, McCartney HA (2003) The potential of optical canopy measurement for targeted control of field crop diseases. Annual review of Phytopathology 41(1):593–614, DOI 10.1146/annurev.phyto.41.121702.103726, URL http://www.annualreviews.org/doi/abs/10.1146/annurev.phyto.41.121702.103726

Williams EB, Kuc J (1969) Resistance in Malus to Venturia Inaequalis. Annual Review of Phytopathology 7(1):223–246, DOI 10.1146/annurev.py.07.090169.001255, URL http://www.annualreviews.org/doi/abs/10.1146/annurev.py.07.090169.001255?journalCode=phyto{&}

Williamson B, Tudzynski B, Tudzynski P, Van Kan JAL (2007) Botrytis cinerea: the cause of grey mould disease. Molecular plant pathology 8(5):561–80, DOI 10.1111/j.1364-3703.2007.00417.x, URL http://www.ncbi.nlm.nih.gov/pubmed/20507522

Wu Y, Ianakiev K, Govindaraju V (2002) Improved k-nearest neighbor classification. Pattern recognition 35(10):2311–2318

Young J, Griffin M, Alford D, Ogilvy S (2001) Reducing agrochemical use on the arable farm: the talisman and scarab projects. London: Defra

Zaman Q, Salyani M (2004) Effects of foliage density and ground speed on ultrasonic measurement of citrus tree volume. Applied Engineering in Agriculture 20(2):173

Zhang H, Chang M, Wang J, Ye S (2008) Evaluation of peach quality indices using an electronic nose by mlr, qpst and bp network. Sensors and Actuators B: Chemical 134(1):332–338

Zhang L, Furumi S, Muramatsu K, Fujiwara N, Daigo M, Zhang L (2006) Sensor?independent analysis method for hyperspectral data based on the pattern decomposition method. International Journal of Remote Sensing 27(21):4899–4910, DOI 10.1080/01431160600702640, URL http://dx.doi.org/10.1080/01431160600702640, http://dx.doi.org/10.1080/01431160600702640

Zhang M, Qin Z, Liu X, Ustin SL (2003) Detection of stress in tomatoes induced by late blight disease in California,

USA, using hyperspectral remote sensing. International Journal of Applied Earth Observation and Geoinformation 4(4):295–310, DOI 10.1016/S0303-2434(03)00008-4, URL http://www.sciencedirect.com/science/article/pii/S0303243403000084

Zomlefer WB (1994) Guide to flowering plant families

List of Figures

List of Tables